New Mexico Bureau of Mines & Mineral Resources

A DIVISION OF
NEW MEXICO INSTITUTE OF MINING & TECHNOLOGY

Guidebook to the Socorro area, New Mexico

Compiled by Virginia T. McLemore and Mark R. Bowie

New Mexico Bureau of Mines and Mineral Resources, Socorro, NM 87801

24th annual meeting of the Clay Minerals Society

and

36th annual Clay Minerals Conference

Guidebook for the 1987 conference

SOCORRO 1987

Original Printing 1987

Published by Authority of State of New Mexico, NMSA 1953 Sec. 63-1-4
Printed by University of New Mexico Printing Plant, October 1987
Available from New Mexico Bureau of Mines & Mineral Resources, Socorro, NM 87801

Preface

Welcome to Socorro! The roadlogs in this guidebook were written primarily for the field trips of the 24th annual meeting of the Clay Minerals Society and the 36th annual Clay Minerals Conference held in Socorro, New Mexico, October 19-22, 1987. With permission, the authors have drawn freely on appropriate parts of published roadlogs from field trips in and around Socorro hosted by the New Mexico Geological Society (Foster and Luce, 1963a, b; Weber and Willard, 1963; Smith et al., 1983) and the New Mexico Bureau of Mines and Mineral Resources (Chapin et al., 1978a). Nomenclature and correlation of Cenozoic strata follows that established by Osburn and Chapin (1983a, b). Radiometric ages of major ash-flow tuffs and related cauldron collapse events were updated by high precision $^{40}Ar/^{39}Ar$ dating by McIntosh et al. (1986).

This guidebook is organized into three parts: 1) an introduction to the Socorro area; 2) roadlogs, and 3) short papers that supplement the field trips. The roadlogs have been divided into three trips. The premeeting field trip on Sunday, October 18, 1987 (Trip 1), is to examine clays in the Luis Lopez and Popotosa Formations and to see manganese mineralization in the Luis Lopez mining district. The mid-meeting trip on Tuesday, October 20, has been divided into Trips 2a-d because of its length. We will examine clays and soils of the La Jencia and Socorro Basins (Rio Grande valley) and drive through a structurally complex section of Paleozoic rocks on the east side of the Rio Grande and into the Jornada del Muerto. At the end of the day we will tour the Bosque del Apache National Wildlife Refuge. In case of inclement weather, the mid-meeting trip will consist of Trips 2a, 3, 2c, and 2d (in that order). Nearby attractions and day trips for spouses, family, and friends of conference participants are described in the introduction. We hope you enjoy your stay in Socorro and get the opportunity to visit other areas of the Southwest.

Acknowledgments—We are grateful to the following people for their assistance: Charles Carroll (Bureau of Land Management), Gretchen Roybal (NMBMMR), George Austin (NMBMMR), Linda Frank (NMIMT), and Frank Kottlowski (Director, NMBMMR). Numerous people in addition to the field trip leaders have spent years studying the geology in the Socorro area (C. E. Chapin, C. T. Smith, G. R. Osburn, J. R. MacMillan, M. N. Machette, W. J. Stone, S. E. Hook, and others), and their work is cited where appropriate and gratefully acknowledged. Technical assistance by Shawn Leppert and Linda Frank is appreciated.

Virginia T. McLemore
Geologist, NMBMMR
Field Trip Chairman

Field Trip Committee:
Mark R. Bowie
John W. Hawley
Richard M. Chamberlin
James L. Post

Socorro
May 1987

Contents

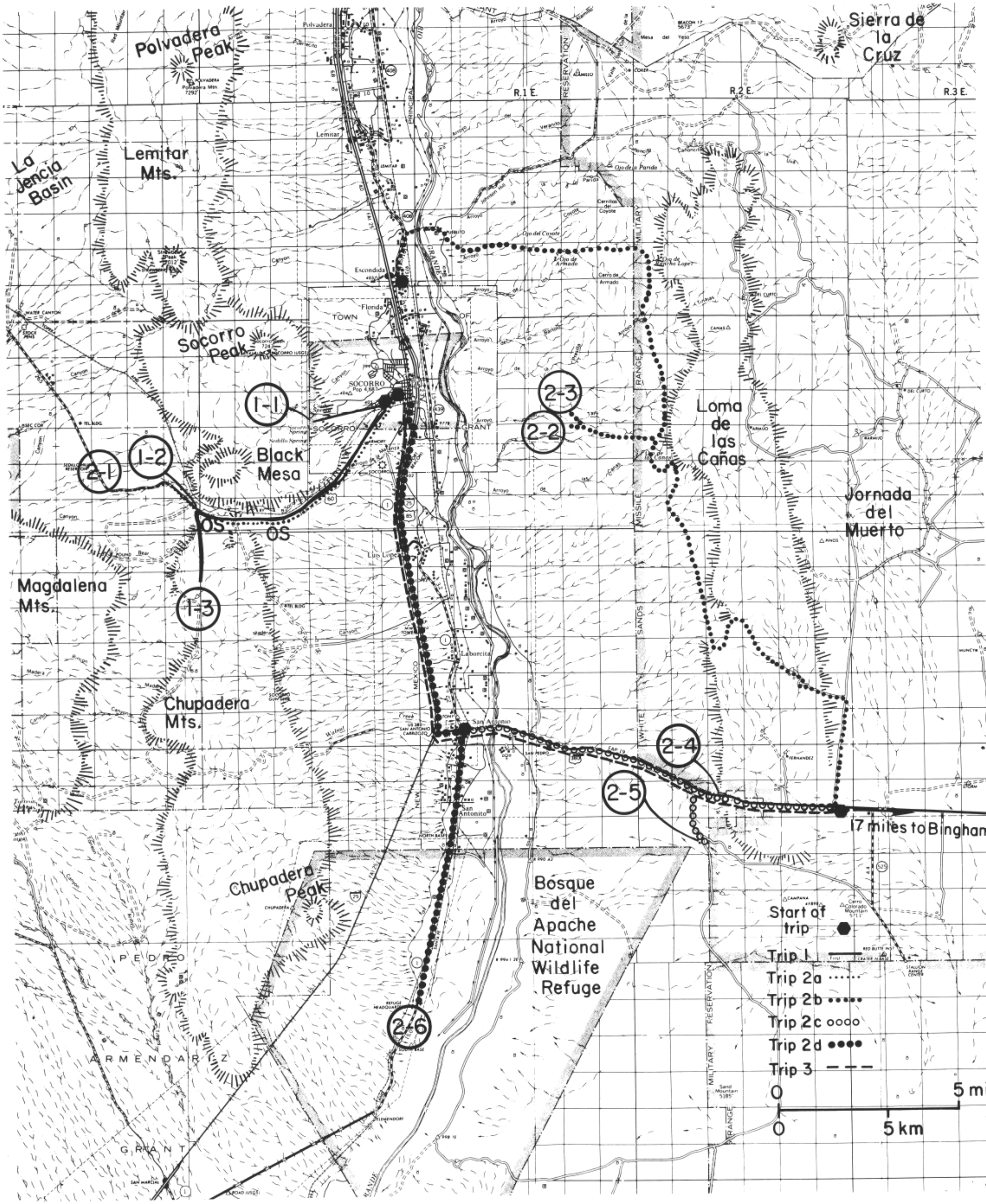

FIGURE 1—Physiographic features of the Socorro area with routes of field trips. **OS** = optional stop.

Introduction

Socorro (pronounced so Kor' ro) is an old city, rich in heritage and history. The word "Socorro," which is Spanish for help or aid, was given by Don Juan de (Mate in June 1598 to a nearby Piro Indian pueblo because the Indians provided his expedition with food. Socorro has since been under the authority of the Spanish, Mexican, and American governments.

Socorro has numerous attractions, including the New Mexico Institute of Mining and Technology, San Miguel mission church, and numerous buildings reminiscent of times past. The Very Large Array (VLA) radio telescope research facility lies about 50 miles to the west via US-60. Socorro will be the headquarters for the Very Large Baseline Array (VLBA) radio telescope facility in the near future. The Bosque del Apache National Wildlife Refuge is about 18 miles to the south and will be visited on Trip 2d.

The Socorro area reveals a complex geologic history strongly influenced by leaky crustal flaws, initially formed as wrench faults, and later reactivated by episodes of crustal shortening, translation of microplates (Colorado Plateau) and crustal stretching along the Rio Grande rift. Mining and exploitation of natural resources has played a vital role in Socorro's development, from early activities of the Native Americans (who were attracted to the area by warm fresh-water springs), to the silver boom of the 1880's, to modern-day quarrying of perlite and road metal. This guidebook describes some of the area's attractions and provides detailed roadlogs for the conference trips that examine the geology and mineral resources of the Socorro area.

Physiographic and geographic setting

Socorro, at an elevation of 4,620 ft, lies near the center of New Mexico in the Mexican Highland section of the Basin and Range physiographic province (Hawley, 1986), a region of distended continental crust characterized by a series of gently sloping alluvium-filled basins separated by complexly faulted mountains or uplifts. Socorro is situated along the Rio Grande (Fig. 1), which flows along a series of linked structural basins that compose the Rio Grande rift from southern Colorado to El Paso, Texas. The Socorro Basin is separated from the stark, desolate plains of the Jornada del Muerto Basin to the east by picturesque hills and mesas of the Loma de las Canas and Carthage areas (Trips 2b, 2c, and 3). The Jornada del Muerto (journey of the dead man) provided a treacherous shortcut for travelers going from Las Cruces (about 150 miles south of Socorro) to Santa Fe (about 135 miles north of Socorro). It was a waterless stretch and an area prone to attacks by Apache Indians; hundreds of travelers perished along this desolate route.

The western edge of the Socorro Basin is bordered by (from north to south) the Lemitar Mountains (elevation 7,929 ft), Strawberry Peak (elevation 7,012 ft), Socorro Mountains (elevation 7,284 ft), and the Chupadera Mountains (elevation 6,179 ft). La Jencia Basin (elevation 6,090 ft; Trip 2a) lies to the west of these mountains. The Magdalena Mountains, rising to over 10,000 ft, can be seen on the southwestern skyline from Socorro.

Climate, vegetation, and wildlife

Socorro has a mild semiarid to arid climate with a wide range of precipitation, temperature, and evaporation rates due to local topographic differences. The average annual precipitation is less than 10 inches, but annual precipitation can deviate from the average by as much as 50%. Precipitation is primarily from rainfall during summer and early fall storms, and it increases with increasing elevation. Total average snowfall in the winter months is approximately 6-7 inches, and the amount of snowfall also increases with increasing elevation. The higher parts of the Magdalena Mountains retain snow throughout the winter months, in contrast to the Rio Grande valley where snow melts within a few days.

Daily temperatures in Socorro range from an average low of 23°F in January to an average high of 93°F in July. Temperature variations between day and night can be as high as 40°F. Radiation and cold-air drainage at night can cause temperature inversions in the valley bottoms, where frost may form in the valleys at night, but temperatures are above freezing on the higher slopes.

Evaporation is influenced by temperature, wind velocity, and relative humidity. Evaporation in Socorro typically exceeds precipitation, especially in summer months, resulting in depletion or complete evaporation of local ponds, springs, and watering holes.

Vegetation and wildlife distribution in the Socorro area, as elsewhere in New Mexico, is dependent upon rainfall, altitude, and temperature. Along the Rio Grande and major arroyos, thick woods or bosques of cottonwood, saltcedar, willows, and Russian olive provide excellent cover, feed, and nesting for wildlife, such as mule deer, coyote, bobcat, gray fox, jackrabbits, cottontail rabbits, dove, quail, roadrunners (New Mexico's state bird), hawks, ravens, and various songbirds, rodents, and reptiles, including the poisonous diamond-backed rattlesnake. Rare, endangered species such as the bald eagle and peregrine falcon may be encountered along the river and arroyos. During winter months, the Rio Grande valley is the home of numerous migratory birds such as snow geese, Canadian geese, ducks, sandhill cranes, and the rare and endangered whooping cranes. The Bosque del Apache National Wildlife Refuge (Trip 2d) offers an excellent view of the habitat of the lower elevations.

As one moves upslope and away from the river, the vegetation changes and is more typical of what one would expect to find in a desert. Vegetation in the Socorro area is typical of that found in the upper Chihuahuan Desert where creosotebush, mesquite, and various grama grasses predominate. Cacti species are varied and plentiful; more than 60 species are found in New Mexico. In the Socorro area, the cane (cholla) and pancake (prickly pear) cacti are the most common. The trees along the Rio Grande have given way in the desert to dwarf and scrubby juniper (cedar) and pirion (pine) trees. The yucca is common in this area as well. Similar species of wildlife inhabit both the Rio Grande valley and the adjacent desert. However, in the Jornada del Muerto one can encounter herds of antelope and wild horses.

In the higher elevations of the Magdalena Mountains, various coniferous and deciduous trees form actual forests that abound with wildlife. The juniper and pirion also occur in this area as tall trees, quite different from their brothers in the lower desert regions. Wildlife species seen in the lower regions, as well as elk, bighorn sheep, and wild turkey are found in the higher elevations.

City of Socorro

Very little is known about the Socorro area before the expedition of Don Juan de Oriate in 1598. At that time the area was inhabited by the Piro Pueblo Indians who based their economy on agriculture and trading with other Pueblo Indians. Several pueblo ruins and numerous petroglyphs and pictographs remain today throughout the Socorro area (see Trip 2b for a visit to a pictograph site).

Spanish missionaries established a church at a Piro pueblo, known by the Spanish as Socorro, sometime between 1615 and 1626. The mission church became the center of the pueblo, similar to other pueblos in the Rio Grande valley. During the Pueblo Revolt of 1680, the Piro Indians at Socorro remained friendly with the Spanish and together they abandoned Socorro and fled south. They resettled along the lower Rio Grande in Texas where the town of Socorro del Sur remains today.

It wasn't until the early 1800's that Socorro was re-established although Don Diego de Vargas reconquered New Mexico in 1693 (Simmons, 1983). Frequent raids by Indians remained a serious problem. A small group of Spaniards applied to the Spanish crown for a land grant in 1817. The mission church was rebuilt during this time on top of the ruins of the original building. Many of the massive adobe walls remaining from the original church were used in rebuilding. Since its completion in 1821, the church has been known as San Miguel. The church was remodeled in the early 1900's and again in 1973 to its present form (Fig. 2). From the time of resettlement to the 1870's, Socorro remained a quiet, poor Spanish community that grew slowly. Its development was hindered by raiding Indians, mostly Apaches. The change from Spanish to Mexican rule in the 1820's and then from Mexican to American rule in 1847 made very little difference to the people of Socorro. Socorro County was created in 1852 by the New Mexico Territorial Legislature with Socorro as the county seat. Fort Craig was commissioned in 1854 to subdue the Indians and then was abandoned in 1885 once this was accomplished.

Between 1867 and 1890, Socorro was the center of a rich silver-mining district (Eveleth, 1983). Unprecedented growth followed. The Atchison, Topeka and Santa Fe (AT&SF) Railroad came to Socorro in 1880, and the stage was set for boom times. In 1882 Socorro was incorporated, and the Billing smelter (later the Rio Grande Smelting Co.) was built in 1883 to process the rich ores brought from the Magdalena district by mule and ox wagon trains. Later a spur of the AT&SF Railroad into Magdalena would facilitate transportation of the Magdalena ore to Socorro. The Socorro Fire Clay Works on Cuba Road began manufacturing bricks for the smelter and later for homes and other buildings in Socorro. The original county courthouse was built in 1884 with local brick. During this period the Illinois Brewery, the first beer brewery and ice plant in the territory, and the Golden Crown Flour Mill were built. The Garcia Opera House (Fig. 3) was built about 1886 with an open trussed roof system supporting a pitched roof and tilted walls. Three hotels served Socorro at the time: the Park, Grand Central, and Windsor; only portions of the Park Hotel remain today.

The end of the boom period came in 1893 with the demonetization of silver resulting in a dramatic decline of silver mining in the area. A series of natural disasters followed. A devastating flood hit Socorro on July 30, 1895, and decimated the lower section of town. Near the train depot the water level reached four feet. A minor earthquake hit Socorro in 1906. Over the years floods and droughts continued to plague the city.

In 1908, Col. Ethan William Eaton completed remodeling on his adobe house to prevent damage by earthquakes. He installed rods through the adobe walls and through the exterior vertical boards. The rods were secured on the inside with bolts and the outside with star washers to help distribute the load (Conron, 1980); the Eaton house still remains today.

Progress was slow after the boom period. Agricul-

FIGURE 2—Front of San Miguel Church, looking west.

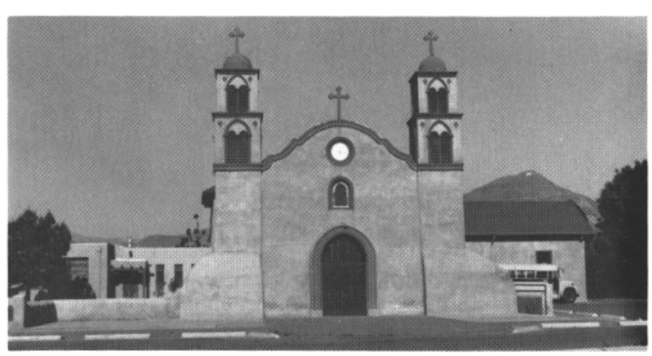

FIGURE 3—Garcia Opera House, looking northwest.

FIGURE 4—Val Verde Hotel on Manzanares Avenue, looking north.

ture became the important means of livelihood in the area. Electricity came to town in 1910, and New Mexico entered the Union as a state in 1912. The first ocean-to-ocean highway (present-day US-60) passed through Socorro in 1910 and helped to revitalize the town. As a result of this major highway, the Val Verde Hotel was built in 1919 and became a popular social gathering site until just before World War II. The Val Verde has since been renovated and part of it has been reopened as a restaurant adjacent to small shops and offices (Fig. 4).

The years since World War II have brought steady growth to Socorro, mainly in response to the growth of New Mexico Tech. Renovation of historic buildings has become popular and some results are seen throughout the town (Fig. 5).

New Mexico Institute of Mining and Technology

New Mexico Institute of Mining and Technology (NMIMT) or New Mexico Tech (Fig. 6) is a small state institution specializing in instruction and research in physical science and mineral engineering. The college was founded in 1889 as the New Mexico School of Mines as a result of extensive mining in the region. The name was changed in 1960 by an amendment to the State Constitution in recognition of its new functions and an enlarged organization. New Mexico Tech consists of four divisions: 1) the College, 2) the New Mexico Bureau of Mines and Mineral Resources, 3) the Research and Development Division, and 4) the New Mexico Petroleum Recovery Research Center.

The College Division consists of undergraduate and graduate programs in basic sciences, computer science, mathematics, technical communication, and mineral engineering, which are supported by humanities, social science, and military science courses. New Mexico Tech is accredited by the North Central Association of Colleges and Secondary Schools as a doctoral-degree-granting institution.

New Mexico Bureau of Mines and Mineral Resources (NMBMMR) is the official state agency responsible for conducting investigations of geology and mineral resources in New Mexico. Information generated by the staff and associates is provided to the public through maps, publications, and direct response to inquiries. Publications are available at the Publications Office in Workman Center. Other infor-

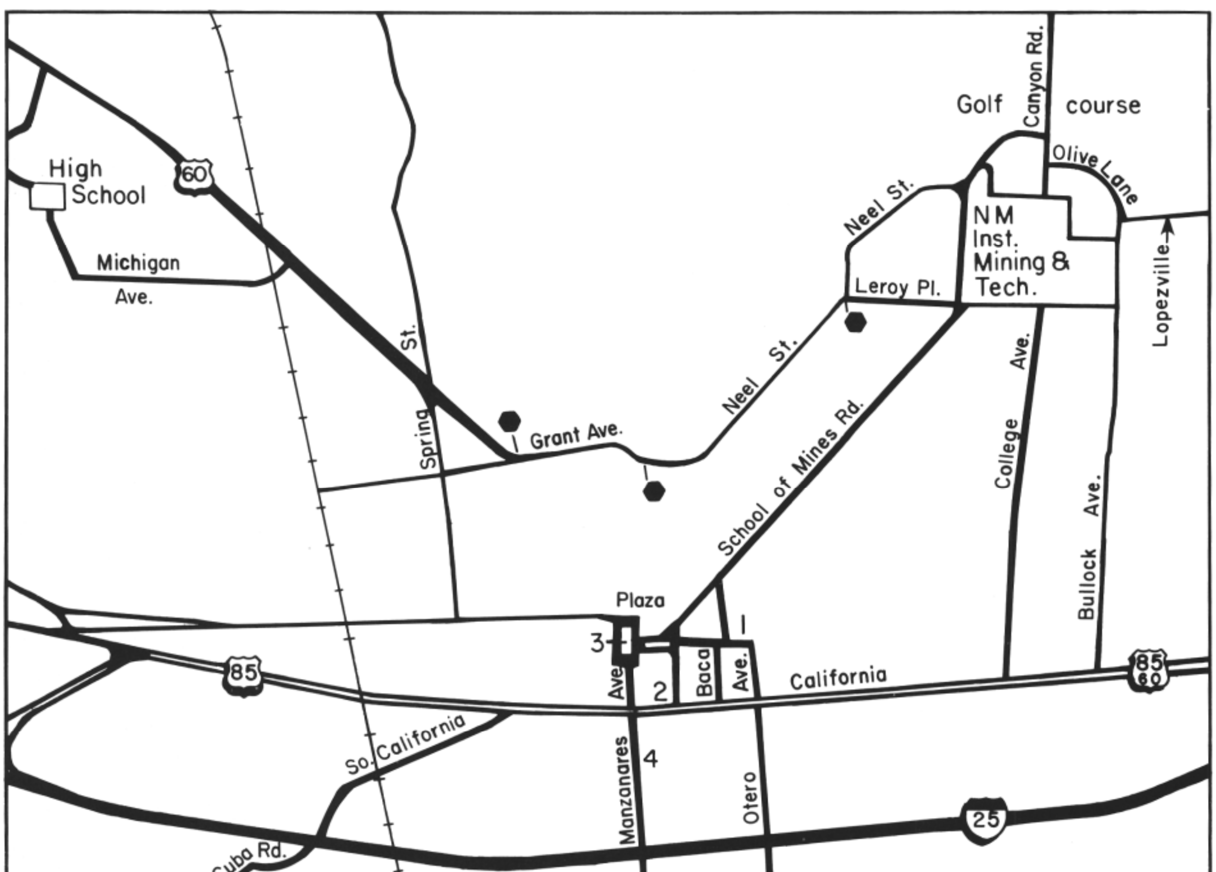

FIGURE 5—Street map of Socorro. **1,** San Miguel Mission; **2,** Garcia Opera House; **3,** Plaza; **4,** Val Verde Hotel. The hexagons indicate stop signs that are mentioned in the roadlog for Trip 1 (p. 19).

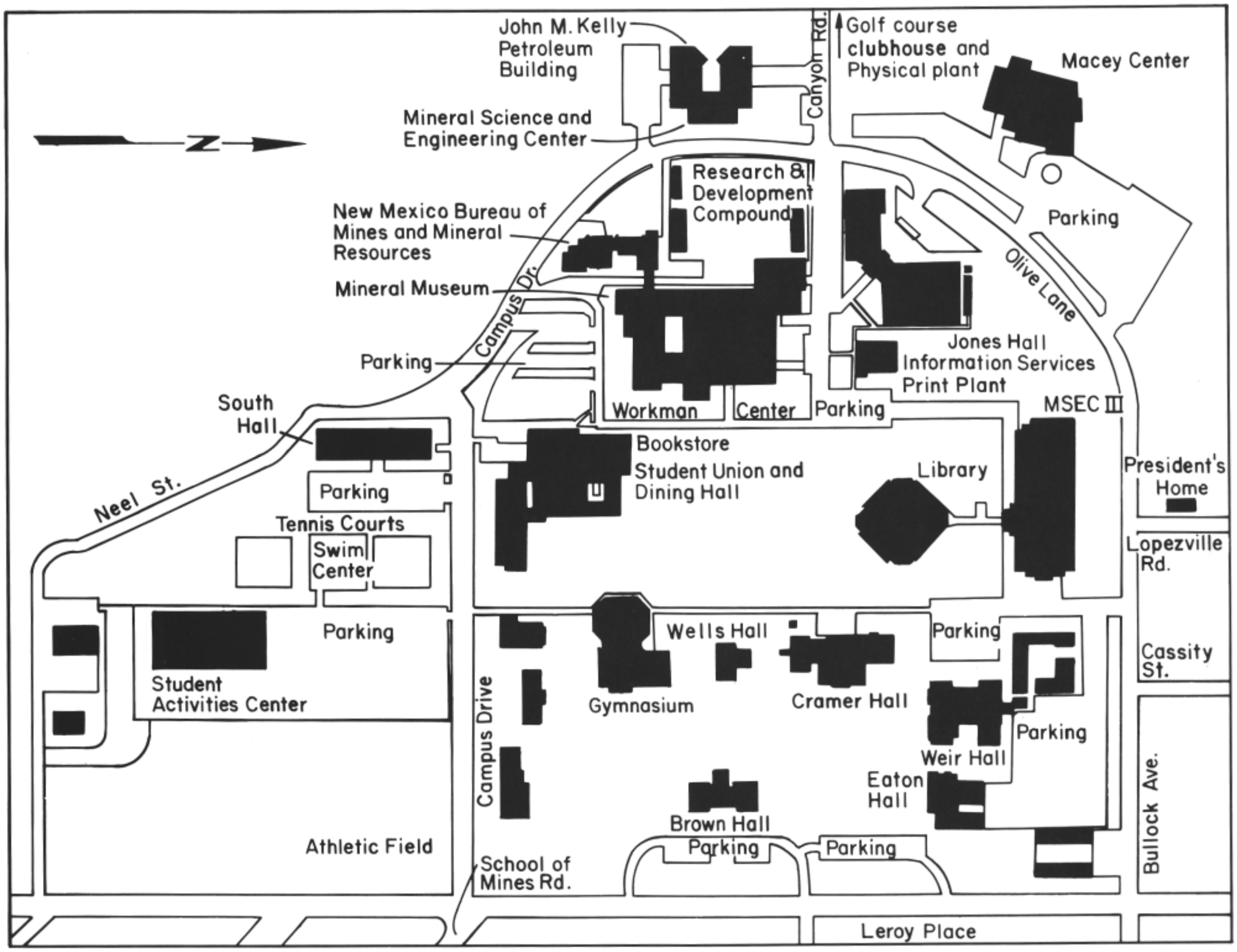

FIGURE 6—Map of New Mexico Institute of Mining and Technology.

mation is available through the Bureau's Geotechnical Information Center.

The NMBMMR Mineral Museum in Workman Center is definitely worth a visit. The museum contains more than 10,000 display and study specimens. The display collection, with more than 2,000 minerals from New Mexico, the rest of the United States, and the world, can be viewed from 8:00 a.m. to 5:00 p.m., Monday through Friday. The study collection contains more than 6,000 specimens and is available to the public for inspection during regular office hours. A micromount collection, where small crystals are mounted in 1 x 1 inch boxes for viewing with a binocular microscope, is also available for examination.

There are four organized components of the Research and Development Division (RDD): 1) the Geophysical Research Center (GRC), 2) the Terminal Effects Research and Analysis group (TERA), 3) the New Mexico Mining and Mineral Resources Research Institute (NMMMRRI), and 4) the Center for Explosives Technology Research (CETR). RDD was established in 1946 in Albuquerque and was moved to Socorro in 1949. The GRC supports research in atmospheric physics and chemistry, air quality, geophysics, and hydrology. The Langmuir Laboratory for Atmospheric Research, located in the nearby Magdalena Mountains, is also supported by the GRC. The TERA group supports research in ordnance and transportation safety and operates the RDD machine shop. NMMMRRI provides research and education in the fields of mining and extractive metallurgy. CETR is RDD's newest group and was established in 1983 to promote research in new materials, explosive devices, rock-blasting techniques, and energetic materials.

The Petroleum Recovery Research Center (PRRC) conducts basic and applied research on enhancement techniques for recovery of petroleum and natural gas.

FIGURE 7—Macey Center, New Mexico Institute of Mining and Technology, looking west.

New Mexico Tech was selected for the home of the PRRC because Tech is the only institution in the state that grants degrees in petroleum engineering. Interaction between the division and the department is extensive.

Socorro is also the home of the New Mexico Tech golf course, which is recognized as one of the best 18-hole courses in the state. The annual Hilton Open and the Chili Chase tournaments are held here.

The Macey Theater/Conference Center (Fig. 7) attracts meetings of all types and hosts many fine arts events. It is located on the northern edge of the campus.

Mining—past and present

Once the Apaches were subdued in the mid-1800's by troops stationed at Fort Craig, prospectors began searching the hills in earnest for gold, silver, and other metals. Lead and silver were discovered in the Magdalena Mountains in 1866, and by 1876 mines in the Magdalena (Kelly), Socorro Peak, and Water Canyon districts were producing (Fig. 8, Table 1). Actual production figures from most of these districts are sketchy, but much more than 30,000 oz of gold and more than 4.8 million oz of silver were produced from Socorro County (North, 1983; North and McLemore, 1986).

Socorro became the center of these silver-rich districts. The Torrance stamp mill and the New Orleans and La Joya smelters initially processed the ore, but in 1883 the Billing smelter went on line and soon was processing ore from throughout the Southwest. It is estimated that $18 million worth of lead, silver, and gold were smelted at this plant from 1883 through 1894 (Eveleth, 1983).

Coal and limestone were mined at Carthage (Trips 2c and 3) as feedstock for the Billing smelter and later as heating fuel. Total coal production through 1964 is estimated at more than 1.8 million tons. An unknown quantity of reserves is still present at Carthage. Quarries in the Popotosa and Luis Lopez Formations near Socorro (Trips 1 and 2a), in the Sandia Formation at Arroyo de la Presilla (near Stop 2-3, Trip 2b), and in the southern Lemitar Mountains supplied clay to the local brick plant. Bricks were used in the smelter and in buildings in town. Most of the fluxing ore was imported from Mexico.

The end of the mining boom commenced in 1893 and 1894 with 1) a duty increase on the Mexican fluxing ore and 2) a steady decrease in demand for silver

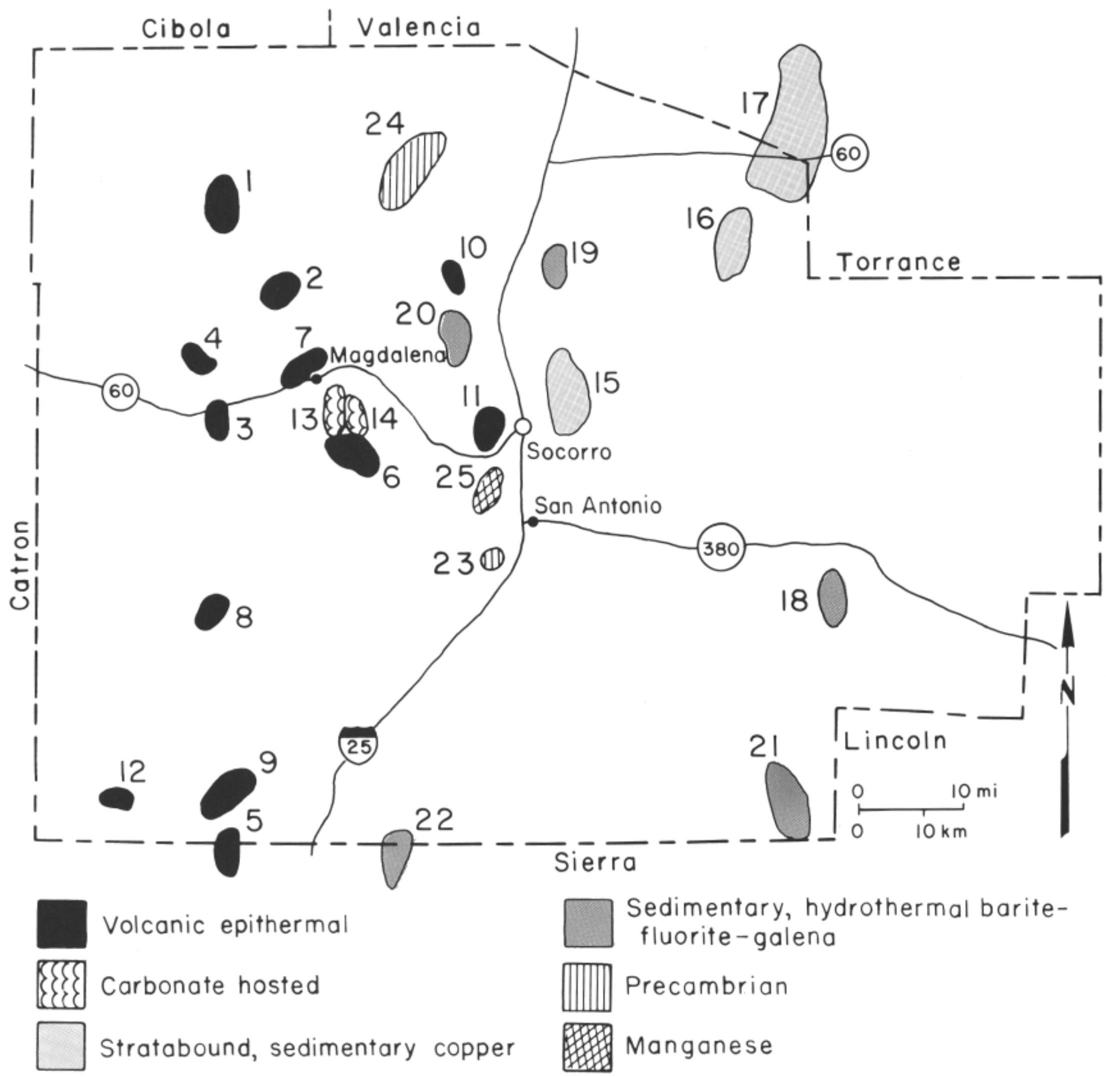

FIGURE 8—Mining districts in Socorro County. Numbers are keyed to Table 1.

(Eveleth, 1983). The Billing smelter closed in October 1894. The closing of the plant crippled the economy of Socorro. Socorro's population in 1890 was 2,300, but by 1900 it had dropped to 1,500.

In the 1900's, mining of gold, silver, and other metals occurred sporadically throughout Socorro County (North, 1983; North and McLemore, 1986). Mines in the Magdalena and Water Canyon districts continued sporadic production until the early 1980's. Other districts produced ore until the 1950's. Exploration for precious metals continues today.

Mines from Socorro County have also yielded barite, fluorite, manganese, uranium, and vanadium. Barite was produced from several areas in the 1970's and milled at Pueblito (Trip 2b). Perlite, a hydrated rhyolitic glass capable of expansion upon heating, was discovered in the Socorro Mountains in the 1960's and is being produced currently. Perlite is used primarily in building materials (e.g., wallboard) and as a filter aid. New Mexico is the leading producer of perlite in the United States. Sand and gravel are the only other raw materials currently produced in Socorro County. They are quarried from Quaternary gravels along the Rio Grande valley.

TABLE 1—Mining districts in Socorro County, New Mexico. Numbers are keyed to Fig. 8.

Volcanic epithermal deposits	
1 Abbe Spring	Cu, Ag (Ba)
2 Bear Mountains	(Cu, Ag, Sb)
3 Cat Mountain	Cu, Au, Ag
4 Council Rock	Pb, Ag (Ba)
5 Goldsboro	Au, Ag
6 Hop Canyon (Mill Canyon)	Cu, Pb, Au, Ag (Zn, Ba, U)
7 North Magdalena (Silver Hill)	Pb, Ba, Cu, V, Ag (Zn)
8 Rosedale	Au, Ag (F)
9 San Jose	Cu, Pb, Zn, Au, Ag
10 San Lorenzo	Cu, Ag (U)
11 Socorro Peak	Pb, Ag (Ba, F)
12 Taylor (Ojo Caliente #2)	Cu, Pb, Ag
Carbonate-hosted deposits	
13 Magdalena (Kelly)	Ag, Au, Zn, Pb, Cu (F, Ba)
14 Water Canyon	Ag, Au, Cu, Pb, **Zn** (Mn)
Stratabound, sedimentary copper deposits	
15 Chupadero	Cu, Ag (U)
16 Rayo	(Cu, Ag)
17 Scholle	Cu, Ra, Pb, Ag, Au (U, V)
Sedimentary-hydrothermal barite-fluorite-galena	
18 Hansonburg	Pb, F, Ba, Cu, Ag, Au
19 Joyita Hills	Pb, F, Ag (Cu)
20 Lemitar Mountains	Cu, Pb, Ba, Ag (F, Zn, U, V)
21 Mockingbird Gap	Pb, Ag (Cu, Ba, F, Zn)
22 Fra Cristobal Mountains	(Cu, Pb, Ag, Au, F, Ba, Mn)
Precambrian	
23 Chupadera Mountains (Coyote Hills)	(Au, Ag, Cu, Pb, Zn, Ba)
24 Ladron Mountains	U, Cu, Pb, Ag, F (Zn, Ba)
Manganese deposits	
25 Luis Lopez	Mn (Au, Ag, Zn, W)

Regional attractions

Fort Craig

Fort Craig is located 25 mi south of Socorro, but is currently closed to the public until restoration of the fort is completed. The site is administered by the U.S. Bureau of Land Management (BLM); guided tours of Fort Craig are provided periodically by BLM personnel.

The fort was commissioned in 1854 to provide protection from hostile Indians. It was named for Captain Louis S. Craig of the 3rd Infantry who was killed in California in 1852. At the beginning of the Civil War, Colonel E. R. S. Canby ordered Fort Craig to be strengthened (Wilson and Bieberman, 1983), thereby making it the second largest fort in New Mexico. Fort Union near Las Vegas, New Mexico, was larger and served as the main supply point for the entire Southwest. The first Civil War battle in New Mexico was fought at Val Verde in 1862; Confederate forces were victorious. However, the Confederates failed to capture Fort Craig. They were finally defeated later that year at Glorieta Pass, between Santa Fe and Las Vegas and forced to retreat to Texas. After the Civil War the fort continued to provide protection from the Apache Indians. It was abandoned in 1885.

Very Large Array

The Very Large Array (VLA) is an astronomical observatory operated by the National Radio Astronomy Observatory and is located on the San Agustin Plains about 50 mi west of Socorro on US-60. Twenty-seven giant, dish-shaped radio telescopes, each weighing 235 tons and standing 100 ft high, make up one of the world's largest astronomical observatories. They are linked electronically to form, in effect, a single, large radio telescope. Each antenna is computer-controlled and collects incoming radio signals and sends them to a central computer where they are processed. By using many antennae, VLA researchers can make detailed, high resolution pictures of extremely faint near- and far-distance celestial objects. The VLA, one of the most powerful radio telescopes in the world, operates 24 hours a day, 7 days a week. The visitor center contains several displays about radio astronomy and the operation of the VLA. A walking tour takes visitors around the central portion of the observatory, including the control and computer rooms, the antenna assembly building, the service area, and the closest of the antennae.

Water Canyon and Langmuir Laboratory

Water Canyon is a popular picnic and camp site in the Magdalena Mountains. It is located about 20 mi west of Socorro on the road that leads to Langmuir Laboratory. The laboratory, which was built in 1963 at an elevation of 10,630 ft, is used for research in atmospheric physics and was named in honor of the late Dr. Irving Langmuir, Nobel Prize winner for research in cloud physics and weather modification at New Mexico Tech, 1946-1957. In cooperation with the Goddard Space Flight Center of NASA and New Mexico Tech, the Joint Observatory for Cometary Research was built at the site in 1973.

Salinas National Monument

Salinas National Monument, which is about 60 mi northeast of Socorro near Mountainair, includes the ruins of three Indian pueblos—Abo, Quarai, and Gran Quivira—and their nearby 17th century Spanish mission ruins. The National Park Service headquarters is in the historic Shaffer Hotel in Mountainair and houses a museum display and audiovisual program. Park personnel present excellent seminars describing the Indian culture, history, and subsequent influence by the Spanish. The pueblo of Abo (10 mi west of Mountainair) was fully settled by A.D. 1150 along a major Indian trade route. Spanish records and the extensive ruins suggest that Abo was one of the largest communities in central New Mexico. Gran Quivira is about 33 mi southeast of Abo (25 mi southeast of Mountainair) and was first occupied by at least A.D. 700. Mission activity began with the construction of San Isidro church in 1629. Quarai, which is 8 mi north of Mountainair (33 mi north of Gran Quivira), was a thriving community by A.D. 1300. The Nuestra Senora de la Purisima ConcepciOn de Cuarac church was constructed about 1630. All three sites were abandoned during the 1670's and 1680's. Today, preservation and excavation of the ruins, including churches, Indian rooms, and kivas, can be seen along trails at each of the three sites.

Albuquerque

New Mexico's largest city, Albuquerque, lies about 75 mi north of Socorro, also on the Rio Grande. The Villa of Alburquerque was established at Old Town in 1706 by the colonial governor Don Francisco Cuervo y Valdez. The villa was named after the Duke of Alburquerque and Viceroy of New Spain. The "r" in the second syllable was dropped by 19th century English-speaking people. Today, Old Town Plaza is a popular attraction where Indian vendors display their wares along sidewalks in front of the many shops and restaurants. The Indian Pueblo Cultural Center, the Albuquerque Museum, and the Natural History Museum are near the Old Town Plaza area. Sandia Peak Tramway, the world's longest, spans 2.7 mi from the foothills of the Sandia Mountains (elevation 10,378 ft). An excellent panoramic view of the Albuquerque area can be seen from the Summit House and restaurant at the top. The geology of the Albuquerque area, including the route of the tramway, is described by Kelley (1982) in NMBMMR's Scenic Trip No. 9.

Roadlogs

Use of roadlogs

The following series of roadlogs point out geologic features, historical information, and other items of interest in and around Socorro. Passenger cars can be used on all trips; however, travel on dirt roads in Trips 1 and 2b is not advised during wet weather. Many features can be seen while driving, but please do not try to read the logs while driving! Have a passenger read the logs or pull over in a safe place to read and observe. A few stops include short walks. Dress appropriately for the weather, carry water, and beware of snakes. Odometers on different vehicles often do not agree, so allow for differences at major landmarks. "Where to look" is usually given in clock-face terminology: 12:00 is straight ahead, 9:00 is due left, and 3:00 is due right. Stratigraphic nomenclature is given in Table 2.

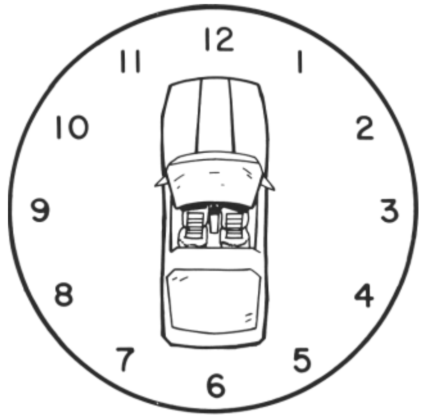

TABLE 2–Stratigraphic nomenclature for the Socorro area (from *Osburn and Chapin, 1983a, b; Osburn and Lochman-Balk, 1983; Hook, 1983; Osburn, 1984; McIntosh et al., 1986).* Ages in parentheses are approximate ranges; ages in brackets are from one or more age dates.

Geologic age	Geologic unit	Thickness (ft)	General lithology
Cenozoic			
Quaternary	undifferentiated alluvial, eolian, basin floor, and piedmont deposits	variable	unconsolidated sands, silts, and gravels
Quaternary–Tertiary	Upper Santa Fe Group		
Pliocene–Pleistocene	Sierra Ladrones Formation includes basalt of Sedillo Hill, basalt of Socorro Canyon [4.1 ± 0.3 m.y.], basalt of San Acacia	0-1000	poorly indurated fanglomerates intertonguing mudstone and siltstone; basalt flows
Miocene	Popotosa Formation includes basalt of Broken Tank basalt of Bear Canyon Socorro Peak Rhyolite [7-12 m.y.]	0-3000	lower unit is well indurated mudflow deposits overlain by red and green playa shales; fanglomerates, mudstones, and sandstones interfingered with local volcanic deposits
	Magdalena Peak Rhyolite [14.8 m.y.]		
	basalt of Kelly Ranch		
	basalt of Council Rock [17.4 m.y.]		
	rhyolite of Water Canyon Mesa [20.5± 0.8 m.y.]		
Oligocene	South Canyon Tuff [27.36 m.y.]	0-650	ash-flow tuff
	La Jara Peak Basaltic Andesite	0-1100	basaltic andesite flows
	Lemitar Tuff [27.97 m.y.]	0-400	ash-flow tuff
	La Jencia Tuff [28.7 m.y.]	0-500; ..-2500	ash-flow tuff
	Vicks Peak Tuff [28.46 m.y.]	0-800	ash-flow tuff
	Luis Lopez Formation includes rhyolite of Cook Spring	0-3500	rhyolite lavas and domes, intermediate lavas, ash-flow tuffs, and sedimentary rocks including mudstones
	Hells Mesa Tuff [32.04 m.y.[	0-800; >3000	ash-flow tuff
	tuff of Granite Mountain	0-200	ash-flow tuff
	Datil Group		
	Spears Formation [33.1-39.6 m.y.]	0-3000	volcaniclastic rocks and lavas, andesitic
Eocene	Baca Formation (37-41 m.y.)	0-1000	red to buff sandstones and claystones with minor conglomerates
Mesozoic			
Cretaceous	Crevasse Canyon Formation	0-1115	mudstone, sandstone, and siltstone with some coals
	Gallup Sandstone (89-88 m.y.)	0-110	sandstone
	D–Cross Tongue of Mancos Shale (90-89 m.y.)	50-300	noncalcareous shale with some limestone
	Tres Hermanos Formation (93-90 m.y.)	190-300	
	Fite Ranch Sandstone Member	75-90	sandstone
	Carthage Member	100-150	predominantly shale and several sandstones; coal
	Atarque Sandstone Member	10-100	sandstone
	Rio Salado Tongue of Mancos Shale	200	basal limestone overlain by calcareous and noncalcareous shales
	Twowells Tongue of Dakota Sandstone	0-100	sandstones
	lower part of Mancos Shale	0-450	shales
	Dakota Sandstone (95-93 m.y.)		sandstone with interbedded shale and local coal
Triassic	Dockum Group		
	Chinle Formation	0-550	maroon and gray shales and siltstones with local sandstones
	Santa Rosa Sandstone	200-250	red sandstones with interbedded shales and siltstones
Paleozoic			
Permian	Bernal Formation	0-100	mudstone and siltstone with minor sandstone
	San Andres Limestone	20-60	limestone and dolostone with gypsum, siltstone, and shale
	Glorieta Sandstone	0-115	cliff-forming quartzose sandstone with local siltstones
	Yeso Formation		
	Joyita Member	0-160	quartzose sandstone with local siltstone
	Callas Member	0-300	gypsum, limestone, and siltstone
	Torres Member	100-600	interbedded sandstone, shale, gypsum, and limestone
	Meseta Blanca Member	130-400	sandstone with minor siltstone and shale
	Abo Formation	0-1000	dark reddish brown sandstone, shale, and siltstone

Geologic age	Geologic unit	Thickness (ft)	General lithology
	Magdalena Group		
	Bursum Formation	28–234	purplish-red and green shales, limestones, and arkoses
Pennsylvanian	Madera Formation	200–2400	
	arkosic limestone member		sandstones, limestones, and shale
	gray limestone member		limestone with interbedded shales and siltstones
	Sandia Formation	30–700	siltstones, sandstones, and shales with minor conglomerates
Mississippian	Kelly Limestone	0–75	limestone
	Caloso Limestone	0–40	limestone with minor shales and sandstones
Ordovician	dikes	—	carbonatite dikes in the Lemitar and Chupadera Mountains [449 ± 16 m.y.]
Precambrian	undifferentiated (1.6–0.6 b.y.)	—	granitic plutons (Tajo granite, Polvadera granite), mafic igneous rocks, and metamorphic rocks

Trip 1:
Socorro Peak area and
Luis Lopez manganese district

Roadlog from Socorro to Blue Canyon area of Socorro Peak, to US-60 clay pit, and to Luis Lopez manganese district.

by Richard M. Chamberlin, Virginia T. McLemore, Mark R. Bowie, and James L. Post
New Mexico Bureau of Mines and Mineral Resources, Socorro, NM 87801 and California State University, Sacramento, CA 95819-2694

Sunday, 18 October 1987

Assembly point: Macey Center, New Mexico Tech campus
Departure time: 1:00 p.m.
Distance: 23.4 mi
Stops: 3

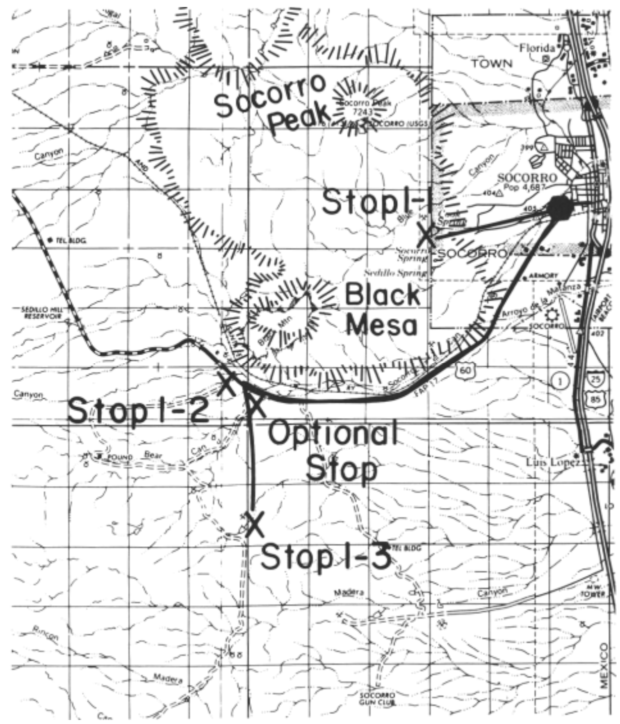

Summary

This half-day excursion provides a brief introduction to the geologic and tectonic setting of two different types of clay deposits as well as the hydrothermal manganese deposits found on the periphery of the Socorro Mountains. As shown in Figure 9, the north-trending basins and ranges of the Socorro region (including Socorro Peak) are predominantly tilted fault blocks (half basin, half uplift) formed by westward extension of the continental crust along the Rio Grande rift. Twentieth century uplift, historic seismicity, thermal springs, and high-heat flow in the Socorro Peak-Socorro Basin area are reasonably attributed to an active sill-like magma body, about 11 mi below the Rio Grande valley, and numerous dike-like bodies about 2.5-8.5 mi below Socorro Peak (Sanford, 1983).

The 2,000-ft escarpment forming the east face of Socorro Peak represents a late-stage tilted-fault-block uplift within the Rio Grande rift. Less than 7 m.y. old, the Socorro-Lemitar uplift has disrupted an early closed basin of the rift known as the Popotosa Basin. Silicic lava flows and domes, that now form the skyline west of "M" Mountain, were erupted, episodically, onto the playa floor of the Popotosa Basin from 12 to 7 m.y. ago. Claystones of the upper Popotosa Formation (Fig. 10) lack sufficient strength to support the flanks of the uplifted lava flows. The Socorro Mountains are therefore surrounded by a hummocky apron of Pleistocene landslide blocks, compositionally equivalent to lava flows found immediately upslope.

The bold cliffs on the east face of Socorro Peak (below the "M") are formed by extremely well indurated debris-flow deposits of the lower Popotosa Formation (Figs. 10, 11). These coarse matrix-supported clastics occur as thick wedges in narrow strike valleys (3 mi wide) adjacent to low-angle early rift faults. A widespread angular unconformity at the base of the Popotosa (20-30°) and abrupt thickness variations in underlying ash-flow tuff sheets indicate that domino-style crustal extension began along the rift axis about 29 m.y. ago.

Thermal springs flowing from the east flank of the Socorro Mountains lie at the intersection of the range-bounding fault zone and the Socorro transverse shear zone—a broad domain boundary separating westerly tilted fault blocks on the north from easterly tilted fault blocks on the south (Fig. 9).

The relatively young Socorro Mountain block transects the northeastern topographic wall and structural margin of the 32-m.y.-old Socorro cauldron (Fig. 9).

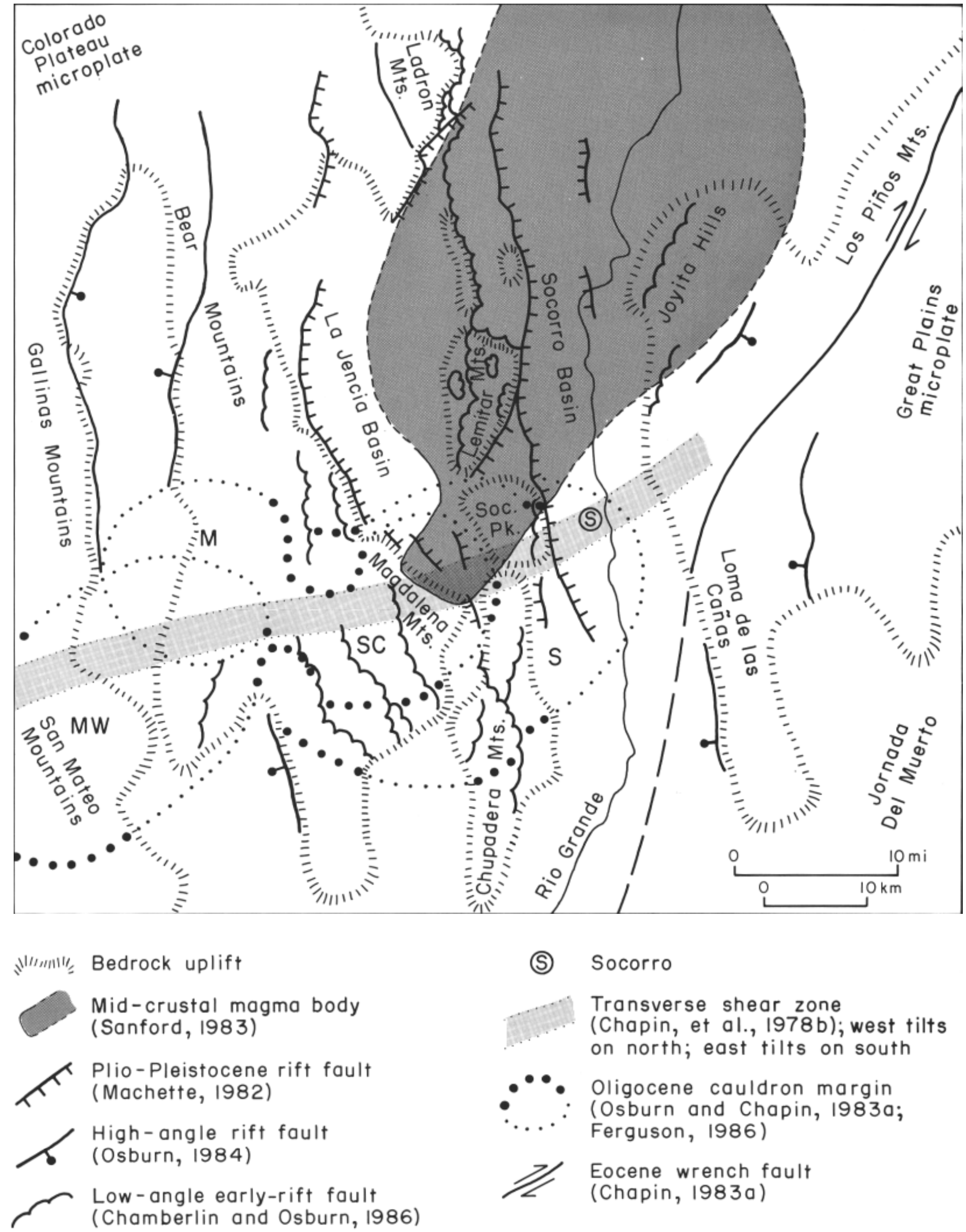

FIGURE 9—Sketch map of major structural features in the Socorro region. Cauldrons: **S**, Socorro; **SC+M**, composite Sawmill Canyon–Magdalena; **MW**, Mount Withington (*compiled by R. M. Chamberlin*).

The uplift thus provides a cross-section-like view of the cauldron margin. Pennsylvanian limestones (Madera Formation) in the middle slope of Socorro Peak define the structurally high rim of the cauldron; and a large rhyolite lava dome in the caldera moat (north of Blue Canyon) is considered to mark a point on the ring-fracture zone. Moat deposits, collectively assigned to the Luis Lopez Formation, thin abruptly by at least 700 ft, northward across the buried rim of the Socorro cauldron.

The middle Tertiary caldera complex southwest of Socorro and the area of strong domino-style extension along the axis of the rift are superimposed on a late Laramide (Eocene) transpressional welt locally bound by right-lateral wrench faults (Fig. 9). The Socorro region can be considered a relatively soft (warm) zone in the continental lithosphere that has been periodically squeezed, transposed, intruded, and stretched between two relatively rigid (cold) microplates, represented by the Colorado Plateau and the Great Plains provinces (Fig. 9). More details on the geology and tectonic setting of this area are by Chapin et al. (1978b), Chamberlin (1980, 1981, 1983), and Chamberlin and Osburn (1986).

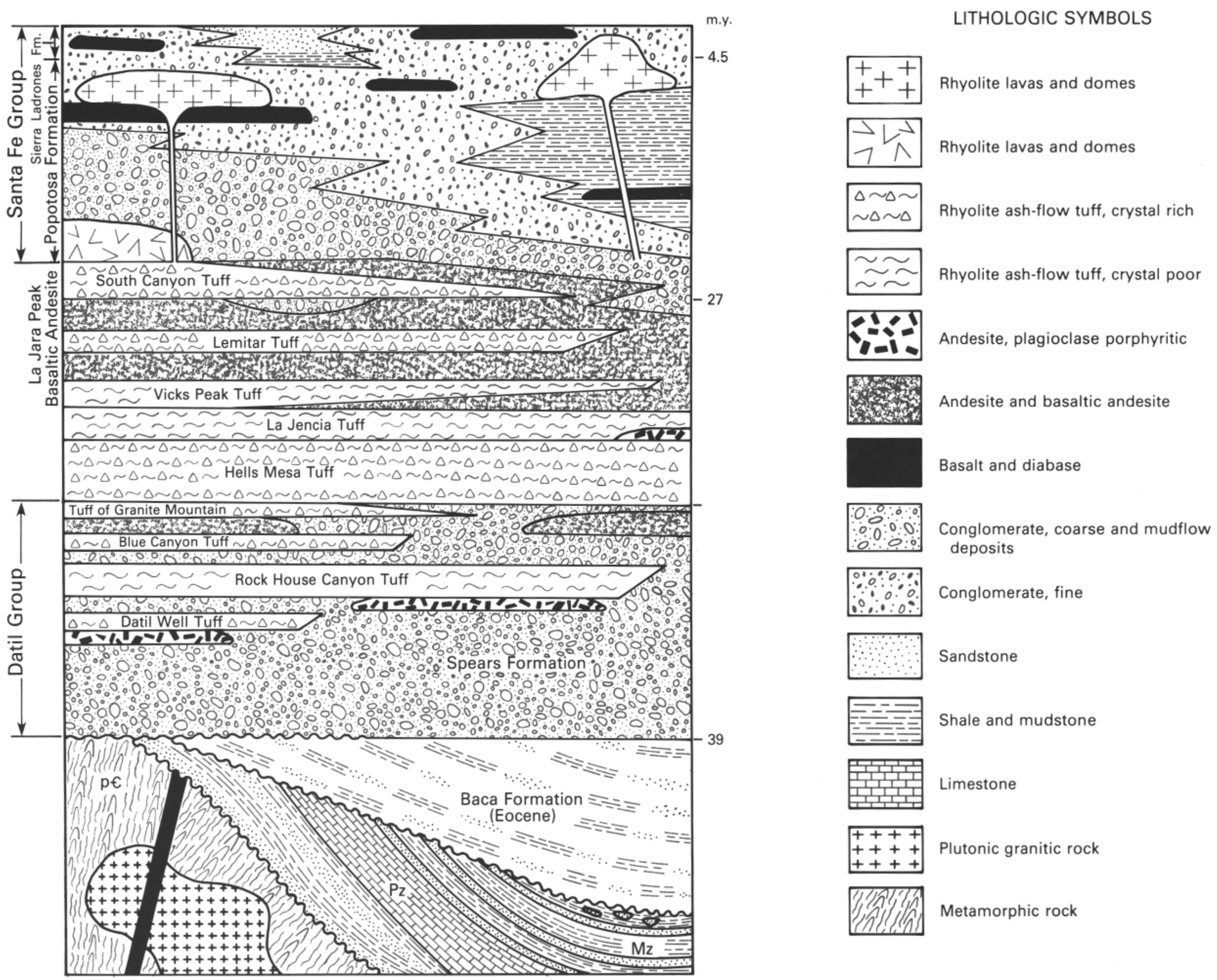

FIGURE 10—Generalized stratigraphic column for the northeast Mogollon–Datil volcanic field, New Mexico (*by Osburn and Chapin, 1983a; modified after McIntosh et al., 1986*).

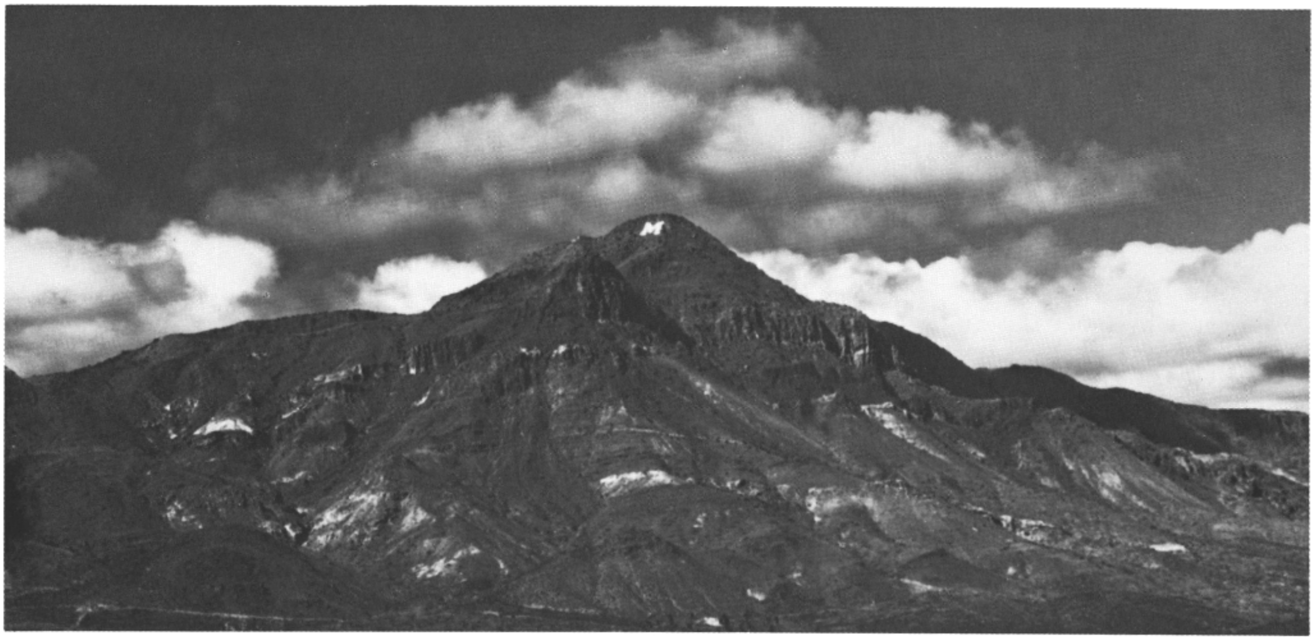

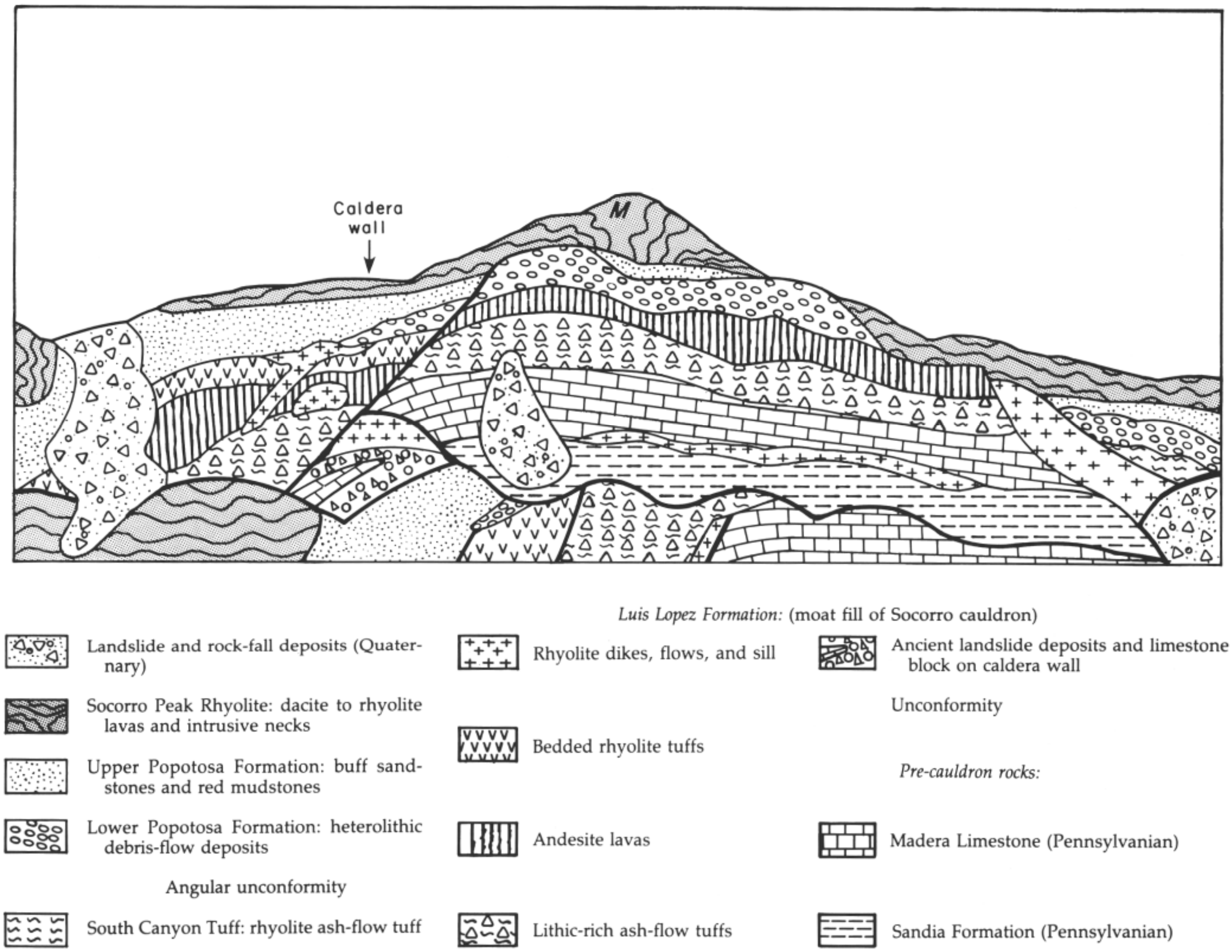

FIGURE 11—Looking west at Socorro Peak from the New Mexico Institute of Mining and Technology campus, 1979. The northern margin of Socorro cauldron (Oligocene) truncates well-stratified limestones and shales of Pennsylvanian age near center of photograph. The topographic margin is onlapped and buried by moat deposits of Luis Lopez Formation (Oligocene). Rhyolitic domes and flows of Socorro Peak Rhyolite (late Miocene) form the skyline. *Photo by G. R. Osburn. Sketch of geologic units by R. M. Chamberlin.*

Total Milage

0.0 Drive west on Canyon Road at intersection with Campus Drive. Macey Center on right and Petroleum Recovery Research Center (Kelly Building) on left. Drive past green oasis of the New Mexico Tech golf course. As much as 1,000 ft of water-saturated sands deposited by the ancestral Rio Grande underlie much of the Socorro Basin. Shallow wells in this unit can produce 1,000 gpm, enough for golfers, farmers, and other Socorroans who appreciate greenery. Machette (1978) named these fluvial sands and intertonguing piedmont-slope deposits (shed from modern ranges) the Sierra La- drones Formation (Fig. 10; Table 2). 0.1

0.1 Slow, duck crossing. 0.3

0.4 Tech Physical Plant on right. 0.2

0.6 Security check point just west of drainage bottom. Passage into this explosives-testing area requires being with a leader familiar with safety procedures and a visitor's pass from TERA (Terminal Effects Research and Analysis group). This drainage is part of the Socorro flood-control ditch, which diverts runoff from the Socorro Mountains northward around the city. 0.4

1.0 "M" Mountain and Socorro Peak (with radio towers) on crest of range at 1:30 (Fig. 11). Blue-green propylitized ash-beds near foot of range at 12:00 give Blue Canyon its name. Small cut at 12:15, in the same unit of altered pyroclastics, was a clay pit of the Socorro Fire Clay Works at the turn of the century (1880-1920). Cottonwood trees and water-storage tank at 11:00 to 11:15 are natural and manmade indications of thermal springs (90°F) that provide a large part of Socorro's water supply. The springs are located where the range-bounding fault cuts moat deposits of the Socorro cauldron and intersects a transverse shear zone of the Rio Grande rift. The transverse shear zone represents reactivation of an ancient crustal flaw, the Morenci lineament of Chapin et al. (1978b), within the strongly extended axial zone of the rift. 0.9

1.9 Pass under telephone wires. Approaching mountain front. 0.1

2.0 STOP 1.1. Turn right onto dirt road leading to TERA storage area. Park and walk upslope about 200 yds to old clay pit. Clay (see pp. 48-49) was mined from this pit during the late 1800's and early 1900's to produce fire bricks at the Socorro Fire Clay Works. Talmage and Wootton (1937, p. 69) described clays from this pit as "kaolinitic material . . . derived from a rhyolite flow"; and also stated that "Bricks made from it are buff-colored and very hard." Recent analyses by J. L. Post have shown that this altered rhyolite contains abundant 1M illite and about 8% K_2O. The best illite material is found in the wash to the south of the pit. Concentrations of 6-11% K_2O are widespread in Oligocene volcanic rocks to the north and west of Socorro. This large region of potassium metasomatism has been interpreted as both a fossil geothermal system (D'Andrea-Dinkelman et al., 1983) and alternatively as diagenetic alteration by alkaline waters descending into the volcanic section from playa deposits in the early-rift Popotosa Basin (Chapin and Lindley, 1986).

Near the entrance to the pit, weathered surfaces reveal blocky fragments of altered pumice that show flattened and elongated vesicles typical of a viscous foam. In unweathered pit walls this altered pumice breccia looks relatively massive; it is broken only by joint-like fracture sets and discontinuous silica veinlets. Only the weathered pumice blocks and sparse andesitic lithic fragments in the pit walls attest to its pyroclastic origin.

Retrace route to campus. 2.0

4.0 At junction of Canyon Road and Campus Drive turn right onto Campus. Pass Kelly Building (Petroleum Recovery Research Center) on right and New Mexico Bureau of Mines and Mineral Resources on left. At junction of Campus and Neel (2-way stop), bear right and follow road to 4-way stop. South Hall Dormitory on left. 0.5

4.5 Stop sign. Junction of Leroy Place and Neel St. Continue straight. 0.5

5.0 Stop sign. Junction of Neel St., Fisher Ave., Grant Ave., and Blue Canyon Rd. Continue straight onto Grant Ave. 0.2

5.2 Stop sign. Junction of Grant Ave. and US-60. Bear right onto US-60. 0.2

5.4 Junction of US-60 and Spring St. Continue straight. 0.4

5.8 Railroad crossing, Grefco spur of the AT&SF. Ascend hill onto remnant of mid-Pleistocene fan surface. Stockpiles of manganese concentrates on the right. 0.4

6.2 Socorro High School on left. 0.4

6.6 Socorro General Hospital on left. 0.9

7.5 Entrance on right to Grefco perlite operation.

Commercial perlite is hydrated volcanic glass, usually of rhyolitic composition, which can be expanded when heated, producing a lightweight, nearly inert product. Perlite is used as a lightweight aggregate in construction products (wallboard) and as filter aids. New Mexico is the leading producer of perlite in the U.S. The Grefco perlite deposit was the principle domestic source of perlite during the infant years of the industry (Weber and Austin, 1982). The Socorro perlite deposit is the youngest of a series of siliceous lava domes (the Socorro Peak Rhyolite) guided to the surface by the deep plumbing of the Morenci lineament (transverse shear zone) and north-trending faults of the rift. This high-silica (78% SiO_2) rhyolite dome is about 7.4 m.y. old, as determined by K-Ar dating on a whole-rock sample (Osbum and Chapin, 1983a). 0.1

7.6 Bridge across concrete ditch that diverts water from Socorro Canyon southward into Arroyo de la Matanza; milepost 136. Light-colored sands of the ancestral Rio Grande exposed at eastern base of ridge. These beds form the oldest part of the Sierra Ladrones Formation fluvial facies and intertongue westward with piedmont-slope alluvium. Pale-red, ledge-forming outcrops of fanglomerate are piedmont facies of Sierra Ladrones Formation shed from the eastern Magdalena Range. This Plio-Pleistocene basin-fill unit is the youngest formation of the Santa Fe Group in the Socorro-Albuquerque Basin area (Machette, 1978). 0.3

7.9 Milepost 136. Stockpiles of manganese concentrates on left. Spur at 3:00 of lower Pliocene olivine basalt; flat-topped basalt overlies Sierra Ladrones Formation and is distinctly offset by range-bounding fault zone. 0.4

8.3 Piedmont fault scarp at apex of Pleistocene alluvial fan at mouth of Socorro Canyon. Recurrent movement on this range-bounding fault offsets the late Pleistocene terrace (foreground) about 10 ft, middle Pleistocene gravels (9:00) about 100 ft, and the Pliocene basalt flow (3:00) by at least 200 ft. 0.4

8.7 Foundations of old Great Lakes Carbon perlite mill on Pleistocene arroyo terrace to the right. Waste dumps of perlite fines (white) at 3:00. 1.1

9.8 Milepost 134; bend in road. At 1:30, hummocky landslide blocks of basalt are derived from Black Mountain (mesa on skyline). Unusually large exposure of red Popotosa claystones in north wall of Socorro Canyon at 2:00. Incompetent Popotosa claystones underlie all of the landslide terrane below Black Mountain; this is the same basalt flow that rests on the ancestral Rio Grande deposits at the mountain front. See pp. 49-51 for description of Popotosa clay mineralogy. 1.2

11.0 Crossing east boundary fault of Chupadera Range. Roadcut in deposits of rhyolitic tuff faulted against underlying porphyritic andesite lavas, all part of the Luis Lopez Formation (Oligocene). The formation is the collective name for the heterogeneous moat fill of the Socorro cauldron. The white rhyolitic tuff has been zeolitically altered (clinoptilolite). 0.4

11.4 Roadcut on left of variegated red and green gypsiferous mudstone and clay and interbedded thin basaltic flow or sill(?). 0.4

11.8 Milepost 132. Crossing fault contact between Popotosa Formation on east and volcanic moat deposits (Luis Lopez Formation) on west. **0.1**

11.9 Bridge over Box Canyon; milepost 131. Entering large roadcut in Luis Lopez Formation dikes and tuffs, which are overlain by red debris- flow deposits and fanglomerates of lower Popotosa Formation (Fig. 12). 0.4

12.3 STOP 1.2. Caution! High speed traffic traveling downhill. Clay pit on left (Fig. 13). Turn left into pit and park. Variegated red, green, and gray beds are in upper Popotosa Formation. The contact between the upper and lower members of the Popotosa Formation is concealed in the valley to the east. Talmage and Wootton (1937) reported that experimental bricks, made from red clays scattered around the Socorro Mountains (Popotosa claystones), are hard and chocolate brown. Roadcuts along US-60 provide some of the best exposures of these red gypsiferous claystones, which are otherwise exposed mostly in deep gullies recently cut into the landslide terranes. Samples from the US-60 clay pit have been identified as a diverse mixture of dominantly illite and mixed-layer illite smectite, with minor chlorite and sodium smectite (see pp. 46-54). This diversity probably reflects the detrital origin of these clays derived from a large watershed draining the southeast margin of the Colorado Plateau and the Magdalena-Bear Mountains uplift (Fig. 9).

Return to US 60, turn right. 0.1

12.4 Turn right onto dirt road. Road is on lower member of Popotosa Formation. 0.2

12.6 Cattleguard. Andesitic lava forming ridge on left. 0.2

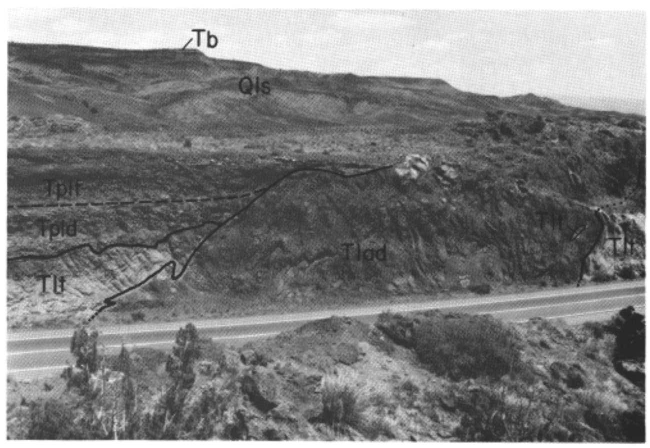

FIGURE 12—Roadcut at mile 11.9 along US–60. Cut exposes sheeted andesite porphyry dike **(Tlad)** intruding poorly welded, lithic-rich ash-flow tuff **(Tlt)**, both of which are unconformably buried by debris flows **(Tpld)** and fanglomerates **(Tplf)** of the lower Popotosa Formation. Dike and tuff are moat-fill units of the Socorro cauldron, collectively assigned to the Luis Lopez Formation. Mesa on left is capped by 4-m.y.-old basalt flow **(Tb)**, which rests on playa claystones of the upper Popotosa Formation. Note that hummocky landslide blocks and basaltic colluvium **(Qls)** effectively conceal underlying "slippery" claystones.

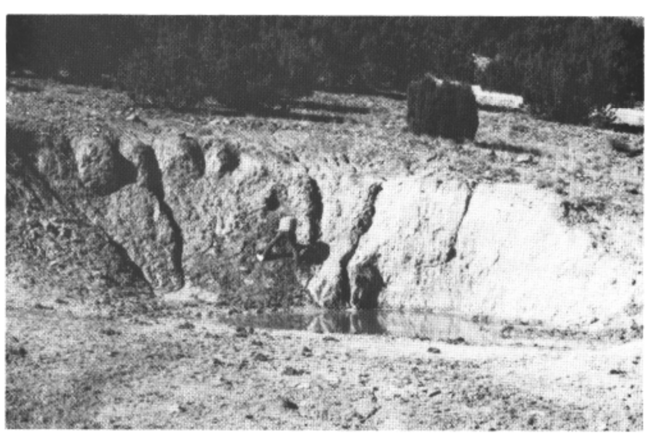

FIGURE 13—Clay pit in Popotosa Formation near US–60 at Stop 1–2.

12.8 Discontinuous playa beds of Popotosa in roadcuts on right. 0.1

12.9 Road junction. Turn left into arroyo leading into Box Canyon to the north. 0.1

13.0 Optional stop at arroyo. Park on northeast side of arroyo and walk down arroyo to Bear (Box) Canyon to examine the breached margin of a volcanic vent in the Luis Lopez Formation, exposed in west (left) wall of canyon (Fig. 14). White beds below cliff are tuffs, mudflows, and sandstone; purple andesitic cinders form wall of vent.

Return to vehicles. Ascend hill. 0.8

13.8 Pit on left exposes minor manganese mineralization. 0.1

13.9 Pit on left. 0.1

14.0 Road junction. Take right fork uphill. South Canyon Tuff forms top of hill at 9:00. Most hills from 11:00-12:00 in middle skyline are "sea" of intracaldera Hells Mesa Tuff on resurgent dome of Socorro cauldron. 0.3

14.3 Rhyolite intrusion forms south wall of canyon at 10:00-11:00. Notch of Black Canyon at 9:00 formed by thick andesite lava flow strongly tilted to east. The Gloryana mine is on top of the hill at 3:00. 0.1

14.4 STOP 1-3. Turn around and park. Dumps of Gloryana mine are visible on top of the hill to the west. Mineralization at the Gloryana is in the South Canyon Tuff. Below, to the east, are pits and dumps of the Grand Canyon mine where manganese mineralization is in basaltic andesite lavas. To the south, cuts of the Tower mine are in the Lemitar Tuff. "Rats hair" psilomelane [(Ba,K,Mn,Pb,Co)Mn,0,,,•H,0], a felty manganese mineral, occurs along fractures and can occasionally be found by breaking open large boulders. Other manganese minerals include pyrolusite (MnO_2), cryptomelane (KMn$_8$0,), hollandite (BaMn$_8$0,,), among other manganese oxides. Black and white calcite and rhodochrosite are also found. For more information see pp. 68-73.

The Gloryana mine lies on the eastern edge of the 28.8 m.y. old Sawmill Canyon cauldron, where the cauldron cuts across the resurgent core of the Socorro cauldron (Fig. 9). Jasperoidal silica veinlets and younger (crosscutting) manganese-calcite veinlets in the Gloryana pit are hosted by the 27.4-m.y.-old South Canyon Tuff. Conformable to unconformable relationships below the South Canyon Tuff locally define the older Sawmill Canyon caldera margin. In the Luis Lopez mining district, jasperoidal silica is commonly associated with Oligocene caldera structures and early rift faults of late Oligocene to early Miocene age. In comparison, manganese and manganiferous calcite mineralization is commonly associated with late-stage rift structures and locally cuts late Miocene rhyolite lavas. These relationships suggest that the crosscutting veinlets in the Gloryana pit represent two long-lived hydrothermal systems—the older one active from about 32 to 20 m.y. ago and the younger one active from about 12 to 7 m.y. ago.

"Rats hair" psilomelane may be found in pockets along manganese veinlets that are *not* associated with calcite. Good luck! 9.0

23.4 Retrace route back to Socorro.

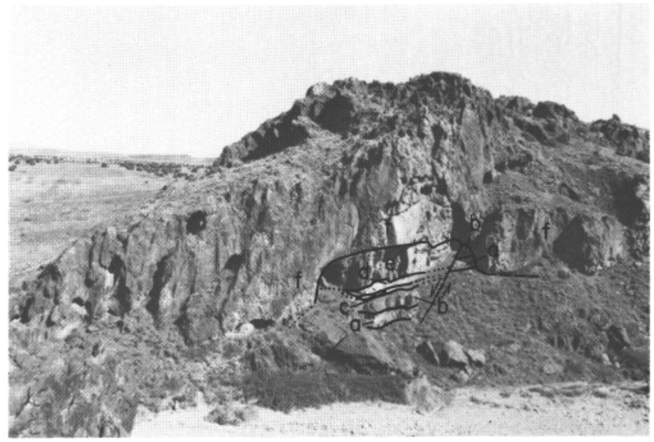

FIGURE 14—Northeast wall of Bear (Box) Canyon cut in moat-fill deposits of the Luis Lopez Formation. Margin of volcanic vent is defined by: **a**, lithic-rich, pumiceous, ash-flow tuff with thin sandy partings; **b**, massive mudflow breccia; **c**, rhyolitic sandstone; **d**, pumiceous tuff; and **e**, crudely bedded andesitic cinders and rounded bombs (vent agglomerate). Andesite lava **(f)** forms steep intrusive contacts and flattens out across top of agglomerate unit. Units "c–d–e" fill down-faulted block buried by the lava flow.

Trip 2a:
Socorro Canyon area and Sedillo Hill

Roadlog from Socorro to Sedillo Hill and to Escondida

by Richard M. Chamberlin, Virginia T. McLemore, Mark R. Bowie, and John W. Hawley

New Mexico Bureau of Mines and Mineral Resources, Socorro, NM 87801

Tuesday, 20 October 1987

Assembly point: Macey Center, New Mexico Tech campus
Departure time: 8:00 a.m.
Distance: 26.2 mi
Stops: 1

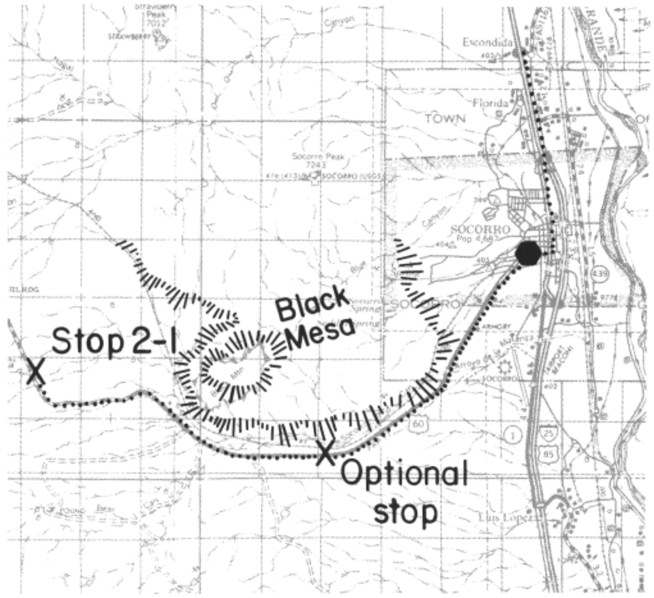

Summary

The first part of this field trip will be to ascend Sedillo Hill into the La Jencia Basin, west of Socorro for an overview of the regional geology. We will examine a red argillic soil profile developed on alluvial-fan deposits of the Sierra Ladrones Formation. The soils are developed in a stable zone on the axis of the tilted Socorro—La Jencia block. The trip offers an excellent view of the Socorro transverse shear zone and morphology of the Rio Grande rift. An optional stop can be made to examine the Socorro Canyon fault, which offsets arroyo terrace gravels of middle and late Pleistocene age. The roadlog ends at Escondida, north of Socorro; Trip 2b begins there.

Total Mileage

0.0 Junction of US-60 and Spring St. Continue straight on US 60. 0.4

0.4 Railroad crossing, Grefco spur of the AT&SF. Ascend hill onto remnant of mid-Pleistocene fan surface. Stockpiles of manganese concentrates on the right. 0.4

0.8 Socorro High School on left. 0.4

1.2 Socorro General Hospital on left. 0.9

2.1 Entrance on right to Grefco perlite operation.

Commercial perlite is hydrated volcanic glass, usually of rhyolitic composition, which can be expanded when heated, producing a lightweight, nearly inert product. Perlite is used as a lightweight aggregate in construction products (wallboard) and as filter aids. New Mexico is the leading producer of perlite in the U.S. The Grefco perlite deposit was the principle domestic source of perlite during the infant years of the industry (Weber and Austin, 1982). The Socorro perlite deposit is the youngest of a series of siliceous lava domes (the Socorro Peak Rhyolite) guided to the surface by the deep plumbing of the Morenci lineament (transverse shear zone) and north-trending faults of the rift. This high-silica (78% SiO_2) rhyolite dome is about 7.4 m.y. old, as determined by K—Ar dating on a whole-rock sample (Osburn and Chapin, 1983a). **0.1**

2.2 Bridge across concrete ditch that diverts water from Socorro Canyon southward into Arroyo de la Matanza; milepost 136. Light-colored sands of the ancestral Rio Grande exposed at eastern base of ridge. These beds form the oldest part of the Sierra Ladrones Formation fluvial facies and intertongue westward with piedmont-slope alluvium. Pale-red, ledge-forming outcrops of fanglomerate are piedmont facies of Sierra Ladrones Formation shed from the eastern Magdalena Range. This Plio-Pleistocene basin-fill unit is the youngest formation of the Santa Fe Group in the Socorro-Albuquerque Basin area (Machette, 1978, 1982). 0.3

2.5 Milepost 136. Stockpiles of manganese concentrates on left. Spur at 3:00 of lower Pliocene olivine basalt; flat-topped basalt overlies Sierra Ladrones Formation and is distinctly offset by range-bounding fault zone. 0.4

2.9 Optional stop. Piedmont fault scarp at apex of Pleistocene alluvial fan at mouth of Socorro Canyon. Recurrent movement on this range-bounding fault offsets the Pleistocene terrace (foreground) about 10 ft, middle Pleistocene gravels (9:00) about 100 ft, and the Pliocene basalt flow (3:00) by at least 200 ft. 0.4

3.3 Foundations of old Great Lakes Carbon perlite mill on Pleistocene arroyo terrace to the right. Waste dumps of perlite fines (white) at 3:00. 1.1

4.4 Milepost 134; bend in road. At 1:30, hummocky landslide blocks of basalt are derived from Black Mountain (mesa on skyline). Unusually large exposure of red Popotosa claystones in north wall of Socorro Canyon at 2:00. Incompetent Popotosa claystones underlie all of the landslide terrane below Black Mountain; this is the same basalt flow that rests on the ancestral Rio Grande deposits at the mountain front. See pp. 49-51 for description of Popotosa clay mineralogy. 1.2

5.6 Crossing east boundary fault of Chupadera Range. Roadcut in deposits of rhyolitic tuff faulted against underlying porphyritic andesite lavas, all part of the Luis Lopez Formation (Oligocene). The formation is the collective name for the heterogeneous moat fill of the Socorro cauldron. The white rhyolitic tuff has been zeolitically altered (clinoptilolite). 0.4

6.0 Roadcut on left of variegated red and green gypsiferous mudstone and clay and interbedded basalt flow or sill(?). 0.4

6.4 Milepost 132. Crossing fault contact between Popotosa Formation on east and volcanic moat deposits (Luis Lopez Formation) on west. 0.1

6.5 Bridge over Box Canyon; milepost 131. Entering large roadcut in Luis Lopez Formation dikes and tuffs, which are overlain by red debris-flow deposits and fanglomerates of lower Popotosa Formation (Fig. 12). 0.4

6.9 Clay pit on left. See Trip 1, Stop 1-2 and Fig. 13 (p. 20) for description. Roadcuts ahead in Popotosa Formation. 1.0

7.9 Ascending Sedillo Hill. Sierra Ladrones fan gravels capping Popotosa playa fades on right. Basalt-capped hills in right foreground. Magdalena Mountains form skyline ahead. 1.9

9.8 STOP 2-1. Top of Sedillo Hill. Park in rest area to the right.

This site is at the south end of La Jencia Basin on a high-level remnant of the piedmont plain that extends from the base of the Magdalena Mountains. To the northwest of this point, the plain is cut by late Quaternary piedmont fault scarps (Machette, 1986).

Figure 15 shows the location of major points of interest and is keyed to the following outline of features west of the Rio Grande:

1) The peak of the Ladron Mountains on the northern skyline, elevation 9,176 ft, is on Precambrian rocks with Upper Paleozoic rocks forming the western slopes of the uplift. Use this peak as 12:00 for orientation in locating the features seen from this stop.

2) Red Mountain at 12:15 is a hogback on the west slope of Lemitar range. Basal debris flows of the Popotosa Formation rest on upper Oligocene volcanic rocks and dip about 30° westward into La Jencia Basin.

3) Polvadera Mountain (peak formed by 32-m.y.-old Hells Mesa Tuff) at 12:30-12:45 is the high point of the Lemitar Range. Field relationships suggest that the Lemitar uplift was forming throughout Popotosa deposition (Miocene time), but major topographic expression of the uplift occurred after 7 m.y. ago.

4) Just to the right of the Lemitar Mountains at

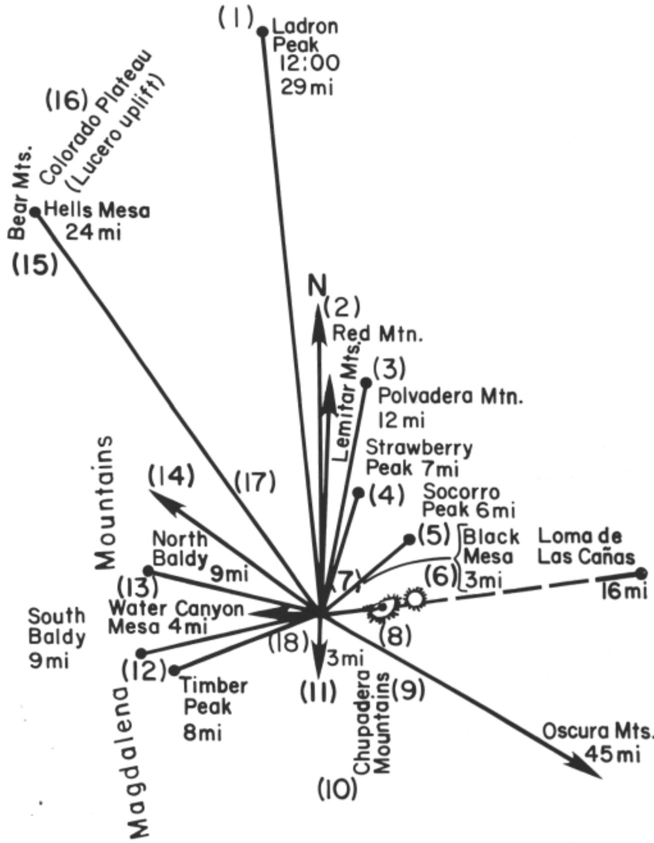

FIGURE 15—Panoramic view from Stop 2-1, La Jencia Basin at top of Sedillo Hill. Numbered sites are described to the left.

12:45 is Strawberry Peak, an 11.8-m.y.-old rhyodacite dome and remnant flow. The vent is on the southeast side of the peak.

5) At 2:00 rhyolite to rhyodacite flows and domes lead up to Socorro Peak and bury the northern Socorro cauldron margin.

6) Flat-topped rhyodacite lava flow, just left of 3:00, occurs at the same elevation as Black Mesa, which led to earlier interpretations that it was a dome truncated by a Pliocene erosion surface. Vertical columnar joints perpendicular to flat cooling surface and an equivalent flat-topped flow overlapped by 11-m.y.-old rhyolite (on Socorro Peak) refute the earlier interpretations.

7) Note west dips in 4-m.y.-old basalt of Sedillo Hill at 1:30 in foreground. This flow remnant is north of the transverse shear zone and is being rotated westward with the Socorro Peak block.

8) Basalt on Black Mesa, immediately right of 3:00 and lying on the shear zone, is nearly horizontal.

9) Resurgent dome of Socorro cauldron at the north end of the Chupadera Mountains at 4:00-5:00.

10) Basalt of similar age and position to the Sedillo Hill unit caps high mesas at 5:30 on west flank of Chupadera Mountains.

11) From 6:00-8:30 a field of east-tilted blocks of upper Miocene rhyolite lavas equivalent to those on Socorro Peak forms the eastern foothills of the Magdalena Range.

12) Timber Peak—South Baldy—South Canyon area of the Magdalena Mountains at 8:30-9:00 is west of Socorro cauldron margin and forms the north margin of the Sawmill Canyon cauldron.

13) North Baldy area of Magdalena Mountains and northwest margin of Socorro cauldron is at 9:30-10:00 on the skyline beyond the mouth of Water Canyon. The light-colored rocks just south of North Baldy are hydrothermally altered Hells Mesa Tuff abutting against the topographic wall of the cauldron. Mudflow deposits of andesitic debris are interbedded in the Hells Mesa Tuff at this locality.

14) Precambrian rocks are exposed along the northeastern front of the Magdalena Range from 10:00-10:30.

15) Bear Mountains at 10:45-11:00 form the northwest border of La Jencia Basin. Hells Mesa overlooking the Rio Salado valley forms the prominent peak at the north end of the Bear Range.

16) High mesas (including Sierra Lucero) of the southeastern Colorado Plateau margin are on the distant skyline at 11:00-11:30, northwest of Ladron Peak.

17) A COCORP (Consortium for Continental Reflection Profiling) seismic profile from east of Magdalena to Sedillo Hill closely parallels US-60 in the basin northwest of this stop. The profile indicates a structurally complex sub-fill basin floor.

18) A shallow dike-like magma body appears to underlie this tour stop at a depth of about 3 mi (Sanford, 1978, 1983).

Looking east of the Rio Grande through the gap between Socorro Peak and Black Mesa, Abo Pass is at 2:30 on the far skyline between the Manzano Range (north) and Los Pinos Mountains (south). South of Black Mesa, Chupadera Mesa is on the distant skyline at 3:30. Slopes east of these uplifts (Sacramento section of the Basin and Range physiographic province) are transitional to the Great Plains province—Pecos Valley section. The lower chain of mesas, cuestas, and hills from 2:30-4:00 (just east of the river valley) composes the Loma de las Callas uplift (Trip 2b). These highlands form the eastern border zone of the rift. They are composed mostly of complexly faulted Pennsylvanian and Permian rocks, capped by San Andres and Yeso Formations. The Mesozoic—lower Tertiary section and at least 2,000 ft of Oligocene volcanic rocks have been stripped by erosion associated with uplift of the blocks. Thick sections of Mesozoic and lower Tertiary sedimentary rocks are preserved only in downfaulted blocks in the Carthage area (4:00) and on the eastern flank of the Joyita Hills (2:30). The east side of the Rio Grande rift is structurally higher than the west side through most of its length.

High ranges visible to the southeast beyond the northern end of Jornada del Muerto Basin include Sierra Oscura at 3:45-4:15 beyond Cerro Colorado and the northern San Andres Mountains at approximately 5:00. If you had been standing here at 5:29 a.m. on July 16, 1945, you would have seen the blinding flash of light and the mushroom cloud from the first atomic bomb detonated at Trinity site at the base of the Oscura Mountains.

Examine soil developed in Sierra Ladrones fan alluvium (see pp. 55-67).

Return to Socorro by retracing roadlog. An excellent view to the east of Rio Grande valley. 10.2

20.0 Junction of Spring St. and US-60. Turn right onto Spring St. 0.6

20.6 Turn right at traffic light onto California St. **0.8**

21.4 Enter 1-25 ramp. (Trip 3 roadlog south to San Antonio begins here.) Stay in left lane and get on 1-25 north. Continue straight on 1-25 on low fan-terrace surface bordering the Rio Grande floodplain. 3.2

24.6 North exit 150 to Socorro. Continue north on 1-25 across Rio Grande floodplain. Socorro Peak is at 9:00; Strawberry Peak is at 10:00; Polvadera Peak (highest point in Lemitar Mountains) is at 11:00; Ladron Mountains are at 12:00; Loma de las Callas are at 3:00 across Rio Grande. The geology of Socorro Peak is discussed in Trip 1 (pp. 15-21).

Tertiary volcanic strata in the Lemitar Mountains generally dip 45-70° to the west. This strong westerly rotation of Tertiary and underlying Paleozoic strata (paraconformable) are the most obvious indication of 100-200% domino-style extension since 29 m.y. ago (Chamberlin, 1983).

The east side of the Lemitar Mountains (Polvadera Peak) consists of Precambrian granites, schists, pegmatites, diabase dikes, and Ordovician carbonatite dikes (McLemore, 1987). Near the south end of the Lemitar Mountains, 80 ft of Mississippian and 1,000 ft of Pennsylvanian rocks overlie the Precambrian. Shale from the Pennsylvanian Sandia Formation (600 ft thick) was mined in the late 1800's for brick manufacture at the Socorro Fire Clay Works. Just below Polvadera Peak, about 400 ft of gray Pennsylvanian limestones (Madera Formation) and 150 ft of Sandia Formation unconformably overlie reddish-orange Precambrian granite. A Late Mississippian to Early Pennsylvanian thrust fault caused this change in stratigraphic relationships (Chamberlin, 1983, fig. 1). A typical 4,000-ft-thick outflow volcanic section (Fig. 10) unconformably overlies the Pennsylvanian rocks. Near the north and south ends of the Lemitar uplift, strongly tilted fan and playa deposits of the Popotosa Formation are exposed. West of the ridge, topped by Polvadera Peak, Precambrian, Pennsylvanian, and Tertiary volcanic rocks are repeated by a major low-angle normal fault (rotated early rift fault) to form a dual hogback range. Permian beds predominate in the Loma de las Callas (east of the river) accompanied by some Precambrian and Pennsylvanian strata in small fault slices (see Trip 2b). 1.4

26.0 Bridge over Nogal Arroyo and Socorro diversion channel. Bluffs across the river are reddish Sierra Ladrones beds capped with valley-fill alluvium and eolian sand. Excellent view to the west of the large landslide area on the north side of Socorro Peak. Hills ahead are alluvial fill. 0.2

26.2 Take exit 152 at Escondida turnoff. End of Trip 2a. Trip 2b roadlog begins here with mileage 0.0.

Trip 2b:
Loma de las Callas area

Roadlog from Escondida to Pueblito, Loma de las Callas, and junction of county road A-129 and US-380 near Carthage (including a stop at Arroyo del Tajo interpretive site)

by John W. Hawley, Virginia T. McLemore, and Mark R. Bowie
New Mexico Bureau of Mines and Mineral Resources, Socorro, NM 87801

Tuesday, 20 October 1987

Distance: 36.4 mi
Stops: 2

Summary

Loma de las Callas separates the Socorro Basin of the Rio Grande valley from the Jornada del Muerto Basin. We travel from 1-25 at Escondida (which means hidden in Spanish) and cross the Rio Grande at Pueblito to view interfingering relationships of piedmont deposits shed from the east side of the valley with axial river sands of the ancestral Rio Grande. At STOP 2-2 we will examine the Sierra Ladrones gravels and pedogenic calcrete (petrocalcic horizon). At STOP 2-3 (lunch stop) we will examine the Arroyo del Tajo interpretive site, where pictographs, presumably from the Piro Pueblo Indians, can be seen on the canyon walls. The entire route passes through excellent exposures of the red, orange, pale-yellow, and gray beds of the Abo, Yeso, Glorieta, and San Andres Formations, spectacular views reminiscent of scenes on the Colorado Plateau. The route ends in the Jornada del Muerto; Trip 2c begins there.

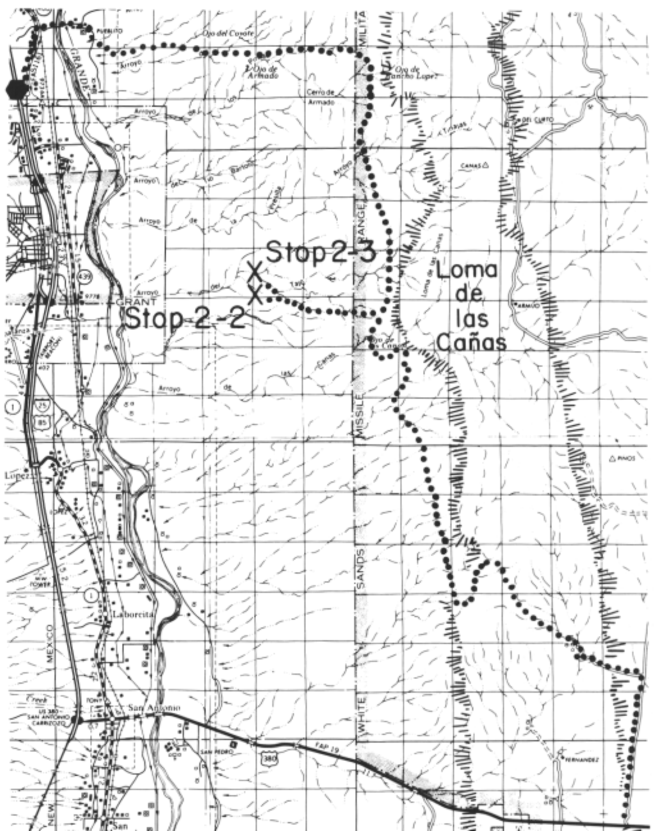

Total
Mileage

0.0 Stop sign at intersection of 1-25 exit 152 and NM-408. Turn right on NM-408 and continue east into village of Escondida. 0.2

0.2 Turn sharp left (north). Route skirts western edge of Rio Grande floodplain. Holocene fan alluvium of small tributary arroyos overlaps and intertongues with axial-river deposits in this area. 0.2

0.4 Bluffs and hillslopes to left veneered with valley-fill alluvium and colluvium of late Quaternary age. These gravelly deposits form a discontinuous cover on a stepped sequence of valley-border erosion surfaces cut on Santa Fe Group—Sierra Ladrones Formation basin fill. The Sierra Ladrones is of Plio-Pleistocene age and comprises two major facies: 1) piedmont alluvium, predominantly derived from bedrock and older basin fill exposed in flanking mountain uplifts; and 2) a basin-floor fluvial facies, here primarily deposits of the ancestral Rio Grande. The river-channel and floodplain deposits, mainly sand and rounded pebble gravel with local silt-clay beds, intertongue with gravelly alluvial-fan deposits of distal piedmont facies. The middle to upper Quaternary valley fill in this area also exhibits complex intertonguing of tributary (arroyo) alluvium and axial-river deposits. Note irrigation canal and farmland on right. Primary crops grown in the Socorro area are corn and alfalfa; other crops include permanent pasture, chili, melons, onions, blue corn, and a limited amount of grapes, wheat, barley, and soybeans. 0.4

0.8 Sierra Ladrones fluvial sands and gravels with ripup clasts of fine-grained sediments exposed in cuts to left. 0.7

1.5 Pueblito Point. Turn right, cross irrigation canal and AT&SF tracks, and continue east across Rio Grande floodplain. Recent test drilling at San Acacia (10 mi to north) and water-well logs in this area (Clark and Summers, 1971) indicate that upper Quaternary fill of the inner river valley ranges from about 70 to 110 ft thick. Below a thin surface layer of clay and silt, the valley-fill section is mainly sand with clay-silt and pebble-gravel lenses. Pebble-to-cobble gravel is common in lower part of the section. These river-channel deposits are unconformable on upper Santa Fe basin fill in most places. 0.2

1.7 County park at Escondida Lake to left; cross main river conveyance channel. Two lane bridge ahead. 0.1

1.8 Crossing Rio Grande. 0.2

2.0 End of pavement. Note prominent, stepped sequence of valley-border geomorphic surfaces rising east of the Rio Grande floodplain. The lowest surface, about 30 ft above the valley floor and of late Holocene age, is formed by coalescent arroyo-mouth fans. Throughout the Rio Grande valley during much of Holocene time, fans of tributary arroyo systems prograded over marginal floodplain areas. When the laterally shifting river channel impinges on these deposits, truncation of distal-fan segments produces low scarps such as the one crossed by the tour route ahead. 0.25

2.25 Top of hill. Pueblito ahead; roadcuts in Holocene alluvial-fan deposits capped with recent car bodies. Pueblito is a very old community that formerly consisted of many houses, small farms, and vineyards. The route of the nation's first transcontinental highway (ocean-to-ocean highway) was established through Pueblito in 1911 and crossed the Rio Grande near the present bridge (Henderson, 1956; McKee and Wilson, 1975; Smith et al., 1983). Abandoned barite mill at 11:00 on top of hill. 0.05

2.3 Turn right (south) on Bosquecito Road along eastern edge of Rio Grande floodplain. 0.3

2.6 Bluffs to left capped with upper Pleistocene gravelly alluvium and Holocene eolian sand that mantle stepped sequence of valley-border surfaces cut on fluvial facies of Sierra Ladrones Formation. The surface just east of the road, about 90 ft above floodplain, is underlain by intertonguing axial-river deposits and older tributary-fan gravels. Archeological sites occur on top of many of these hills. 0.7

3.3 Road junction. Turn left through cattleguard and continue east up valley of Arroyo del Coyote on graded **BLM** Quebrados Road. Route for next 1.8 mi is on Holocene arroyo-terrace and channel deposits, which form younger valley fill. Fluvial and alluvial-fan facies of older valley fill and the Sierra Ladrones Formation are exposed in roadcuts and valley walls ahead. 0.6

3.9 Older valley-fill deposits exposed in high arroyo cuts to right appear to be graded to an ancestral river base level about 90 ft above modern floodplain. 0.3

4.2 Roadcut to left in older valley-fill alluvium. 0.5

4.7 Approximate eastern limit of ancestral Rio Grande (fluvial) facies in Sierra Ladrones Formation. 0.25

4.95 Roadcut and valley-wall exposures of reddish-brown conglomeratic sandstones and mudstones of Sierra Ladrones piedmont facies ahead on left and right. 0.35

5.3 Crossing Arroyo del Coyote. Sierra Ladrones piedmont facies exposed in valley walls to left. 0.2

5.5 Cattleguard. Route ascends ridge. Roadcut in piedmont facies of Sierra Ladrones Formation. 0.7

6.2 Top of hill at road junction. Keep left on main road. Cerrillos del Coyote at 12:00 capped by San Andres Limestone and Glorieta Sandstone with lower slopes cut in Yeso Formation (Fig. 16). Ridge on skyline at 1:00 is an uplifted fault block that exposes upper arkosic limestone member of Madera Formation. Roadcuts ahead in uppermost Sierra Ladrones piedmont facies. 0.1

6.3 High ridge on skyline at 2:30-3:30 consists of gently folded lower gray limestone member of Madera Formation; the lower slopes and westerly exposures are Sandia Formation. Beds on eastern shoulder of ridge are overturned to west and are upper arkosic limestone member of Madera Formation. 0.1

6.4 Trail to right leads to Bursum "Spring" (Ojo de Amado), a favorite swimming hole and picnic area in wet years. It is not a spring but a plunge pool beneath an overhanging cliff formed by steeply east-dipping, overturned limestone beds of Pennsylvanian age. 0.1

6.5 Road junction. Keep left on main road. Road

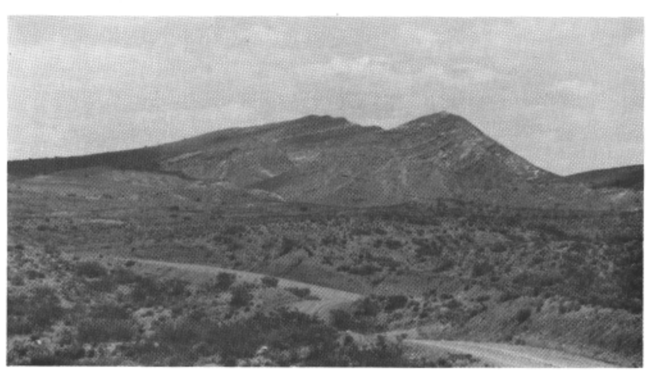

FIGURE 16—Cerrillos del Coyote near mile 6.2.

to right leads to Minas del Chupadero copper prospects, a stratabound, sedimentary copper deposit consisting of malachite, azurite, chalcanthite, and chalcocite in interbedded carbonaceous shales and limestones of upper arkosic limestone member of Madera Formation (Jaworski, 1973). 0.6

7.1 Contact of Santa Fe (Sierra Ladrones) fanglomerate with Abo Formation in valley wall to left. Continue up hill. 0.1

7.2 Top of hill. Cuts ahead in Abo Formation mudstone and sandstone; clay mineralogy is described on pp. 50, 52. Peaks of Cerrillos del Coyote (11:00-1:00) capped with San Andres Limestone and Glorieta Sandstone. 0.2

7.4 Road to left and right. Route for next 0.6 mi in Abo Formation. 0.6

8.0 Side road on right. Roadcuts to east of junction are in gypsiferous Torres Member of Yeso Formation; road has crossed a major north-trending fault. 0.05

8.05 Crossing Yeso-Abo contact ahead. Complex faulting in this area has formed slivers of several stratigraphic units. Pennsylvanian limestones of upper arkosic member of the Madera Formation at 1:00-2:00. A major north-northeast-trending fault juxtaposes Pennsylvanian rocks on east against Abo red beds on west. 0.35

8.4 The broad slope at 9:30 is broken by four thin, cliff-forming units of the Yeso, Glorieta, and San Andres Formations, which are not in proper stratigraphic order, thus indicating possible imbricate structure on a low-angle fault. 0.1

8.5 Cross arroyo and major north-northeast-trending fault at mile 8.05. 0.1

8.6 Small gullies to right over next mile are eroded along minor north-trending faults with a few tens of feet displacement. The road is entirely in Pennsylvanian shale of upper arkosic member of Madera Limestone. 0.4

9.0 Ridge to left is upper arkosic member of Madera Limestone, but is lower in section than shale on which road is built. Another north-trending fault cuts through saddle ahead and passes east of steep, west-dipping limestone beds behind you at 6:00. 0.2

9.2 Cross saddle and fault. Lowest massive limestone cliff on right is Council Spring Limestone of Thompson (1942), equivalent to part of arkosic limestone member of the Madera Formation (Wilpolt and Wanek, 1951). The Council Spring Limestone hosts sedimentary-hydrothermal galena-fluorite-barite deposits in the Hansonburg (Bingham) mining district approximately 30 mi to the east (Trip 3). 0.05

9.25 Massive west-dipping limestone at 12:00 is narrow west-tilted fault block of uppermost part of arkosic limestone member of Madera Formation with reddish, arkosic conglomerates of Bursum Formation to east and lower part of arkosic limestone member in valley to west. On skyline is north end of Loma de las Catias. Note low-angle faulting with San Andres Limestone resting on tilted Glorieta Sandstone and units of the Yeso Formation. 0.35

9.6 Cross arroyo. Outcrops to right across arroyo are arkosic conglomerates of Bursum Formation. The fault, which bounds the east side of the tilted block discussed at mile 9.2, crosses road in this vicinity. 0.05

9.65 Cattleguard. 0.05

9.7 Road junction. **Keep right** on main road. 0.1

9.8 Blocky outcrops at 2:00 are slivers of Bursum Formation along fault that splits and outlines tilted Madera block at mile 9.2. Road is on Bursum Formation for next 0.5 mi, then crosses contact with Abo Formation. Beds dip gently to east. 0.5

10.3 Arroyo crossing. Drainage through water gap on right superimposed in fault block in Madera Formation. See article on pp. 46-54 for discussion of clay mineralogy. 0.2

10.5 Road is now on lower Abo Formation. 0.6

11.1 Cross northeast-trending fault with lower Abo beds to west and Bursum arkosic conglomerates to east. Outcrops on hills to east are upper Abo Formation. Cross arroyo. 0.25

11.35 Cross another arroyo. Good exposures of arkosic conglomerates and purple shales of Bursum Formation in arroyo bank. Road is again on Bursum Formation. 0.5

11.85 Contact of Bursum Formation and arkosic member of Madera Formation in gully to right of road. 0.4

12.25 Mesa on eastern skyline capped by limestones in lower part of Torres Member of Yeso Formation. Rounded yellowish-red, cliff-forming sandstone beds are Meseta Blanca Member of Yeso Formation. Road is on Abo Formation and follows a south-trending strike valley, which eroded along beds that are overturned to east and dip steeply to west. As the road progresses south, sandstone and mudstone beds of Abo Formation in right-hand bar ditch gradually steepen and become vertical. 0.6

12.85 Sandstones and mudstones of Abo Formation in right-hand bar ditch now dip vertically. Ridge to left is in Yeso Formation. 0.5

13.35 At 12:30, thin-bedded red and gray sandstones and mudstones of uppermost Abo Formation dip 30°W and are overturned (Fig. 17). Vertical buff-colored sandstone ridges at 12:00 are Meseta Blanca Member of Yeso Formation. 0.3

13.65 Cross north fork of Arroyo del Tajo. 0.1

13.75 Cross northeast-trending fault with lower limestone bed of Torres Member of Yeso Formation faulted against uppermost Abo Formation; Torres on left and Abo on right. 0.1

13.85 Cross arroyo. Water gap to right exposes large overturned (to east) anticline in upper part of arkosic member of Madera Formation. Magdalena Range and South Baldy Peak on skyline to the west. At 1:00, Meseta Blanca Member of Yeso Formation is overlain by first limestone bed of Torres Member. 0.4

FIGURE 17-Small syncline on top of knob (Torres Member of Yeso Formation) near mile 13.35, looking south. Overturned beds of Abo Formation to right of knob.

14.25 Cross south fork of Arroyo del Tajo. 0.2
14.45 Fault in arroyo at 9:00 with gypsum and limestone beds of upper part of Torres Member of Yeso Formation downfaulted against lowermost Torres units. 0.3
14.75 Tightly contoured beds of lowermost limestone in Torres Member at 3:00. Beds forming battlement on skyline are overturned to east and dip sharply west. 0.2
14.95 Lowermost limestone beds of Torres Member of Yeso Formation at 1:00 are overturned (almost recumbent) and dip gently west. 0.1
15.05 Cross arroyo. Ascend steep grade across west-dipping Yeso strata capped with carbonate-cemented piedmont gravel of upper Sierra Ladrones Formation. 0.15
15.2 Road junction. Turn sharp right. Continue west on high piedmont surface described at STOP 2-2 (mile 15.65). 0.2
15.4 Cattleguard. Socorro Peak at 2:00; Chupadera Mountains lower ridge at 10:00 to 12:00; skyline formed by Magdalena Mountains. 0.2
15.6 Gate on right to STOP 2-3 (entry 17.5). Continue ahead to STOP 2-2. 0.05
15.65 STOP 22. Turn around and park at road junction. After an introduction to the geologic and geomorphic setting, walk down road on left to roadcut exposure of Sierra Ladrones gravels and pedogenic calcrete (petrocalcic horizons; see pp. 55-67).

Panoramic view (west at 12:00), Socorro cauldron (Trip 1), and geomorphic surfaces-Chupadera Mountains are at 11:30-12:30; marked break at 12:15 with flat-topped mesa in background is Nogal Canyon. South end of San Mateo Range (Vicks Peak) on skyline behind and south of Nogal Canyon. Socorro and Socorro Peak are at 2:30. Topographic margin of north side of Socorro cauldron exposed on Socorro Peak below the "M" (Trip 1); topographic margin of south side of Socorro cauldron marked by highest point at south end of Chupadera Mountains (11:00). The distended Socorro cauldron has a north-south diameter of about 12 mi and an extended east-west dimension of 18-20 mi. A resurgent dome in Socorro cauldron makes up the northern part of Chupadera Mountains at about 1:00. Low areas between resurgent dome and north and south topographic margins compose the moat of Socorro cauldron and are underlain by a complex series of rhyolitic domes, flows, local ash-flow tuffs, and various types of breccias and volcaniclastic rocks, collectively known as Luis Lopez Formation. High point of Magdalena Range on skyline from 12:30-2:00 is within both the Socorro cauldron and a younger, nested, Sawmill Canyon cauldron.

The stop is on a high-level piedmont surface capped with gravelly alluvium and now deeply incised by the valley of Arroyo de las Canas; note surficial zone of pedogenic calcrete. The basal contact of the alluvial deposits on deformed beds of the San Andres and Yeso Formations can be seen in upper valley walls to the south and east. The gravel cap locally includes fan and channel-fill deposits up to 100 ft thick, as well as thin alluvial veneers on extensive rock pediments. This surface appears to be one of the oldest and highest members of stepped sequence of surfaces graded to the ancestral Rio Grande.

Reconnaissance geomorphic investigations in this area by NMBMMR staff document the presence of at least three major valley-border surfaces between this level and the Holocene fills of larger arroyo valleys. These geomorphic surfaces of both erosional and constructional origin have been tentatively correlated with the Tio Bartolo, Valle de Parida, and Canada Mariana stepped sequence of Kirk Bryan (1932) and Charles Denny (1941). Elevations of projected surface profiles above the present floodplain approximate the ancestral river base levels suggested by Denny (1941) and Sanford et al. (1972): Tio Bartolo-200-225 ft, Valle de Parida-100-180 ft, and Canada Mariana-40-90 ft. The high-level piedmont surface at this stop, informally designated "Las Carias surface" by W. Stone and L. Fleischhauer, appears to grade to a river-base level more than 300 ft above the modern valley floor. However, this surface has been offset (down-to-west) by a rift-boundary fault located about 1.5 mi to the west. Projected base-level estimates of older members of the valley-border sequence may be considerably in error due to faulting and tectonic warping. The gravelly alluvium with pedogenic calcrete that caps the "Las Carias" surface is included in the youngest piedmont facies of Sierra Ladrones Formation and is probably of early to middle Pleistocene age (>0.5 m.y.).

Return to vehicles and retrace route to STOP 2.3. 0.05

15.7 Turn left through gate and continue northwest across "Las Carias" surface. 0.7
16.4 At 1:00 orange-brown hills of Precambrian Tajo granite are overlain by dark beds of Sandia Formation (Fig. 18). Route descends from "Las Carias" surface to lower valley-border erosion-surface complex (possible fault offset). **0.8**
17.2 Steep downgrade. Crossing major boundary fault zone of Rio Grande rift. Hillslopes to west are cut of upper Santa Fe Group basin fill (Sierra Ladrones Formation). Veneers of gravelly alluvium and colluvium cap mid-to-late Qua-

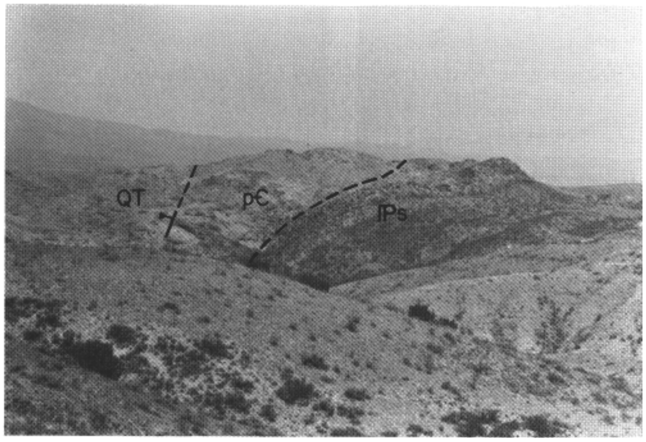

FIGURE 18—Precambrian Tajo granite overlain unconformably by dark beds of Sandia Formation, looking north. **p€,** Precambrian granite; **IPs,** Sandia Formation; **QT,** Santa Fe Group.

ternary valley-border erosion surfaces. 0.3

17.5 STOP 2-3 at windmill—lunch. Discussion of panoramic view and examination of Arroyo del Tajo interpretive site.

Follow the trail downhill and across the arroyo for about 0.2 mi to the Arroyo del Tajo interpretive site, which consists of a group of pictographs—pictures painted on rock by Native Americans, probably the Piro Pueblo Indians.

Panoramic view: Socorro Peak ("M" Mountain) to west (12:00); Magdalena Mountains on southwestern skyline. To the east at 5:00 are orange-brown hills of the Precambrian Tajo granite (Fig. 19). During the late 1970's, the granite and adjacent rock was explored for uranium (McLemore, 1983). Uranium mineralization with fluorite occurs along fractures. Barite and fluorite veins are common along the western fault contact with the Santa Fe Group; some barite and fluorite were mined.

Fire clay was produced from several stratigraphic horizons in the Sandia Formation (Pennsylvanian) at the Houlett deposit (2.5 mi to the north) for brick manufacture at the Socorro Fire Clay Works during the late 1800's (Talmage and Wootton, 1937). Three carloads of clay were shipped to the International Brick Co. in El Paso, Texas, in 1910 and three carloads were shipped to the Denver Fire Clay Co. in Denver, Colorado, between 1910 and 1920 (J. Van Sandt, written comm. 1964). The clay mineralogy of this site is described on pp. 50, 52-53.

Arroyo del Tajo interpretive site (Fig. 20) was discovered by Robert Weber, NMBMMR, and has been examined by the National Park Service for possible preservation. The National Park Service concluded that any high technological preservation methods would accelerate deterioration. Please use caution in examining this site and do not touch the paintings because they are extremely fragile. Despite administration by the U.S. Bureau of Land Management as an Area of Critical Environmental Concern (ACEC) and a special management area, some vandalism of the site has occurred.

Although interpretation of this site is controversial, it is almost certainly of Piro origin. The Piro Pueblo

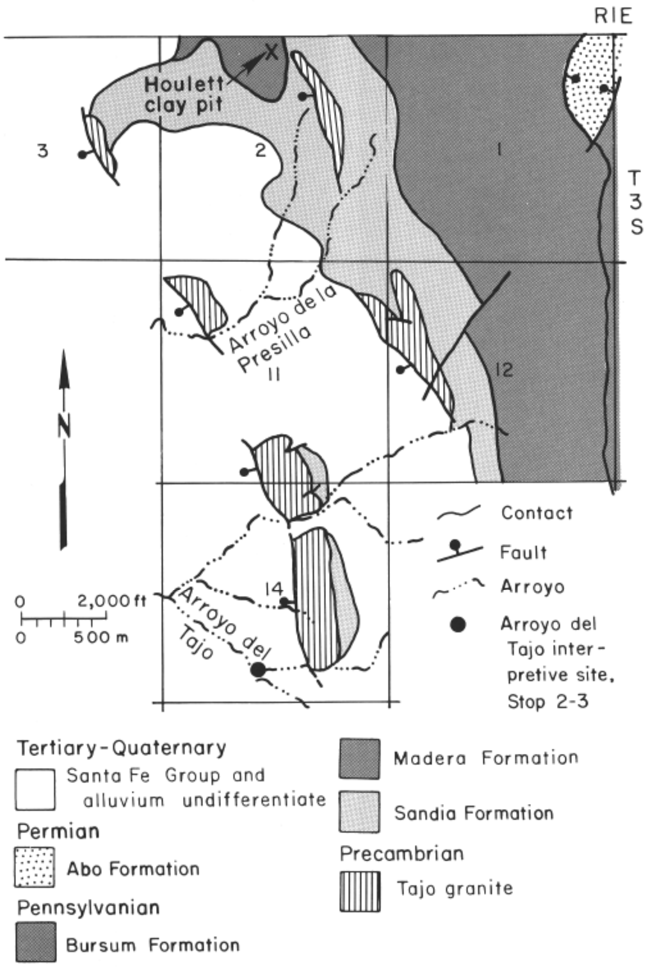

FIGURE 19—Geologic map of Tajo area (*simplified from Osburn, 1984; McLemore, 1983; Bauch, 1982; and Wilpolt and Wanek, 1951*).

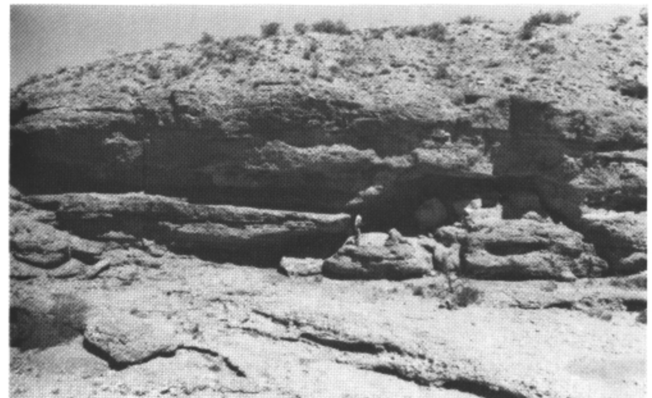

FIGURE 20—Arroyo del Tajo interpretive site, looking north.

Indians were an agriculture-based people and had 12-44 settlements along the Rio Grande during the late 1500's. The closest known pueblos to this site are near Luis Lopez and in Socorro, both on the west side of the Rio Grande (Cordell and Earls, 1983). The population of the Piro Indians declined during the 1640's and 1650's due to an influx of European diseases, including smallpox, and to raids and massacres by Apache Indians. Many Piros also died of starvation and famine resulting from severe draughts during the 1660's. The Piros did not participate in the Pueblo Revolt of 1680; most left for the south with the Spaniards.

The pictographs (Fig. 21) are on the north side of Arroyo del Tajo in a natural amphitheater with excellent acoustics that may have been used as a teaching area. Interpretations of the paintings suggest that they are of post-Spanish contact (A.D. 1540-1680), as evidenced by pictures of a goat and horse.

Early Piro history is depicted in these scenes according to various interpretations. Some figures are painted white, symbolizing light-skinned Indians, whereas others are red, symbolizing dark-skinned Indians. There was a war between the two peoples as shown by swords and other instruments of warfare. Legend suggests the dark-skinned Indians, ancestors of modern Indians, overcame the light-skinned Indians. Other figures represent medicine men and gods. A painted face encircled with dots may represent the God of Nature.

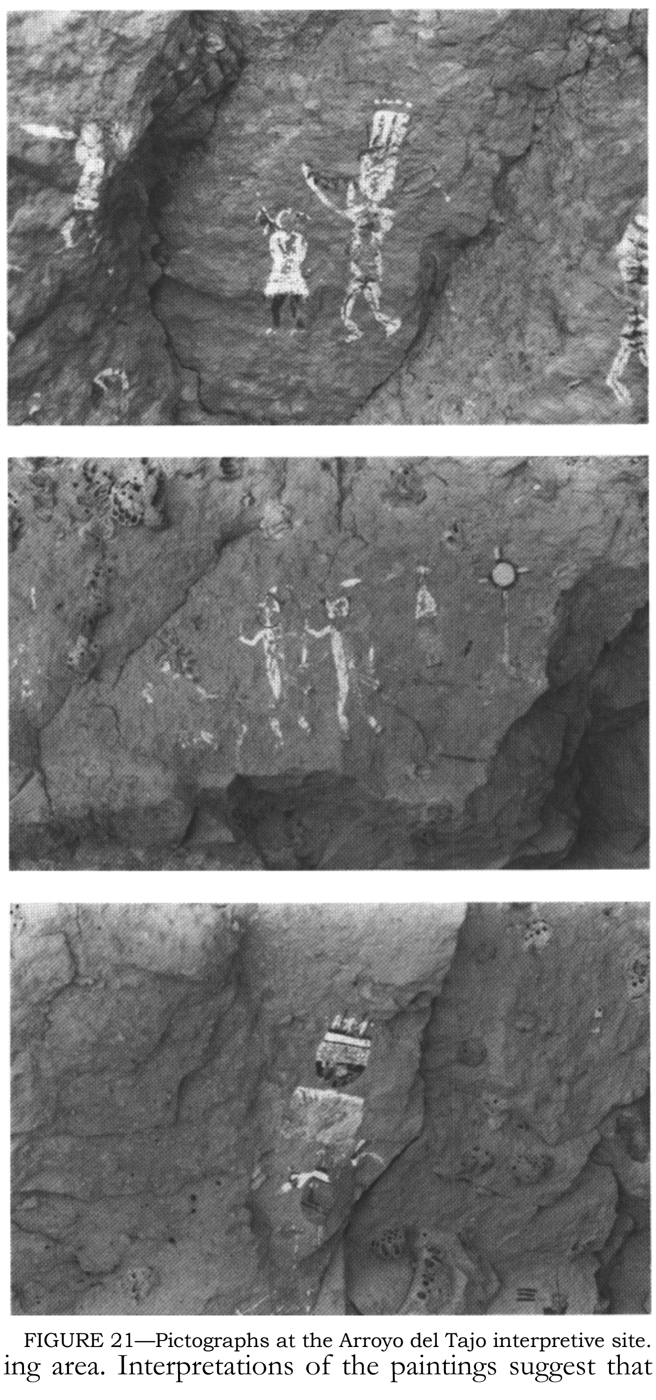

FIGURE 21—Pictographs at the Arroyo del Tajo interpretive site.

Retrace roadlog to gate and Quebrados Road junction at mile 15.2. 1.8

19.3 Gate. **Turn left.** 0.2

19.5 Cattleguard. 0.2

19.7 Junction of Quebrados Road. **Turn right.** Route continues east across "Las Catias" surface remnant, then drops abruptly into upper valley (cationcito) of Arroyo de las Carias. 0.25

19.95 Road bends right and begins descent into Ojo de las Carias, a spring high in carbonate and sulfate, which feeds Arroyo de las Catias in the reach visible on the right. Narrow zone of strong deformation noted at mile 14.75 continues beneath Sierra Ladrones Formation on which we are driving and crosses Arroyo de las Catias below the recent sand dunes and piedmont gravels visible on south side of arroyo. Note well-developed pedogenic calcrete (Bkm horizon) in upper part of piedmont gravel deposit, which is about 50 ft thick here. The base of the Sierra Ladrones Formation is a nonpedogenic conglomeratic calcrete. 0.1

20.05 **Caution: steep grade.** On skyline, the Glorieta—San Andres contact is visible at 12:00 at color break; dark brownish-gray limestone is above and buff to gray-white sandstone is below. Pinkish sandstone and mudstone exposed here and there beneath buff sand is the Joyita Member of Yeso Formation and is partially interbedded with it. 0.05

20.1 Roadcut in basal Sierra Ladrones Formation conglomerate that is angularly unconformable on Yeso Formation. 0.05

20.15 Roadcuts on left after bend in road expose Torres Member of Yeso Formation. See pp. 50, 52 for description of clay mineralogy. Note laminated gypsum beds in Torres Member. 0.2

20.35 Cross Arroyo de las Caftas. As road ascends south bank note successive limestone units in Torres Member. These beds cannot be used as markers because they are lithologically very similar and contain little or no fossils. Gravelly alluvium caps terraces above inner arroyo valley at 12:00-3:00. 0.75

21.1 Cattleguard. Route ahead ascends east-dipping Yeso section to another remnant of the "Las Callas" surface. 0.3

21.4 Cuts in veneer of Sierra Ladrones gravel, with pedogenic calcrete, at edge of "Las Canas" surface remnant. Note extensive cover of Holocene eolian sand. Route for next 5 mi crosses dissected piedmont erosion surface (rock pediment) cut across deformed beds of upper Paleozoic section. 0.25

21.65 Limestone beds with interbedded gypsum, siltstone, and mudstone of Torres Member of Yeso Formation on either side of road. 0.5

22.15 Road turns to follow strike of Yeso beds. 0.55

22.7 Cross arroyo. 0.15

22.85 Slow: steep grade ahead. Driving on small gravel-capped remnant of "Las Carias" surface with well-developed pedogenic calcrete. Road continues to follow strike of Yeso beds. Note local gypsum outcrops. 0.3

23.15 Cross arroyo. East-dipping limestones of Torres Member of Yeso Formation on right. 0.2

23.35 Red sandstones and mudstones from 9:00-12:00 are a fault block of Abo Formation. Contorted beds of Torres Member of Yeso Formation at 3:00-4:00 dip steeply west. 0.3

23.65 Entering San Antonio 71/2 min quadrangle. 0.4

24.05 Good exposure of limestones in Torres Member of Yeso in canyon to right. 0.3

24.35 Another remnant of "Las Carias" surface with gravelly pedogenic calcrete and sample site is described on p. 63, Table 6. Good exposures of Cafias and Joyita Members of Yeso Formation overlain by Glorieta Sandstone and San Andres Limestone on north end of mesa at 9:30-11:30. 0.1

24.45 Westward dip slope of San Andres Mountains in distance at 11:00, Little San Pasquel Mountain at 11:30, eastward dip slope of Fra Cristobal Mountains at 12:00. 0.3

24.75 Slow. Downgrade. 0.3

25.05 Cross arroyo. A spectacular buckle-type fold is exposed downstream along the arroyo walls (Smith et al., 1983, stop 5). 0.05

25.1 Cattleguard. 0.6

25.7 Road crosses northwest-trending fault that juxtaposes lower Abo Formation on southwest against middle part of Torres Member of Yeso Formation on northeast. 0.5

26.2 Road on right. Hills of tilted Madera limestones on right. 0.8

27.0 Cattleguard. Route ahead curves to east through water gap (north fork of San Pedro Arroyo) and across southern part of Loma de las Carias uplift. Road on Abo Formation with exposures of channel sandstone to either side. 0.15

27.15 Cross arroyo. Stratigraphic section from 11:00-12:00 is Joyita Member of Yeso Formation at base of slope, overlain by Glorieta Sandstone (light colored in lower half, reddish near top), which, in turn, is overlain by San Andres Limestone on upper slopes (Fig. 22). 0.2

27.35 Outcrops along arroyo to left contain gradational contact of Abo Formation and Meseta Blanca Member of Yeso Formation in zone of green mudstone and siltstone. Contact crosses road near this point. 0.4

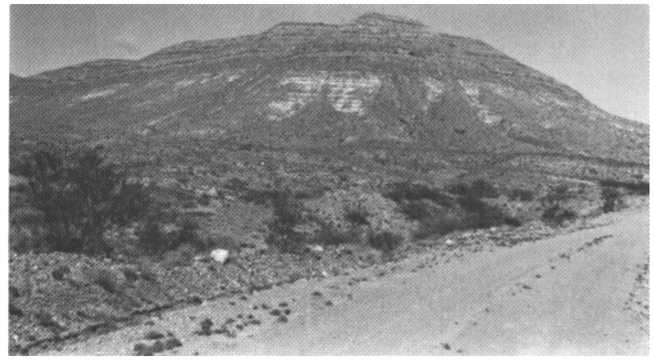

FIGURE 22-Southern part of Loma de las Carias at mile 27.15.

27.75 Entering Canon Agua Bueno 772 min quadrangle. Fault block of Abo at 10:00. 0.2

27.95 Cross arroyo. Abo Formation in arroyo bottoms. 0.1

28.05 Cross fault described at mile 25.7. Abo Formation is to southwest, Torres Member of Yeso Formation to northeast. 0.05

28.1 Arroyo crossing. Entering zone of complex structure including low-angle faulting in slope from 2:00-2:30. 0.5

28.6 Red beds on steep slope to right are Torres Member of Yeso Formation. Massive outcrop near crest is San Andres Limestone. A low-angle fault separates these units. 0.3

28.9 Entering flat-floored valley. Rocks from 7:30-10:30 are Glorieta Sandstone and San Andres Limestone in upper plate above low-angle fault (some imbricate faulting in upper plate). Valley floor is underlain by red mudstones and sandstones of the Chinle Formation (Triassic) and a small amount of overlying buff to white Dakota Sandstone (Upper Cretaceous) at 1:00. The Cretaceous rocks are downfaulted against Yeso Formation to south along same northwest-trending fault as miles 25.7 and 28.05. Low-angle faults are also present from 3:00-4:30 beneath San Andres Limestone. (This shallow valley in Triassic and Cretaceous rocks surrounded by topographically higher Permian rocks suggests that the Permian might be thrust again over younger units with the thrust somewhat modified by later faulting.) 0.6

29.5 Road bends to left. Good exposures of Chinle Formation red beds in roadcuts and gullies. 0.2

29.7 Road tops divide between north fork and Agua Bueno forks of San Pedro Arroyo. Jornada del Muerto and distant Oscura Mountains at 12:00-1:00. Note thin cap of gravelly alluvium on high pediment surfaces flanking hills to north and south. 0.5

30.2 Unusual buff to yellow-gray sandstone interbedded in Chinle Formation on left. Paleoweathering zone? 1.1

31.3 Cattleguard. Road continues on Chinle Formation. 0.3

31.6 Road junction. Gonzales well and old ranch house 0.3 mi via left fork. Possible weathering profile on Chinle Formation in roadcut at 6:30. Continue southeast on main road across upper valley of Canon Agua Bueno arroyo. Ridges ahead and to left capped with mid-Pleistocene alluvial fill of Jornada del Muerto Basin. 0.2

31.8 Cross arroyo. Route ahead on thin upper Quaternary valley-fill deposits. 0.1

31.9 Cross arroyo. Approaching Jornada del Muerto closed basin. 0.4

32.3 Route ascends to Jornada del Muerto Basin surface. Thick gravelly fill is fan-piedmont facies of Sierra Ladrones Formation (here mostly middle Pleistocene) with discontinuous veneer of upper Quaternary alluvium and eolian deposits. 0.1

32.4 Broad plains of northern Jornada del Muerto Basin from 10:00 to 2:00 (elevation 5,400-4,700 ft) are about 500 ft above the floor of the Rio Grande valley.

The Jornada del Muerto extends southward from Chupadera Mesa to Las Cruces and the Desert Project area (Gile et al., 1981). It was named "journey of the deadman" because hundreds of people perished enroute from Chihuahua to Santa Fe due to lack of water and attacks by Apache Indians (Pearce, 1965). Oscura Mountains are on the skyline at 12:30-1:30, Mockingbird Gap is at 3:00, northern San Andres Mountains and Salinas Peak are at 2:00-2:30. The regional dip shifts from eastward in the Oscura Mountains to westward in the San Andres Mountains across Mockingbird Gap. The Bliss Sandstone and the rest of the lower Paleozoic section present in southern New Mexico pinch out at the south end of the Oscura Mountains. Layered rocks overlying Precambrian rocks on the crest of the Oscura block are Pennsylvanian—Permian limestones, mostly Missourian, Desmoinesian, and Virgilian in age. Scars near the lower north end of the Oscura block are mines in the Hansonburg barite-fluorite-galena district. 0.4

32.8 Road junction. Continue straight ahead. Cross divide ahead between Rio Grande drainage (Arroyo Agua Buena) and internal drainage of Jornada Basin.

Jornada surface drainage is southward to a large playa that was formerly inundated by pluvial Lake Trinity (Neal et al., 1983). Groundwater discharge from northern Jornada area is westward to Rio Grande valley (Weir, 1965). Hogbacks of Oligocene volcanic strata at 10:00 may be underlain by a low-angle listric fault. The beds dip 40-50°W in the eastern hogback, generally steeper than underlying Paleozoic and Mesozoic rocks. The western hogbacks dip much more gently than the eastern ones and, locally, dip either east or west. Localized areas of steeply dipping beds such as these suggest listric faulting. 0.3

33.1 Road junction. Turn right (south) on graded road (county road A-129). Route descends gentle piedmont slope graded to Jornada del Muerto Basin floor. Conical hills at 12:00 are Oligocene volcanic rocks (mainly andesitic lavas of Spears Formation) at north end of White Sands Missile Range. White buildings at 11:00 are Stallion Site Range Station, the security and tracking headquarters for the north end of the missile range. 3.2

36.3 Cattleguard. 0.1

36.4 Cattleguard and junction with US-380. Turn right. End of Trip 2b. Trip 2c begins here at mileage 0.0

Trip 2c:
Carthage area

Roadlog from junction of county road A-129 and US-380 west to Carthage and San Antonio

by John W. Hawley, Virginia T. McLemore, and Mark R. Bowie

New Mexico Bureau of Mines and Mineral Resources, Socorro, NM 87801

Tuesday, 20 October 1987

Distance: 24.1 mi
Stops: 2

Summary

This trip takes us from the Jornada del Muerto (end of Trip 2b) west along US-380 through the structurally complex Carthage coal field. At STOP 2-4 we will examine a roadcut exposing the Triassic Chinle Formation—Dakota Sandstone (Cretaceous) contact. An excellent calcic soil profile on top of the Sierra Ladrones Formation can be viewed at STOP 2-5. The unconformity between the Sierra Ladrones Formation and the Gallup Sandstone is beautifully exposed at this stop. The route continues west into San Antonio where it joins Trip 2d.

Total Mileage

0.0 Junction of county road A-129 (dirt) and US-380. 0.3

0.3 Buried archeological site at north edge of highway. Thin surficial deposits of Holocene age unconformably overlie thick calcic horizon of paleosol on Jornada surface. 0.35

0.65 Milepost 11. Cross divide between Jornada and Rio Grande (San Pedro Arroyo) drainage basins. 0.15

0.8 Roadcut in gravels of Baca and Spears Formations dips about 40° east. Baca conglomerates (Eocene) at west end of cut contain Precambrian, Paleozoic, and some Mesozoic clasts that were transported eastward from a Laramide uplift, now mostly downfaulted beneath the Rio Grande rift (Cather, 1983). Several fossil teeth (Titanotheres, etc.) recovered in the Carthage area indicate a Bridgerian provincial age for the lower part of the Baca (Lucas et al., 1982; Lucas, 1983). The Baca—Spears contact, which is placed at the first occurrence of Tertiary volcanic clasts (here mainly plagioclase-rich andesitic rocks), is exposed about midway in the outcrop. Volcanic clasts increase gradationally over 15-30 ft until almost all clasts are volcanic. 0.7

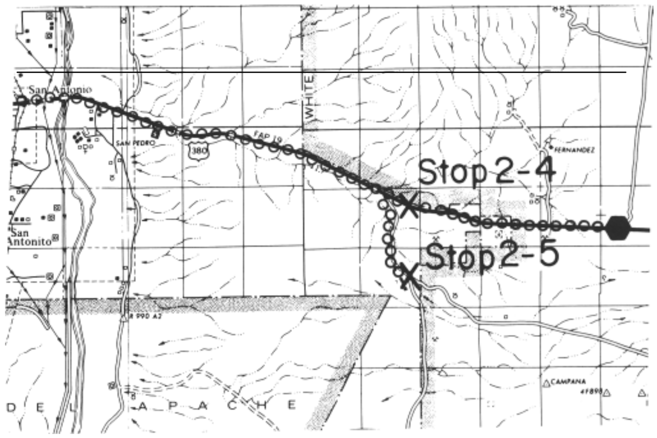

1.5 Junction with county road A-137 on Baca Formation. Crossing covered contact (late Quaternary valley fill) ahead between Baca Formation and underlying Upper Cretaceous rocks. Route for next 4.5 mi is mainly on Cretaceous strata that dip predominantly south and east and are cut by numerous north-trending faults. See map (Fig. 23) for details.

At 9:00 are old dumps and tipples of Hart and Hilton coal mines, the northeasternmost coal producers in the Carthage mining district (Fig. 24; Osburn, 1983). The Hilton mine (marked by reddish dumps behind tipples) closed before 1920. The Hart mine was operated until 1967; in later years it was operated by A. B. Baca of Socorro under the name Carthage mine. Some coal was used by the Santa Fe Railroad and for domestic use in Socorro and San Antonio, but most was shipped to Socorro, El Paso, and Chihuahua as smelter fuel. A. B. Baca supplied coal to the steam plant at New Mexico Tech until 1953 and to Albuquerque Public Schools until 1967.

The mines were developed in a 4-ft-thick coal bed in the lower part of the Crevasse Canyon Formation (Upper Cretaceous). The mine site currently consists of a westward-sloping, timbered decline, a loadout facility, small buildings, mine dumps, and a railroad grade that marks the eastward terminus of the New Mexico Midland Railroad. Westward mine development was halted at a north-trending fault that juxtaposes the Crevasse Canyon Formation and the Carthage Member of the Tres Hermanos Formation. 0.1

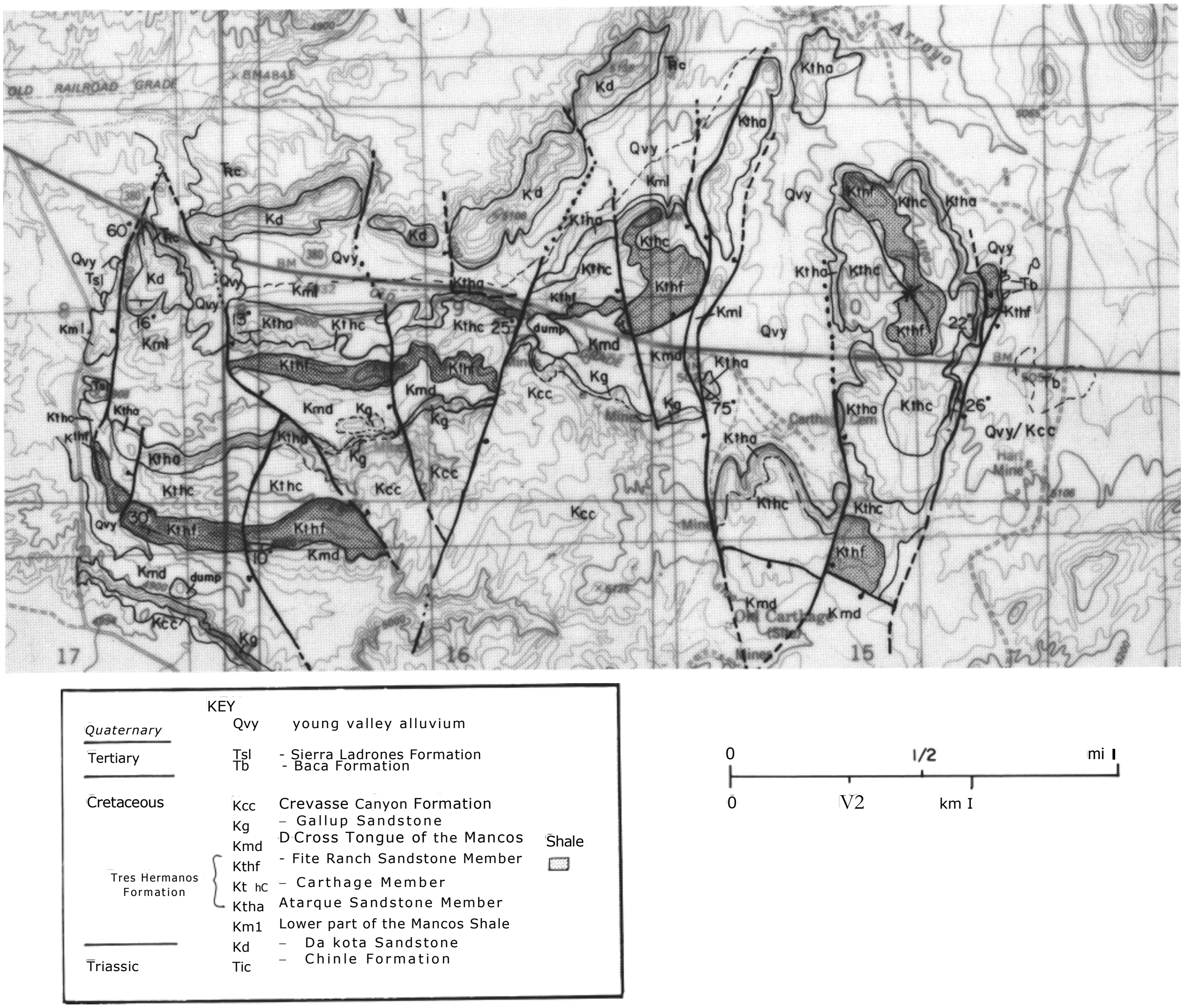

FIGURE 23—Geologic map of the Carthage area *(by Osburn, 1983).*

1.6 Milepost 10. Ridge from 12:30 to 2:00 formed on west-dipping Atarque Sandstone—the basal member of the Tres Hermanos Formation (see Table 2, pp. 13-14, for stratigraphic nomenclature). The Atarque is a regressive, coastal-barrier sandstone that ranges up to 75 ft thick in the Carthage area (Hook et al., 1983). It consists of an alternating sequence of massive, 3-4-ft-thick beds of flat to low-angle cross-bedded sandstones, and 2-3-ft-thick, fine-grained, burrowed and bioturbated sandstones that weather to form minor reentrants. At 3:00 the Atarque is faulted against the Fite Ranch Sandstone Member of the Tres Hermanos Formation to the east and this, in turn, is faulted against the Baca Formation. 0.1

1.7 Dip slope on Atarque Sandstone Member at 3:00; dip flattens immediately westward. Highway crosses the axis of a small syncline where soft, paludal shales and thin splay and overbank sandstones of the Carthage Member overlie the Atarque Sandstone Member. Locally, the Carthage Member is 115 ft thick. At 9:00, immediately south of the highway, a dip reversal takes place in the Atarque. This change in attitude from westward dipping north of the highway to eastward dipping south of the highway reflects influence of the syncline to the north and drag folding to the south. It may also indicate that on the north side of the highway the fault is offset to the east and thus no drag folding is seen in the Atarque Sandstone. South of the highway the fault trends north–south and the Atarque and lower part of the Carthage Member are in fault contact with the Crevasse Canyon Formation; vertical separation is approximately 500 ft. 0.1

1.8 Fite Ranch Sandstone Member of Tres Hermanos Formation along north side of highway. This unit represents transgressive upper part of Tres Hermanos. The type section of Fite Ranch Sandstone Member is 2 mi to southwest in sec. 17, T5S, R2E (Hook et al., 1983), where it is 72 ft thick. Along the highway, it is about 66 ft thick; the basal 40 ft is made up of a lower, grayish-orange, fine-grained sand-

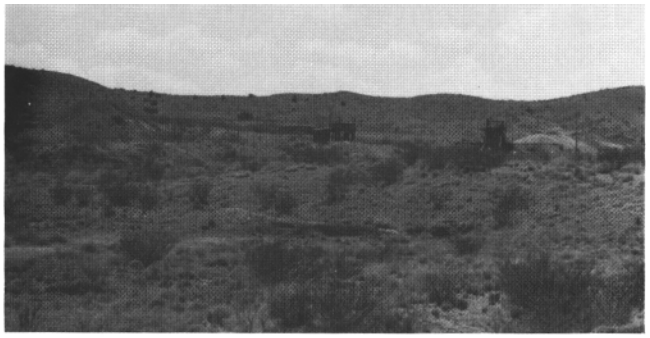

FIGURE 24—Dumps and tipples of Hart and Hilton coal mines, looking south.

stone, mottled, and bioturbated in its lower portion and containing *Lopha bellaplicata* (marine oyster) in middle and upper parts. The upper Fite Ranch Sandstone Member (Hook et al., 1983) is 20 ft of white to grayish-yellow, fine-grained, unfossiliferous sandstone. A 5-ft-thick, moderate yellowish-brown sandstone forms the distinctive top of the Fite Ranch Sandstone Member. This bed has been interpreted as a disconformity based on missing faunal zones and presence of phosphatized internal molds of bivalves, gastropods, and ammonite chambers (Hook et al., 1983). *Lopha bellaplicata* also occur in this bed. 0.2

2.0 Contact between Atarque and Carthage Members on south side of highway. Carbonaceous shales and siltstones form base of Carthage Member here. East-dipping Atarque Formation is present in roadcut immediately to right on west limb of syncline. 0.05

2.05 Highway descends into valley developed on lower part of Mancos Shale. Valley fill is of Holocene and latest Pleistocene age. 0.25

2.3 Railroad bed formerly serving Carthage mine on left. Rails were removed between 1935 and 1940 and shipped to Japan as scrap. Excellent bricks of several colors were made in Socorro from clay from the Cretaceous units in the Carthage area (Talmage and Wootton, 1937). During the 1930's, Mr. B. H. Kinney had a few shipments of clay sent to his New Mexico Clay Products Co. plant in Albuquerque. Some clay was also used in a small roofing-tile plant at San Antonio during the 1930's (Talmage and Wootton, 1937). 0.1

2.4 Road to left leads to Carthage cemetery and townsite. Sandstone ledge capping cliff at 9:00 is Gallup Sandstone (Kg). Coal dump is from Manilla mine where a coal seam about 50 ft above the Gallup was exploited. Wastes were trammed north from the mine and dumped over Gallup cliff. Highway crosses north-trending fault. Light-colored Bridge Creek Limestone beds of the Mancos Shale on east (upthrown) block are in fault contact with D-Cross Tongue of Mancos Shale on west (downthrown) block. The Atarque Sandstone Member, which lies approximately 164 ft stratigraphically above Bridge Creek beds, is present on ridge at 3:00 and caps knob at 9:00. Coal dumps at 10:00-11:00. 0.1

2.5 Brown sandstone flatirons on dip slope at 3:00 are top of Fite Ranch Sandstone Member. 0.25

2.75 An erosion surface developed on D-Cross Tongue of Mancos Shale is seen on both sides of road. At 9:00 note upper half of D-Cross, containing very large calcareous concretions and overlain by Gallup Sandstone. At 3:00 note dip slope on uppermost distinctive brown bed of Fite Ranch Sandstone Member of Tres Hermanos Formation. 0.2

2.95 Highway crosses north-trending fault; abandoned coal mine at 9:00. All three members of Tres Hermanos Formation are exposed in ascending order south of highway along west (upthrown) side of fault, which here cuts out coal-bearing Crevasse Canyon Formation. Archeological sites dating back to Old Carthage (late 1800's) throughout the area. 0.1

3.05 Atarque Sandstone Member caps ridge that parallels highway on south. Old railroad grade along north side of highway is on dissected valley-fill alluvium of Holocene age. At 3:00 note dip slope formed on highly fractured and hematite-stained Dakota Sandstone. Strike valley ahead cut in lower part of Mancos Shale. 0.25

3.3 Bridge Creek Limestone beds of Mancos Shale form a light-colored zone in a low ridge along the south side of the highway. Associated with the limestone beds, which individually range from 1 to 6 inches thick, are numerous thin, white- to orange-weathering bentonites from which selenite crystals commonly weather out. These beds mark a transgressive maximum of the shallow seaway. The *Sciponoceras gracile* (ammonite) zone in lower part of this calcareous interval was previously designated as the Cenomanian—Turonian boundary; this boundary has now been moved up several faunal zones. Also present in lower half of Bridge Creek Limestone beds are the guide fossil *Pychodonte newberryi* (oyster) and ammonites *Metoicoceras geslinianum* and *Euomphaloceras (kanabiceras) septemseriatum*. The uppermost Bridge Creek Limestone contains *Inoceramus mytiloides* (clam) and other fossil debris. Fossil agate wood is found throughout the area. The calcareous interval represented by the Bridge Creek Limestone is about 50 ft thick. 0.15

3.45 Old railroad grade passes through water gap in Dakota Sandstone hogback at 3:00. Bridge Creek Limestone beds parallel highway on south; Atarque Sandstone Member caps ridge beyond. 0.2

3.65 At 9:00 the south-dipping Atarque is cut out by a sinuous, northwest-trending fault. Dip slope of Dakota Sandstone on right forms east-trending hogback. 0.25

FIGURE 25-Roadcut at mile 4.1 (Stop 2-4) exposing contact between Chinle Formation on left and Dakota Sandstone on right (south side of highway).

FIGURE 26-Roadcut at mile 4.1 (Stop 2-4) exposing a high-angle fault between Chinle Formation on right and Santa Fe Group on left (north side of highway).

3.9 Milepost 8. Highway crosses fault between Dakota Sandstone (Cretaceous) on east and Chinle Formation (Triassic) on west. 0.2

4.1 STOP 2.4. Roadcut exposes Chinle-Dakota contact on left (Fig. 25). White, clayey zone at base of Dakota may represent Morrison-like beds (Jurassic) or a weathering zone at top of Triassic. See pp. 50-52 for a synopsis of the clay mineralogy of this outcrop. A major high-angle fault at west end of roadcut on right (Fig. 26) juxtaposes Triassic mudstones (Chinle Formation) against conglomeratic calcrete of upper Santa Fe Group. 0.1

4.2 Cut in sands and clays of Sierra Ladrones Formation. Prepare for sharp left turn ahead. 0.3

4.5 Turn left onto Fite Ranch Road (Socorro County road A-153). Cuts ahead in soft mudstones and sandstones of Sierra Ladrones Formation. These beds are distal piedmont facies and intertongue 1 to 2 mi to west with fluvial (ancestral Rio Grande) facies. 0.3

4.8 At 10:00-11:00 are isolated remnants of Sierra Ladrones conglomerates (Santa Fe Group) resting on lower part of Mancos Shale. On skyline beyond is dip slope of Dakota Sandstone passing under buff to gray Mancos Shale. 0.2

5.0 West-dipping Sierra Ladrones sandstone to left. For more information see Smith et al. (1983, stop 6). 0.25

5.25 Tres Hermanos Sandstone to left capped by prominent ledge of dark-brown sandstone. Many minor faults offset this unit. Note change in strike, which now is southeast, rather than east as seen to the north. 0.2

5.45 Valley to left now cut in upper D-Cross Tongue of Mancos Shale. Ridge on skyline (10:00-11:30) is capped by Gallup Sandstone at base of Mesaverde Group. Ascend winding road to Jornada del Muerto Basin floor. 0.1

5.55 Crossing unconformable contact of Sierra Ladrones piedmont facies on Gallup Sandstone and D-Cross Tongue (Fig. 27). Basal Santa Fe beds are locally well cemented with calcite derived from ground water that previously circulated above basin fill-bedrock contact. Coal dumps to left. 0.3

5.85 STOP 2.5. Examine soil profile on top of Sierra Ladrones Formation and unconformity between Gallup Sandstone and Sierra Ladrones Formation (see pp. 55-67 for more information). After stop, turn around and return to US-380. 1.35

7.2 Turn left on US-380 and continue west down valley of San Pedro Arroyo. Quarries in San Andres Limestone on hillside to far north (Fig. 28). Limestone was used in the smelters in Socorro during the late 1800's. 0.2

7.4 Crossing San Pedro Arroyo. The distal-piedmont facies of Sierra Ladrones Formation is well exposed in valley wall from 9:00-11:00. Bluffs flanking arroyo valley are capped with thin deposits of eolian sand and older valley fill. 1.2

8.6 Bridge. Milepost 6. 0.5

9.1 Gray-brown sand and reddish clay of Sierra Ladrones fluvial facies exposed in arroyo bank to right. The belt of intertonguing distal-piedmont and fluvial facies, first observed along Arroyo de la Parida (Trip 2b), continues south through this area and extends southeastward

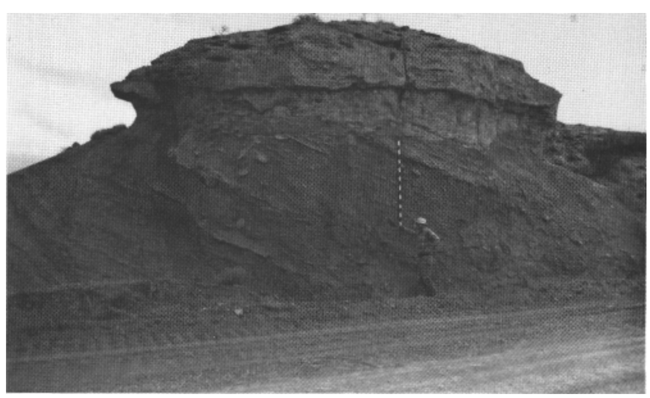

FIGURE 27-Unconformity between Sierra Ladrones Formation (upper beds) and Gallup Sandstone, at mile 5.55 (just before Stop 2-5).

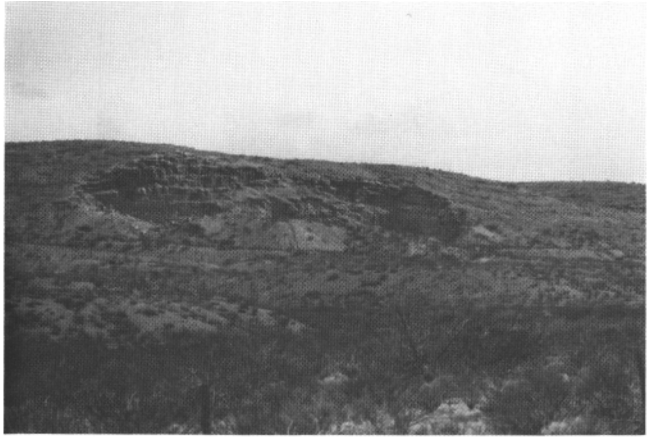

FIGURE 28—Limestone quarries as seen from Fite Ranch Road (looking north at mile 7.2).

FIGURE 29—Thick bed (about 15 ft) of gravelly pumice interbedded with Santa Fe Group fluvial units, looking west about 1 mi northeast of mile 10.9.

across the northern Jornada del Muerto Basin. Route ahead on arroyo terraces capped with middle to upper Quaternary alluvium. 0.8

9.9 Bridge. Conglomeratic sandstone, pebbly sand, and minor clay and mudstone of Sierra Ladrones fluvial facies is well exposed south of San Pedro Arroyo for next 1.1 mi. 0.2

10.1 Sands of Sierra Ladrones fluvial facies with veneer of arroyo-terrace gravel in roadcuts ahead. The thin terrace fill probably correlates with deposits of lowest major valley-border surface of Pleistocene age (Canada Mariana surface of Denny, 1941). 0.8

10.9 Bridge over San Pedro Arroyo. Fluvial sand and clay of Sierra Ladrones Formation exposed in valley wall to left. Route for next 1.4 mi on Holocene arroyo terrace and fan deposits, with low bluffs to right underlain by middle to upper Pleistocene valley fill. A large deposit of volcanic ash and gravelly pumice (mostly pebble to cobble size) approximately 1 mi to northeast is derived from Cerro Toledo Rhyolite and basal Bandelier Tuff of the Jemez Mountains (Fig. 29; Izett et al., 1981). This pumice mass is interbedded with the fluvial facies and was probably emplaced as a unit during a catastrophic Rio Grande flood sometime between 1.4 and 1.1 m.y. ago. Older arroyo-fan and terrace deposits in this area are graded to ancestral river-base levels from 60 to 180 ft above the present valley floor. 0.9

11.8 Bosquecito road to right. Route descends fan of San Pedro Arroyo, which has prograded onto the Rio Grande floodplain during middle to late Holocene time. 0.4

12.2 San Pedro townsite to left on toe of arroyo-mouth fan. Route ahead descends to Rio Grande floodplain. 0.5

12.7 East end of Rio Grande bridge. 0.8

13.5 Cross AT&SF Railroad (Albuquerque—El Paso line) at west edge of floodplain. Route ascends Holocene fan of Nogal Canyon drainage and enters San Antonio. The town is named for a mission founded in 1629 by Fray Antonio de Arteaga and Fray Garcia de Francisco de Zuniga (Pearce, 1965) and is the birthplace of hotel entrepreneur Conrad Hilton. A small roofing plant operated intermittently during the 1930's (Talmage and Wootton, 1937); two or three men operated a small kiln to produce tile from local adobe clay and shale from Carthage. 0.3

13.8 Junction with NM-1 and Owl Bar ahead. South margin of Socorro cauldron in southern Chupadera Mountains is to the west. Pleistocene piedmont and valley-border surfaces, grading eastward from base of Chupaderas to bluffs along Rio Grande, are offset by several faults that trend south—southeast toward this area from the foot of Socorro Peak (Sanford et al., 1972). 0.5

14.3 Junction of US-380 and NM-1. Turn left. End of Trip 2c. Trip 2d begins here at mileage 0.0.

Trip 2d:
Bosque del Apache National Wildlife Refuge

Roadlog from San Antonio to Bosque del Apache National Wildlife Refuge and return to Socorro

by Virginia T. McLemore, Mark R. Bowie, and John W. Hawley
New Mexico Bureau of Mines and Mineral Resources, Socorro, NM 87801

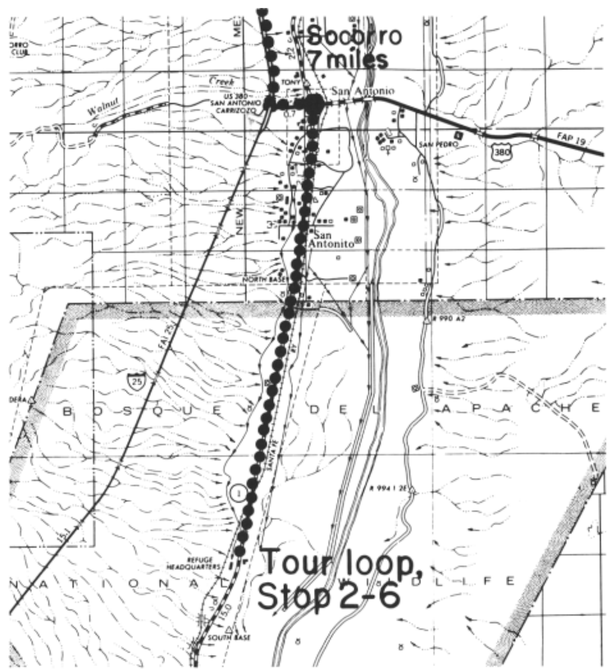

Tuesday, 20 October 1987
Distance: 41.8 mi
Stops: 1 (tour loop)

Summary

Bosque del Apache (woods of the Apache) National Wildlife Refuge was established in 1939 on the Rio Grande as a refuge and breeding ground for water fowl and other wildlife. The 57,191-acre park provides habitat for about 295 different bird species, including the endangered bald eagle, peregrine falcon, and whooping crane, and over 400 different mammals, reptiles, and amphibians. Water is diverted from irrigation channels or pumped from wells to create temporary ponds and marshes during the winter where birds can nest and feed. During the summer months, the ponds are drained and the water is used for agriculture. About 1,400 acres of farmland provide supplemental food for the wildlife.

The Bosque consists of a 15-mi tour loop, open to the public throughout the year from 30 minutes before sunrise to 30 minutes after sunset. Two hiking trails, the Bosque trail (1.75 mi) and the marsh walk (0.75 mi), provide an opportunity to view wildlife more closely. The Bosque also includes 30,287 acres of wilderness for day hikes for the more hardy individual who wants to observe wildlife.

Total
Mileage

0.0 Junction of US-380 and NM-1 in San Antonio. Continue south on NM-1. 0.6

0.6 Foundations on right side of road are all that remain of the Hilton store, boyhood home of hotel entrepreneur Conrad Hilton. Railroad station foundation on left. Route continues on Rio Grande floodplain. 0.95

1.55 Former Mex—Tex barite-fluorite mill on left. These ores were mined from the Hansonburg mining district, Oscura Mountains near Bingham (Trip 3). Low bluffs to right are underlain by terrace and fan gravels of middle to late Pleistocene age that are inset against fluvial sand and gravel of the Sierra Ladrones Formation. 2.7

4.25 Enter Bosque del Apache National Wildlife Refuge. Little San Pascal Mountain at 11:00. 0.6

4.85 Milepost 12. Chupadera Mountains at 1:00. High peak at 1:30 is capped by dark-colored A—L Peak tuff, erupted from cauldrons in the Magdalena area. The underlying light-colored, poorly welded tuffs dip southeast and rest on silicified Mississippian sandstones and limestones, which, in turn, overlie Precambrian granites and schists. The Precambrian rocks form low, rounded foothills at 1:30 to 3:00. The light-colored tuff unit probably accumulated in pre-existing topographic lows because the densely welded A—L Peak tuff rests directly on Paleozoic rocks just to south.

Approximately 1,500-2,000 ft of the Oligocene volcanic section is missing in this area. Possible causes are: 1) erosion along the south margin of the Sawmill Canyon cauldron before eruption of the A—L Peak tuff and/or 2) the existence of a Laramide uplift that was beveled to its Precambrian core by the late Eocene erosion surface but that remained topographically high until middle Oligocene time. Transport directions in arkosic channel sands of the Baca Formation (Eocene) north of Magdalena indicate a source region for Precambrian detritus somewhere to the south-southeast.

Note basalt-capped mesa at 2:30 on crest of Chupadera Mountains in saddle at head of • valley. This unit may be correlative with the 4-m.y.-old basalt of Sedillo Hill seen on Trip 1. 2.35

7.2 AT&SF Railroad crossing. Note dissected fans and pediments extending from Chupadera Mountains. Higher ridges to the southwest . underlain by deformed piedmont and basin-floor facies of the Popotosa Formation (lower' Santa Fe Group). 1.6

8.8 STOP 2-6. Headquarters of the Wildlife Refuge. Turn right and continue to Visitors Center parking area. Following visit to refuge headquarters and museum, continue on tour loop of refuge east of NM-1 (tour loop map available at entrance). After tour, retrace route to San Antonio. 22.8

31.6 San Antonio at junction of NM-1 and US-380. Turn left. 0.4

32.0 Turn right (north) onto access ramp of I-25. 0.4

32.4 Roadcuts and arroyo exposures from here to Socorro show complex intertonguing of piedmont-gravel and fluvial-sand facies. Units make up youngest Santa Fe basin fill (Sierra Ladrones Formation) and middle to upper Pleistocene valley fill. 1.5

33.9 Milepost 141. Magdalena Range on western skyline. Socorro Peak at 11:00 and Ladron Peak on distant skyline behind Lemitar Mountains at 11:30. Basalt of Sedillo Hill (4 m.y.) caps mesa in moat of Socorro cauldron at 10:30. Piedmont fault scarp at 11:00 shows displacement of youngest Santa Fe and older valley-fill units. 1.0

34.9 Milepost 142. Relay tower on left. High hills, mesas, and cuestas on skyline east of Rio Grande (Loma de las Cafias uplift) consist mostly of Permian (San Andres, Glorieta, and Yeso) formations (Trip 2b). Pliocene to lower Pleistocene fluvial and piedmont facies of upper Santa Fe Group crop out in bluffs and benches that form eastern border of river valley. 2.3

37.2 Underpass; Luis Lopez Road. 1.6

38.8 Milepost 146. Socorro airport on left. Crossing Socorro Canyon fan. The surface here is probably of pre-Wisconsin, late Pleistocene age. 1.2

40.0 Bridge over Arroyo de la Matanza. Exposures of upper Santa Fe Group basin fill overlain by fan gravel in arroyo and gravel pit to left. 0.2

40.2 Take exit 147. 0.7

40.9 Enter Socorro. 0.7

41.6 Railroad crossing, Grefco spur of the AT&SF. 0.2

41.8 Intersection of California and Spring Streets, junction of US-60 and US-85 (business 1-25). End of log.

Trip 3:
Carthage, Jornada del Muerto, and Bingham

Roadlog from Socorro to San Antonio, Carthage, and Bingham Post Office

by Virginia T. McLemore, Mark R. Bowie, and John W. Hawley
New Mexico Bureau of Mines and Mineral Resources, Socorro, NM 87801

Tuesday, 20 October 1987 (if it rains)

Distance: 37.5 mi
Stops: 1

Summary

Trip 3 is the reverse log of Trip 2c, starting in Socorro and traveling south on 1-25 to San Antonio. From San Antonio, the route progresses east through the Carthage coal field and into the Jornada del Muerto Basin as far east as Bingham. Geology of the Carthage area is shown in Figure 23 (p. 34).

Total Mileage

0.0 South end of Socorro at ramp to 1-25. Proceed south on 1-25. 0.5

0.5 Bridge over Arroyo de la Matanza. Exposures of upper Santa Fe Group basin fill overlain by fan gravel in arroyo and gravel pit to right. 0.4

0.9 Socorro airport on right. Crossing Socorro Canyon fan. The surface here is probably of pre-Wisconsin, late Pleistocene age. 1.9

2.8 Underpass; Luis Lopez Road. 2.2

5.0 Relay tower on right. High hills, mesas, and cuestas on skyline east of Rio Grande (Loma de las Canas uplift) consist mostly of Permian (San Andres, Glorieta, and Yeso) formations (Trip 2b). Pliocene to lower Pleistocene fluvial and piedmont facies of upper Santa Fe Group crop out in bluffs and benches that form eastern border of river valley.

Roadcuts and arroyo exposures from here to San Antonio show complex intertonguing of piedmont-gravel and fluvial-sand facies. Units make up youngest Santa Fe basin fill (Sierra Ladrones Formation) and middle to upper Pleistocene valley fill. 3.0

8.0 Turn right at San Antonio (exit 139). Continue into San Antonio on US-380. San Antonio is named for a mission founded in 1629 by Fray Antonio de Arteaga and Fray Garcia de Francisco de Zufiiga (Pearce, 1965) and is the birthplace of hotel entrepreneur Conrad Hilton. Route descends on Holocene fan surface graded to Rio Grande valley floor. 0.6

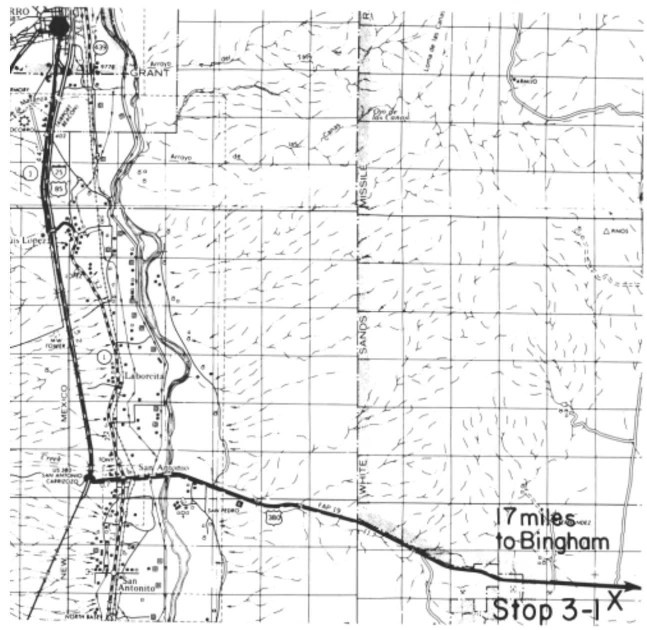

8.6 Junction with NM-1 and Owl Bar ahead. Continue east on US-380. Bosque del Apache National Wildlife Refuge is south on NM-1 (Trip 2d). 0.3

8.9 Cross AT&SF Railroad (Albuquerque-El Paso line) at west edge of Rio Grande floodplain. 0.7

9.6 West end of Rio Grande bridge. 0.6

10.2 San Pedro townsite to right on toe of arroyo-mouth fan. Route ahead ascends fan of San Pedro Arroyo, which has prograded onto the Rio Grande floodplain during middle to late Holocene time. 0.4

10.6 Bosquecito road to left. Ahead on the left, middle to upper Pleistocene fan alluvium is exposed in arroyo walls. Higher ridges to the north are eroded on fluvial sand and gravel of the Sierra Ladrones Formation. A large deposit of volcanic ash and gravelly pumice (mostly pebble to cobble size) approximately 1 mi to northeast is derived from Cerro Toledo Rhyolite and basal Bandelier Tuff of the Jemez Mountains (Fig. 29, Trip 2c, p. 37; Izett et al., 1981). This pumice mass is interbedded with the fluvial facies and was probably emplaced as a unit during a catastrophic Rio Grande flood sometime between 1.4 and 1.1 m.y. ago. Older arroyo-fan and terrace deposits in this area are graded to ancestral river-base levels about 60 to 180 ft above present valley floor. 0.9

11.5 Bridge over San Pedro Arroyo. Fluvial sand and clay of Sierra Ladrones Formation exposed in valley wall to right. Sands of Sierra Ladrones fluvial facies with veneer of arroyo-terrace gravel in roadcuts ahead. Loma de las Catias on skyline at 11:00 (Trip 2b). 1.0

12.5 Culvert. Route ahead on terrace capped with older valley-fill alluvium. 0.4

12.9 Bridge. 0.8

13.7 Gray-brown sand and reddish clay of Sierra Ladrones fluvial facies exposed in arroyo bank to left. The belt of intertonguing distal-piedmont and fluvial facies, first observed along Arroyo de la Parida (Trip 2b), continues south through this area and extends southeastward across the northern Jornada del Muerto Basin. 0.5

14.2 Bridge. Milepost 6. 1.2

15.4 Crossing San Pedro Arroyo. The distal-piedmont facies of Sierra Ladrones Formation is well exposed in valley wall to south (red to yellowish-brown beds) and is capped with thin deposits of eolian sand and older valley-fill alluvium, commonly with multiple buried soils (Trip 2c, Stop 2-5, p. 36). 0.2

15.6 Fite Ranch Road on right (Socorro County road A-153-Trip 2c, Stop 2-5). Continue east on US-380. Quarries in San Andres Limestone at 10:00 (Fig. 28, p. 37). Limestone was used in the smelters in Socorro during the late 1800's. The San Andres Formation caps the high ridge at 9:00. 0.4

16.0 Roadcut exposes Chinle-Dakota contact on right (Trip 2c, Stop 2-4; Figs. 25, 26, p. 36). White, clayey zone at base of Dakota may represent Morrison-like beds (Jurassic) or a weathering zone at top of Triassic. The clay mineralogy of this outcrop is described on pp. 50-52. A major high-angle fault at west end of roadcut on left (Fig. 26, p. 36) juxtaposes Triassic mudstones against conglomeratic calcrete of upper Santa Fe Group. 0.1

16.1 Crossing fault between Dakota Sandstone (Cretaceous) on east and Chinle Formation (Triassic) on west. Dip slope of Dakota Sandstone ahead on left forms east-trending hogback. Route continues up strike valley cut in lower Mancos shale, with thick fill of Holocene and latest Pleistocene age. 0.4

16.5 Old railroad grade passes through water gap in Dakota Sandstone hogback at 9:00. Railroad bed formerly serving Carthage mine on left. Rails were removed between 1935 and 1940 and shipped to Japan as scrap. Atarque Sandstone Member caps ridge on southern skyline. Ridge on left formed on west-dipping Atarque Sandstone-the basal member of Tres Hermanos Formation (see Table 2, pp. 13-14, for stratigraphic nomenclature). The Atarque is a regressive, coastal-barrier sandstone that ranges up to 75 ft thick in the Carthage area (Hook et al., 1983). It consists of an alternating sequence of massive, 3-4-ft-thick beds of flat to low-angle crossbedded sandstones, and 2-3-ft-thick, fine-grained, burrowed and bioturbated sandstones that weather to form minor reentrants. Bridge Creek Limestone beds of the Tres Hermanos Formation (Mancos Shale) form a light-colored zone in a low ridge along the south side of the highway. Associated with the limestone beds, which individually range from 1-6 inches thick, are numerous thin, white- to orange-weathering bentonites from which selenite crystals commonly weather out. These beds mark a transgressive maximum of the shallow seaway. The *Sciponoceras gracile* (ammonite) zone in lower part of this calcareous interval was previously designated as the Cenomanian-Turonian boundary; this boundary has now been moved up several faunal zones. Also present in lower half of Bridge Creek Limestone beds are the guide fossil *Pychodonte newberryi* (oyster) and ammonites *Metoicoceras geslinianum* and *Euomphaloceras (kanabiceras) septemseriatum.* The uppermost Bridge Creek Limestone contains *Inoceramus mytiloides* (clam) and other fossil debris. Fossil agate wood is found throughout the area. The calcareous interval represented by the Bridge Creek Limestone is about 50 ft thick. 0.5

17.0 Coal mine dump on right. Atarque Sandstone Member caps ridge at 11:00; old railroad grade crosses highway. 0.15

17.15 Highway crosses north-trending fault. All three members of Tres Hermanos Formation are exposed in ascending order south of highway along west (upthrown) side of fault, which here cuts out coal-bearing Crevasse Canyon Formation. 0.15

17.3 Milepost 9. Surface developed on D-Cross Tongue of Mancos Shale is seen on both sides of road. At 3:00 note upper half of D-Cross, containing very large calcareous concretions and overlain by Gallup Sandstone. At 9:00 note dip slope on uppermost distinctive brown bed of Fite Ranch Sandstone Member of Tres Hermanos Formation. 0.15

17.45 Highway crosses north-trending fault. Light-colored Bridge Creek Limestone beds of the Mancos Shale on east (upthrown) block are in fault contact with D-Cross Tongue of Mancos Shale on west (downthrown) block. The Atarque Sandstone Member, which lies approximately 164 ft stratigraphically above Bridge Creek beds, is present on ridge at 9:00 and caps knob at 3:00. 0.05

17.5 Road to right leads to Carthage townsite and cemetery. Sandstone ledge capping cliff at 2:00 is Gallup Sandstone (Kg). 0.4

17.9 Roadcut in Atarque Sandstone. East-dipping Atarque is present in roadcut immediately to left on west limb of syncline. 0.05

17.95 Contact between Atarque and Carthage Members on south side of highway. Carbonaceous shales and siltstones form base of Carthage Member here. 0.15

18.1 Fite Ranch Sandstone Member of Tres Hermanos Formation along north side of highway. This unit represents transgressive upper part of Tres Hermanos. The type section of Fite Ranch Member is 2 mi to southwest in sec. 17, T5S, R2E (Hook et al., 1983) where it is 72 ft thick. Along the highway, it is about 66 ft thick; the basal 40 ft is made up of a lower, grayish-orange, fine-grained sandstone, which is mottled and bioturbated in its lower portion and contains *Lopha bellaplicata* (marine oyster) in its middle and upper parts. The upper Fite Ranch Sandstone Member is 20 ft of white to grayish-yellow, fine-grained, unfossiliferous sandstone. A 5-ft-thick, moderate yellowish-brown sandstone forms the distinctive top of Fite Ranch Member. This bed has been interpreted as a disconformity based on missing faunal zones and presence of phosphatized internal molds of bivalves, gastropods, and ammonite chambers (Hook et al., 1983). *Lopha bellaplicata* also occur in this bed. 0.1

18.2 Dip slope on Atarque Sandstone Member at 9:00; dip flattens immediately westward. Highway crosses the axis of a small syncline where soft, paludal shales and thin splay and overbank sandstones of the Carthage Member overlie the Atarque Sandstone Member. Locally, the Carthage Member is 115 ft thick. At 3:00, immediately south of the highway, a dip reversal takes place in the Atarque. This change in attitude from westward dipping north of the highway to eastward dipping south of the highway reflects influence of the syncline to the north and drag folding to the south. It may also indicate that on the north side of highway the fault is offset to the east and thus no drag folding is seen in the Atarque Sandstone. South of the highway the fault trends north-south and the Atarque and the lower part of Carthage Member are in fault contact with the Crevasse Canyon Formation; vertical separation is approximately 500 ft. 0.1

18.3 At 9:00 the Atarque is faulted against Fite Ranch Sandstone Member of the Tres Hermanos Formation to the east and this, in turn, is faulted against the Baca Formation. 0.1

18.4 At 3:00 are old dumps and tipples of Hart and Hilton coal mines, the northeasternmost coal producers in the Carthage mining district (Fig. 24; Osburn, 1983).

The Hilton mine (marked by reddish dumps behind tipples) closed before 1920. The Hart mine was operated until 1967; in later years it was operated by A. B. Baca of Socorro under the name Carthage mine. Some coal was used by the Santa Fe Railroad and for domestic use in Socorro and San Antonio, but most was shipped to Socorro, El Paso, and Chihuahua as smelter fuel. A. B. Baca supplied coal to the steam plant at New Mexico Tech until 1953 and to Albuquerque Public Schools until 1967.

The mines were developed in a 4-ft-thick coal bed in the lower part of the Crevasse Canyon Formation (Upper Cretaceous). The mine site currently consists of a westward sloping, timbered decline, a loadout facility, several small buildings, mine dumps, and a railroad grade that marks the eastward terminus of the New Mexico Midland Railroad. Westward mine development was halted at a north-trending fault that juxtaposes the Crevasse Canyon Formation and the Carthage Member of the Tres Hermanos Formation. 0.05

18.45 Milepost 10. 0.05

18.5 Junction of US-380 and A-137. Continue on US-380. Crossing covered contact between Baca Formation and underlying Upper Cretaceous rocks. 0.6

19.1 Roadcut in gravels of Baca and Spears Formations that dip about 40° east. Baca conglomerates (Eocene) at west end of cut contain Precambrian, Paleozoic, and some Mesozoic clasts that were transported eastward from a Laramide uplift, now mostly downfaulted beneath the Rio Grande rift (Cather, 1983). Several fossil teeth (Titanotheres, etc.) recovered in the Carthage area indicate a Bridgerian provincial age for the lower part of the Baca (Lucas et al., 1982; Lucas, 1983). The Baca-Spears contact, which is placed at the first occurrence of Tertiary volcanic clasts (here mainly plagioclase-rich andesitic rocks), is exposed about midway in the outcrop. Volcanic clasts increase gradationally over 15-30 ft until almost all clasts are volcanic. 0.3

19.4 Milepost 11. Top of hill. Road descends into the Jornada del Muerto Basin. This basin extends southward to Las Cruces and northward to the Los Pinos Mountains and Chupadera Mesa. It was so named because hundreds of people perished en route from Chihuahua to Santa Fe due to lack of water and attacks by Apache Indians (Pearce, 1965). Chupadera Mesa is at 11:00-12:00; Oscura Mountains, 12:00-2:00; Mockingbird Gap, 2:00. 0.6

20.0 Junction of county road A-129 and end of Trip 2b. 0.9

20.9 STOP 3-1. Historical marker at junction with NM-525 to Stallion Site, White Sands Missile Range. Trinity Site, location of the world's first nuclear test is about 20 mi to the southeast. Pluvial Lake Trinity, described by Neal et al. (1983), flooded the Jornada Basin floor south of Trinity Site during Pleistocene pluvial periods. Salinas Peak, in the northern San Andres Range at 2:30, is capped by an aphanitic rhyolite sill of Tertiary age intruded into Pennsylvanian rocks. 0.6

21.5 Ruins of Carthage Post Office and Store. 5.8

27.3 Milepost 19. Hansonburg mining district at 1:00 in the Oscura Mountains. Lower red hills at 2:00 are in Abo Formation. 3.4

30.7 Rest stops ahead. Recent sand dunes have been partially stabilized by vegetation. 1.7

32.4 Roadcuts in limestone of San Andres Formation. Roadcuts ahead in Glorieta Sandstone and gypsum of the Yeso Formation. **3.1**

35.5 Roadcuts in San Andres Formation ahead. Cross west flank of small syncline. **2.0**

37.5 Bingham. Hansonburg mining district to right (Fig. 30). Roadcuts in Abo Formation ahead. See pp. 50, 52 for description of clay mineralogy.

End of roadlog.

Retrace route back to Socorro or continue on US-380 to Valley of Fires field trip (Allen and Kottlowski, 1981).

FIGURE 30—Looking east at the Hansonburg mill and dumps of barite-fluorite-galena mines.

Roadlog references and additional reading (*)

Allen, J. E., and Kottlowski, F. E., 1981, Roswell-Ruidoso-Valley of Fires, including trips to Lincoln, Tularosa, and Bottomless Lakes State Park: New Mexico Bureau of Mines and Mineral Resources, Scenic Trip 3, 3rd edition, 96 pp.

Bauch, J. H. A., 1982, Geology of the central area of the Loma de las Carias quadrangle, Socorro County, New Mexico: Unpublished M.S. thesis, New Mexico Institute of Mining and Technology, 116 pp.

Bryan, K., 1932, Pediments developed in basins with through drainage as illustrated in the Socorro area, New Mexico (abs.): Geological Society of America Bulletin, v. 43, pp. 128-129.

Cather, S. M., 1983, Laramide Sierra uplift-evidence for major pre-rift uplift in central and southern New Mexico: New Mexico Geological Society, Guidebook to 34th Field Conference, pp. 99-101.

Chamberlin, R. M., 1980, Cenozoic stratigraphy and structure of the Socorro Peak volcanic center, central New Mexico: Unpublished Ph.D. dissertation, Colorado School of Mines, Golden, 495 pp.; New Mexico Bureau of Mines and Mineral Resources, Open-file Report 118, 532 pp., 3 pls.

Chamberlin, R. M., 1981, Cenozoic stratigraphy and structure of the Socorro Peak volcanic center, central New Mexico-a summary: New Mexico Geology, v. 3, no. 2, pp. 22-24.

Chamberlin, R. M., 1983, Cenozoic domino-style crustal extension in the Lemitar Mountains, New Mexico-a summary: New Mexico Geological Society, Guidebook to 34th Field Conference, pp. 111-118.

Chamberlin, R. M., and Osburn, G. R., 1986, Tectonic framework, character, and evolution of upper crustal extensional domains in the Socorro area of the Rio Grande rift, New Mexico: Arizona Geological Society Digest, vol. XVI, p. 464.

Chapin, C. E., 1983a, Selected tectonic elements of the Socorro region: New Mexico Geological Society, Guidebook to 34th Field Conference, p. 97.

*Chapin, C. E., editor, 1983b, Socorro region II: New Mexico Geological Society, Guidebook to 34th Field Conference, 344 pp.

Chapin, C. E., Chamberlin, R. M., and Hawley, J. W., 1978a, Socorro to Rio Salado; *in* Hawley, J. W. (compiler), Guidebook to Rio Grande rift in New Mexico and Colorado: New Mexico Bureau of Mines and Mineral Resources, Circular 163, pp. 121-137.

Chapin, C. E., Chamberlin, R. M., Osburn, G. R., White, D. W., and Sanford, A. R., 1978b, Exploration framework of the Socorro geothermal area, New Mexico; *in* Chapin, C. E., and Elston, W. E. (eds.), Field guide to selected cauldrons and mining districts of the Datil-Mogollon volcanic field, New Mexico: New Mexico Geological Society, Special Publication No. 7, pp. 114-129.

Chapin, C. E., and Lindley, J. I., 1986, Potassium metasomatism of igneous and sedimentary rocks in detachment terranes and other sedimentary basins-economic implications: Arizona Geological Society Digest, vol. XVI, pp. 118-126.

Clark, N. J., and Summers, W. K., 1971, Records of wells and springs in the Socorro and Magdalena areas, Socorro County, New Mexico, 1968: New Mexico Bureau of Mines and Mineral Resources, Circular 115, 51 pp.

Conron, J. P., 1980, Socorro, a historic survey: University of New Mexico Press, Albuquerque, 124 pp.

Cordell, L. S., and Earls, A. C., 1983, Piro Pueblo excavation: New Mexico Geological Society, Guidebook to 34th Field Conference, pp. 63-64.

D'Andrea-Dinkelman, J. F., Lindley, J. I., Chapin, C. E., and Osburn, G. R., 1983, The Socorro K_2O anomaly-a fossil geothermal system in the Rio Grande rift: New Mexico Geological Society, Guidebook to 34th Field Conference, pp. 76-77.

Denny, C. S., 1941, Quaternary geology of the San Acacia area, New Mexico: Journal of Geology, v. 49, pp. 225-260.

Eveleth, R. W., 1983, Gustav Billing, the Kelly mine, and the great smelter at Park City, Socorro County, New Mexico: New Mexico Geological Society, Guidebook to 34th Field Conference, pp. 89-95.

Ferguson, C. A., 1986, Geology of the east-central San Mateo Mountains, Socorro County, New Mexico: New Mexico Bureau of Mines and Mineral Resources, Open-file Report 252, 135 pp., 4 maps.

Foster, R., and Luce, P., 1963a, Road log A, Socorro northward to Valencia County line via Interstate 25, U.S. 85, and U.S. 60: New Mexico Geological Society, Guidebook to 14th Field Conference, pp. 6-12.

Foster, R., and Luce, P., 1963b, Road log D, Socorro to Sierra County line, via U.S. 85: New Mexico Geological Society, Guidebook to 14th Field Conference, pp. 26-30.

Gile, L. H., Hawley, J. W., and Grossman, R. B., 1981, Soils and geomorphology in the Basin and Range area of southern New Mexico-guidebook to the Desert Project: New Mexico Bureau of Mines and Mineral Resources, Memoir 39, 222 pp.

Hawley, J. W., 1986, Physiographic provinces; *in* Williams, J. L. (ed.), New Mexico in maps, 2nd edition: University of New Mexico Press, Albuquerque, pp. 23-31.

*Hawley, J. W., and Parsons, R. B., 1984, Glossary of selected geomorphic terms for western soil surveys: West National Technical Service Center, U.S. Soil Conservation Service, Portland, Oregon, 31 pp.

Henderson, E., 1956, U.S. 60: Arizona Highways, v. 32, no. 5, pp. 12-31.

Hook, S. C., 1983, Stratigraphy, paleontology, depositional framework, and nomenclature of marine Upper Cretaceous rocks, Socorro County, New Mexico: New Mexico Geological Society, Guidebook to 34th Field Conference, pp. 165-172.

Hook, S. C., Molenaar, C. M., and Cobban, W. A., 1983, Stratigraphy and revision of nomenclature of upper Cenomanian to Turonian (Upper Cretaceous) rocks of west-central New Mexico; *in* Hook, S. C. (compiler), Contributions to mid-Cretaceous paleontology and stratigraphy of New Mexico-part II: New Mexico Bureau of Mines and Mineral Resources, Circular 185, pp. 7-28.

Izett, G. A., Obradovich, J. D., Naeser, C. W., and Cebula, G. T., 1981, Potassium-argon and fission-track zircon ages of Cerro Toledo Rhyolite tephra in the Jemez Mountains, New Mexico: U.S. Geological Survey, Professional Paper 1199-D, pp. 37-43.

Jaworski, M. J., 1973, Copper mineralization of the Upper Moya Sandstone, Chupadera mines area, Socorro County, New Mexico: Unpublished M.S. thesis, New Mexico Institute of Mining and Technology, Socorro, 102 pp.

Kelley, V. C., 1982, Albuquerque, its mountains, valley, water, and volcanoes, 3rd edition: New Mexico Bureau of Mines and Mineral Resources, Scenic Trip 9, 106 pp.

*Kuellmer, F. J., editor, 1963, Socorro region: New Mexico Geological Society, Guidebook to 14th Field Conference, 240 pp.

*Lasky, S. G., 1932, The ore deposits of Socorro County, New Mexico: New Mexico Bureau of Mines and Mineral Resources, Bulletin 8, 139 pp.

Lucas, S. G., 1983, The Baca Formation and the Eocene-Oligocene boundary in New Mexico: New Mexico Geological Society, Guidebook to 34th Field Conference, pp. 187-192.

Lucas, S. G., Wolberg, D. L., Hunt, Adrian, and Schoch, R. M., 1982, A middle Eocene titanothere from the Baca Formation, south-central New Mexico: Journal of Paleontology, v. 56, pp. 542-545.

Machette, M. N., 1978, Preliminary geologic map of the Socorro 1° x 2° quadrangle, central New Mexico: U.S. Geological Survey, Open-file Report 78-607, scale 1:250,000.

Machette, M. N., 1982, Quaternary and Pliocene faults in the La Jencia and southern part of Albuquerque-Belen Basins, New Mexico-evidence of fault history from fault-scarp morphology and Quaternary geology: New Mexico Geological Society, Guidebook to 33rd Field Conference, pp. 161-169.

Machette, M. N., 1986, History of Quaternary offset and paleoseismicity along the La Jencia fault, central Rio Grande rift, New Mexico: Bulletin of the Seismological Society of America, v. 76, no. 1, pp. 259-272.

McIntosh, W. C., Sutter, J. F., Chapin, C. E., Osburn, G. R., and Ratte, J. C., 1986, A stratigraphic framework for the eastern Mogollon-Datil volcanic field based on paleomagnetism and high-precision $^{40}Ar/^{39}Ar$ dating of ignimbrites; a progress report: New Mexico Geological Society, Guidebook to 37th Field Conference, pp. 183-195.

McKee, J. D., and Wilson, S., 1975, Leave the back of garage and turn left: New Mexico Architecture, v. 17, no. 6, pp. 11-19.

McLemore, V. T., 1983, Uranium in the Socorro area, New Mexico: New Mexico Geological Society, Guidebook to 34th Field Conference, pp. 227-233.

McLemore, V. T., 1987, Geology and regional implications of carbonatites in the Lemitar Mountains, central New Mexico: Journal of Geology, v. 95, pp. 255-270.

Neal, J. T., Smith, R. E., and Jones, B. F., 1983, Pleistocene Lake Trinity, an evaporite basin in the northern Jornada del Muerto, New Mexico: New Mexico Geological Society, Guidebook to 34th Field Conference, pp. 285-290.

*Nieman, C. L., 1972, Spanish times and boom times-toward an architectural history of Socorro, New Mexico: Socorro County Historical Society, Inc., v. 6, 100 pp.

North, R. M., 1983, History and geology of the precious metal occurrences in Socorro County, New Mexico: New Mexico Geological Society, Guidebook to 34th Field Conference, pp. 261-268.

North, R. M., and McLemore, V. T., 1986, Silver and gold occurrences in New Mexico: New Mexico Bureau of Mines and Mineral Resources, Resource Map 15, 32 pp., scale 1:1,000,000.

Osburn, G. R., compiler, 1984, Socorro County geologic map: New Mexico Bureau of Mines and Mineral Resources, Open-file Report 238, 14 pp., 1 map, scale 1:200,000.

Osburn, G. R., and Chapin, C. E., 1983a, Nomenclature for Cenozoic rocks of northeast Mogollon-Datil volcanic field, New Mexico: New Mexico Bureau of Mines and Mineral Resources, Stratigraphic Chart 1, 7 pp., scale 1:1,000,000.

Osburn, G. R., and Chapin, C. E., 1983b, Ash-flow tuffs and cauldrons in the northeast Mogollon-Datil volcanic field-a summary: New Mexico Geological Society, Guidebook to 34th Field Conference, pp. 197-204.

Osburn, G. R., and Lochman-Balk, C., 1983, Stratigraphic nomenclature chart: New Mexico Geological Society, Guidebook to 34th Field Conference, p. 98.

Osburn, J. C., 1983, Coal resources of Socorro County, New Mexico: New Mexico Geological Society, Guidebook to 34th Field Conference, pp. 223-226.

*Patterson, S. H., and Holmes, R. W., 1965, Clays; *in* Mineral and water resources of New Mexico: New Mexico Bureau of Mines and Mineral Resources, Bulletin 87, pp. 312-322.

Pearce, T. M., 1965, New Mexico place names, a geographical dictionary: University of New Mexico Press, Albuquerque, 187 pp.

Sanford, A. R., 1978, Characteristics of Rio Grande rift in vicinity of Socorro, New Mexico, from geophysical studies; *in* Hawley, J. W. (compiler), Guidebook to Rio Grande rift in New Mexico and Colorado: New Mexico Bureau of Mines and Mineral Resources, Circular 163, pp. 116-121.

Sanford, A. R., 1983, Magma bodies in the Rio Grande rift in central New Mexico: New Mexico Geological Society, Guidebook to 34th Field Conference, pp. 123-125.

Sanford, A. R., Budding, A. J., Hoffman, J. P., Alptekin, O. S., Rush, C. A., and Topozada, T. R., 1972, Seismicity of the Rio Grande rift in New Mexico: New Mexico Bureau of Mines and Mineral Resources, Circular 120, 19 pp.

Simmons, M., 1983, The refounding of Socorro, 1816: New Mexico Geological Society, Guidebook to 34th Field Conference, pp. 83-84.

Smith, C. T., Osburn, G. R., Chapin, C. E., Hawley, J. W., Osburn, J. C., Anderson, 0. J., Rosen, S. D., Eggleston, T. L., and Cather, S. M., 1983, First day road log from Socorro to Mesa del Yeso, Joyita Hills, Johnson Hill, Cerros de Amado, Lomas *[sic]* de las Carias, Jornado *[sic]* del Muerto, Carthage, and return to Socorro: New Mexico Geological Society, Guidebook to 34th Field Conference, pp. 1-28.

Talmage, S. B., and Wootton, T. P., 1937, The non-metallic mineral resources of New Mexico and their economic features (exclusive of fuels): New Mexico Bureau of Mines and Mineral Resources, Bulletin 12, 159 pp.

Thompson, M. L., 1942, Pennsylvanian system in New Mexico: New Mexico Bureau of Mines and Mineral Resources, Bulletin 17, 90 pp.

Weber, R. H., and Austin, G. S., 1982, Perlite in New Mexico; *in* Austin, G. S. (compiler), Industrial rocks and minerals of the Southwest: New Mexico Bureau of Mines and Mineral Resources, Circular 182, pp. 97-101.

Weber, R. H., and Willard, M. E., 1963, Road log C, Socorro westward to Catron County line via U.S. 60: New Mexico Geological Society, Guidebook to 14th Field Conference, pp. 20-25.

Weir, J. E., Jr., 1965, Geology and availability of ground water in the northern part of the White Sands Missile Range and vicinity, New Mexico: U.S. Geological Survey, Water-Supply Paper 1801, 78 pp.

Wilpolt, R. H., and Wanek, A. A., 1951, Geology of the region from Socorro and San Antonio east to Chupadera Mesa, Socorro County, New Mexico: U.S. Geological Survey, Oil and Gas Investigations Map OM-121, scale 1:63,360.

Wilson, S., and Bieberman, R. A., 1983, The Civil War in New Mexico-tall tales and true: New Mexico Geological Society, Guidebook to 34th Field Conference, pp. 85-87.

Clay mineralogy of selected sedimentary and volcanic rocks, Socorro County, New Mexico

by Mark R. Bowie and Virginia T. McLemore
New Mexico Bureau of Mines and Mineral Resources, Socorro, New Mexico 87801

Abstract

Oriented slide semi-quantitative x-ray diffraction (XRD) analyses of the <2 micron-size fraction of selected sedimentary rocks from Socorro County, New Mexico, were undertaken to examine temporal and lateral trends in their clay mineralogy and to ascertain whether variations in detrital clay mineral deposition or diagenetic processes are responsible for sharp color differences between beds and within individual beds of the same rock units. Claystones from the playa fades of the Popotosa Formation (Miocene) southwest of Socorro consist dominantly of either illite or dioctahedral sodium smectite (montmorillonite). Variations in clay mineralogy are reflected in color differences of the rock. The observed clay mineralogy may be the product of potassium metasomatism of detrital clay minerals.

The D-Cross Tongue of the Mancos Shale (Cretaceous) near Carthage is illitic, with lesser mixed-layer illite/smectite (I/S) and kaolinite. Also near Carthage, white kaolinitic claystones previously assigned to the base of the Cretaceous Dakota Sandstone may represent a zone of weathering at the top of the Chinle Formation (Triassic). Varicolored Chinle claystones immediately underlying the Dakota are also kaolinitic but grade downward into mostly I/S and illite-bearing purple and gray claystones. Different-colored sandy claystones of the Torres Limestone Member of the Yeso Formation (Permian) in the Loma de las Calias are uniformly illitic with lesser, subequal amounts of chlorite and kaolinite. Varicolored claystones and sandstones of the Abo Formation (Permian) in the Loma de las Cafias and east of Bingham consistently contain subequal amounts of illite and chlorite. Carbonaceous claystones of the Sandia Formation (Pennsylvanian) at the Houlett fireclay deposit in the Loma de las Cafias are uniformly dominantly kaolinite with subordinate I/S and illite. The consistency of the clay mineralogy of the Yeso, Abo, and Sandia sediments vertically and through several color variations suggest that most of the clays are detrital and were little affected by diagenetic processes that changed the original color of the sediments.

Randomly oriented pressed powder XRD analyses of the <2 micron-size fraction of an altered rhyolite tuff from the Luis Lopez Formation (Oligocene) revealed that it consists dominantly of 1M illite, a polytype which, experimentally, forms at less than 350°C.

Introduction

Sedimentary rocks from the Sandia Formation (Pennsylvanian), the Abo and Yeso Formations (Permian), the Chinle Formation (Triassic), the Dakota Sandstone and Mancos Shale (Cretaceous), the Popotosa Formation (Miocene), and volcanic rock from the Luis Lopez Formation (Oligocene) were sampled in Socorro County, New Mexico, in preparation for semi-quantitative x-ray diffraction (XRD) analyses of the <2 micron-size fraction (Fig. 1). Altered rhyolite ash-flow tuff from the Luis Lopez Formation was collected in Blue Canyon near the base of Socorro Peak. Claystones in the Popotosa Formation were sampled in roadcuts and in a pit along US-60 southwest of Socorro. Claystones, siltstones, and sandstones from the Sandia, Abo, Yeso, and Chinle Formations were sampled along the traverses of Trips 2b, 2c, and 3 (this volume) in the Loma de las Cafias about 7 mi east of Socorro and in roadcuts along US-380 from just east of Bingham to about 7 mi east of San Antonio. The Mancos Shale was sampled in a roadcut on the Fite Ranch about 0.5 mi south of US-380 near Stop 2-5 of Trip 2c (p. 36).

The purpose of the semi-quantitative analyses is severalfold: 1) to supplement the rock descriptions in the roadlogs of this guidebook, 2) to identify the clay mineral assemblage of the <2 micron-size fraction of the rocks and to determine the relative abundances of the major clay mineral groups (illite, smectite, mixed-layer clay minerals, chlorite, and kaolin) present, 3) to examine vertical and lateral trends in the clay mineralogy of the rock units, and 4) to ascertain the origin of sharp, distinct color differences (notably red versus green or gray) between beds and within individual beds of the rock units. Are the color variations controlled by differences in clay mineralogy? Are they the result of the influence of local oxidizing or reducing conditions during deposition of the sediments? Are they a product of diagenesis?

Previous studies

Very few investigations have assessed clay resources in New Mexico. Talmage and Wootton (1937) briefly described clay occurrences, production, and commercial uses in the state. Patterson and Holmes (1965) updated this earlier report. An unpublished manuscript by Van Sandt (1964) provides descriptions of refractory clay occurrences in Arizona and New Mexico; several are in the Socorro and Carthage areas. Van Sandt also tested physical and chemical properties of the clays to evaluate their refractory qualities.

Burlbaw and Siemers (unpubl. report 1975), Cappa (unpubl. report 1975), and Domski (unpubl. report 1987) performed semi-quantitative XRD analyses of the major clay mineral groups in selected Pennsylvanian, Permian, and Tertiary rocks in Socorro County and surrounding areas. Brenner-Tourtelot and Machette (1979) and Asher-Bolinder (1982) analyzed the mineralogy of claystones and altered air-fall tuffs in the Popotosa Formation by XRD and chemical methods. The data generated by the above workers complement data presented in this paper.

Historical production and utilization

In New Mexico, clay deposits have been used since prehistoric times by Native Americans for making pottery and

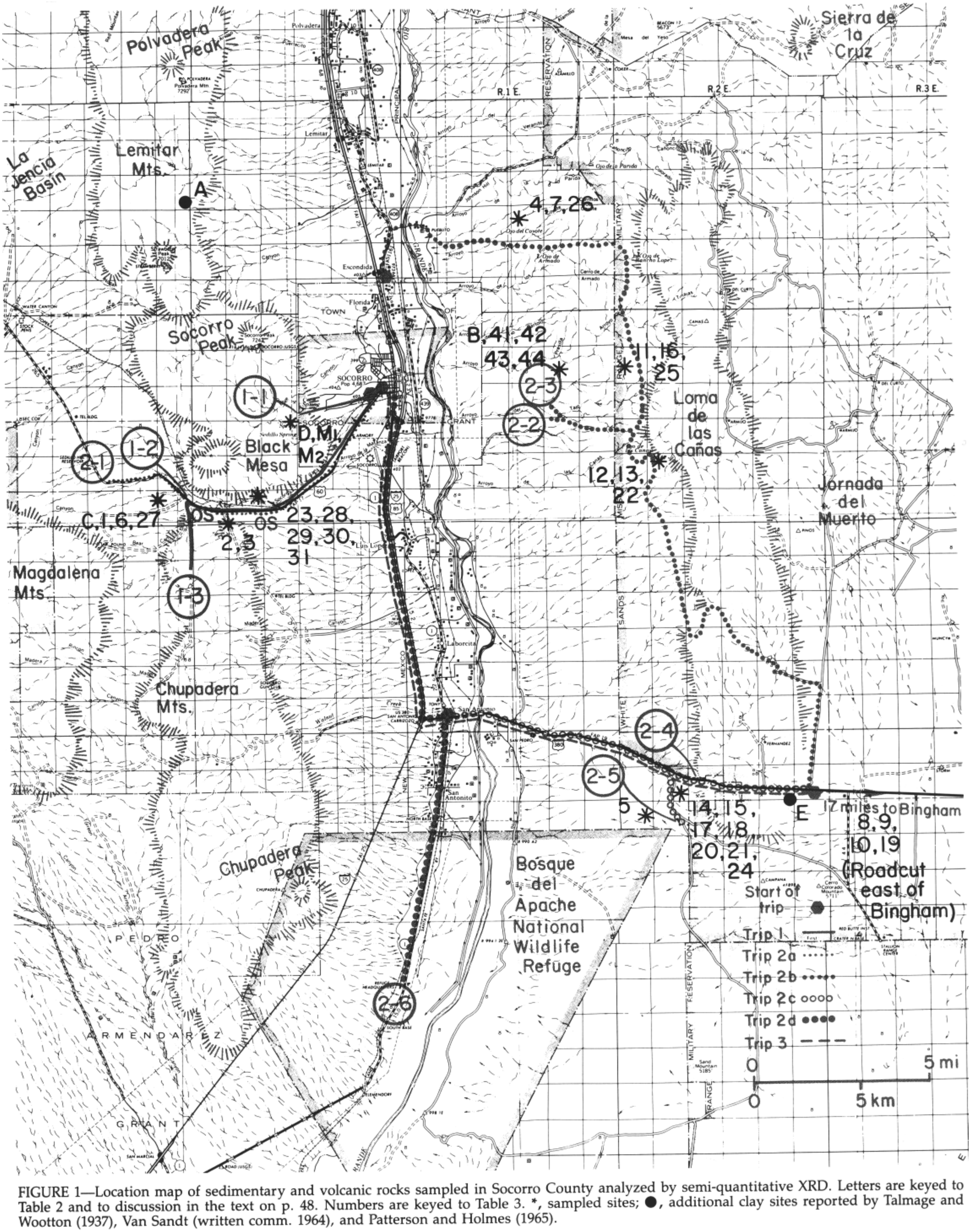

FIGURE 1—Location map of sedimentary and volcanic rocks sampled in Socorro County analyzed by semi-quantitative XRD. Letters are keyed to Table 2 and to discussion in the text on p. 48. Numbers are keyed to Table 3. *, sampled sites; ●, additional clay sites reported by Talmage and Wootton (1937), Van Sandt (written comm. 1964), and Patterson and Holmes (1965).

building homes. Native Americans were making crude adobe bricks when the Spanish first entered the region. Most of the clay material was extracted from alluvial deposits along major rivers and arroyos. Even today, many New Mexicans use local clay material to produce adobe brick. Numerous homes and buildings in Socorro County, including the historic San Miguel Church at Socorro (see fig. 2 on p. 7), are built of adobe (Conron, 1980). Adobe construction remains a very popular form of architecture because it is aesthetically pleasing, inexpensive, and a good insulator. Adobe brick making and adobe construction in New Mexico are discussed by Smith (1982). Clay minerals, most commonly illite-group clays and kaolinite, are the chief binders in adobe brick.

In the late 1800's and early 1900's, common brick and fire brick were manufactured by the Socorro Fire Clay Works. Common brick was produced from a mixture of local alluvial clay material and fireclay. Fire brick was made from fireclay obtained from several localities in Socorro County (the following letters are keyed to Fig. 1): A) Sandia Formation, southern Lemitar Mountains 10 mi northwest of Socorro, B) Sandia Formation, near the head of Arroyo de la Presilla 6 mi east of Socorro, C) Popotosa Formation, Socorro Mountains immediately west and southwest of Socorro, D) Luis Lopez Formation, Socorro Mountains, and E) Cretaceous units, Carthage coal field (Talmage and Wootton, 1937; Van Sandt, 1964). Exact production statistics are not known although the brick industry was an important contributor to Socorro's economy around the turn of the century. Fire brick was used under boilers in several smelters in the Southwest, including the Billing smelter in Socorro (Talmage and Wootton, 1937). Common brick was later used in many buildings in Socorro.

A small roofing-tile plant in San Antonio operated intermittently during the early 1900's. The three-man operation used local adobe material and sometimes clay from Carthage to make the tiles. Some Carthage clay was also shipped to Albuquerque by the New Mexico Clay Products Company who experimented with admixtures of Carthage and Albuquerque clays in the manufacture of brick and tile (Talmage and Wootton, 1937).

Experimental procedure

Fresh select grab samples of a particular zone in outcrop or channel samples of a vertical interval of outcrop were collected for this study. In particular, different-colored beds within the rock units were sampled to determine if the color variations are due to variations in clay mineralogy or depositional or diagenetic processes.

Oriented (sedimented) clay slides were prepared for XRD analyses by immersing the samples in distilled water in a beaker and allowing the coarse material to settle, leaving a residual <2 micron-size fraction at the top of the suspension. An eye dropper was then touched to the surface of the suspension, and the drawn sample was transferred to a petrographic slide where it was allowed to dry at room temperature. Samples that did not disperse after several cycles of immersion and mixing in distilled water were wet ground in a mortar and pestle, and if they remained flocculated, they were treated with a few drops of ammonium hydroxide (NI-1,0H) and remixed. All samples dispersed before or during this stage of preparation.

A Rigaku Geigerflex diffraction unit with Ni-filtered CuKa, (=1.5418 A) radiation was used for the XRD analyses. Five XRD traces (scans) were run on each slide using the same machine settings. Initially, the oriented, untreated slides were continuously scanned at 2° 20/min between 2° 20 and 38° 20. When both kaolinite and chlorite were present in a sample, a scan from 24° 20 to 26°/20 was run at a slower scan speed to help distinguish between the 002 kaolinite reflection at 24.9° 20 and the 004 chlorite reflection at 25.1° 20.

TABLE 1—Equations used for the semi-quantitative XRD analyses. Peaks are designated with numeral subscripts to indicate the order of 001 reflections (e.g., second order illite, 002 reflection, is I_2). Peak intensities are in counts above background. All traces for a particular sample were run on the same slide using the same machine settings. **T,** total counts; **G,** glycolated; **H,** heated; **I,** illite; **S,** smectite; **K,** kaolinite; **C,** chlorite. Note: peaks without "G" or "H" subscripts are from the untreated, oriented slide traces.

With no chlorite present:

$$\text{Illite} = \frac{I_{1G}}{T} \times 10$$

$$\text{Smectite} = \frac{1/4\ S_{1G}}{T} \times 10$$

$$\text{Mixed-layer illite/smectite} = 10A_H - \frac{(1/4\ S_{1G} + I_{1G})}{T} \times 10$$

$$\text{Kaolinite} = \frac{K_1}{T} \times 10$$

$$T = 10\text{Å}_H + \text{untreated } K_1$$

With chlorite present, the following adjustments are made to the above calculations:

$$T = I_{1H} + \frac{(C_3)\ (I_{1G})}{I_2} + \frac{(K_2)\ (C_3)\ (I_{1G})}{(2C_4)\ (I_2)}$$

$$\text{Kaolinite} = \frac{K_2}{2C_4} \times \frac{C_3}{I_2} \times \frac{I_{1G}}{T} \times 10$$

$$\text{Chlorite} = \frac{C_3}{I_2} \times \frac{I_{1G}}{T} \times 10$$

All slides were then placed in an ethylene glycol chamber for 24 hours. Glycolation caused expansion of smectite and interstratified smectite layers within mixed-layer clay minerals and shifts in reflection positions of the untreated, oriented slide traces, which aided in their identification. The glycolated slides were continuously scanned with the diffractometer between 2° 20 and 15° 20. The same slides were then heated at 375-380°C for 30 minutes in a Blue M Lab-Heat Muffle Furnace. They were scanned with the diffractometer between 7.5° 20 and 9.5° 20, then between 2° 20 and 15° 20 immediately after removal from the furnace so that the scan passed over the 10-A peak while the slide was still hot. The scan between 2° 20 and 15° 20 was used to demarcate background scatter on the diffractograms and, subsequently, to determine the relative intensity of the 10A peak. Any enhancement of the 10-A peak by heating was attributed to the collapse of interstratified smectite layers within illite/smectite mixed-layer minerals (Austin and Leininger, 1976).

The semi-quantitative XRD analyses were performed using equations developed by G. S. Austin (written comm. 1987; Table 1) to determine the relative abundance of the major clay mineral groups. This method is based on the heights of 001 peaks above background and quantifies the major clay mineral groups to parts in 10.

A <2 micron-size fraction of altered rhyolite tuff from the Luis Lopez Formation was analyzed by randomly oriented powder XRD using a Phillips Norelco diffraction unit with Ni-filtered CuKa, radiation at 40 kv and 20 ma from 3° to 65° 20, a vertical goniometer, a graphite crystal monochrometer, and receiving and scattering slits of 1/2° and 4°, respectively.

Clay mineralogy of the rock units

Luis Lopez Formation

The Luis Lopez Formation consists of intermediate to mafic lavas and flows and volcaniclastic sedimentary rocks emplaced as moat-fill in the Socorro cauldron (Chamberlin, 1980; Osburn et al., 1981; Eggleston, 1982; Osburn and Chapin, 1983). An altered rhyolite ash-flow tuff of the Luis Lopez was sampled from a clay pit in sec. 16, T3S, R1W in Blue Canyon on the eastern flank of the Socorro Mountains (Fig. 1; Trip 1, Stop 1-1, p. 19). Clay (altered tuff) from this pit was previously described as kaolinitic (Talmage and Wootton, 1937, p. 69), but recent randomly oriented pressed powder XRD analyses by G. S. Austin and J. L. Post (written comm. 1987) of the <2 micron-size fraction of the tuff reveal that it consists dominantly of 1M illite (Fig. 2), a polytype which, experimentally, forms at temperatures less than 350°C (Yoder and Eugster, 1955; Austin et al., 1987).

The sampled tuff lies within a large zone in which Oligocene and early Miocene volcanic and sedimentary rocks have been pervasively altered by potassium metasomatism (D'Andrea-Dinkelman et al., 1983; Chapin and Lindley, 1986). Within this zone, volcanic rocks commonly contain 5-11% K_2O. Unaltered tuffs outside the zone average less than 5% K_2O. Chemical analyses of the illite in the clay pit in Blue Canyon by J. L. Post (written comm. 1987) indicate that it contains about 8% K_2O. Whole rock x-ray fluorescence analyses by the authors of the same illitized tuff indicate that it contains about 4-5% K_2O (Table 2).

The large zone of potassium metasomatism has been interpreted both as a fossil geothermal system (D'Andrea-Dinkelman et al., 1983) and, alternatively, as a zone of diagenetic alteration by alkaline solutions descending into the buried Oligocene and early Miocene volcanic and sedimentary section from an alkaline, saline-lake system of the Popotosa (Miocene) Basin (Chapin and Lindley, 1986). This latter low-temperature alteration is analogous to diagenetic reactions in alkaline saline-lake environments common to Tertiary basins of the Basin and Range Province (Hay, 1966, 1978; Sheppard and Gude, 1968; Surdam and Sheppard, 1978). The abundance of the relatively low-temperature 1M illite polytype in the altered tuff in Blue Canyon lends support to the low-temperature alkaline solutions theory.

TABLE 2-Whole rock x-ray fluorescence analyses of two samples of altered rhyolite ash-flow tuff from the Luis Lopez Formation in a clay pit, sec. 16, T3S, R1W, Blue Canyon, Socorro Mountains. -, analyzed for but not found. Sample numbers refer to locations on Fig. 1.

Oxide	Sample MI	Sample M2
SiO_2	69.2	68.7
Al_2O_3	14.6	15.2
Fe_2O_3 (total Fe)	2.29	2.42
MnO	0.03	0.02
TiO_2	0.15	0.15
MgO	2.09	1.79
CaO	1.52	1.03
Na_2O	1.42	1.47
K_2O	4.36	5.04
P_2O_5		
LOI	5.00	4.68
Total	100.66	100.50

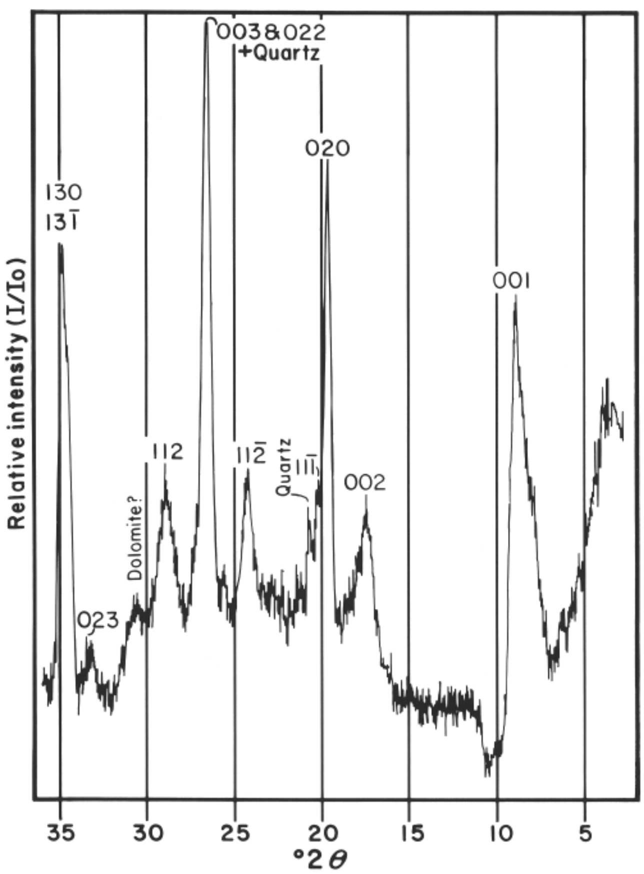

FIGURE 2—X-ray diffractogram of randomly oriented pressed powder mount of altered rhyolite ash-flow tuff from the Luis Lopez Formation. The tuff consists of the 1M illite polytype, quartz, and dolomite(?). The illite reflections are labeled. The 023, 112, and 11$\bar{2}$ reflections are diagnostic of this polytype.

Popotosa Formation

The Popotosa Formation represents early basin fill of the Rio Grande rift and consists of intertonguing fanglomerates, alluvium, and playa deposits (Denny, 1940; Bruning, 1973; Chapin and Seager, 1975; Brenner-Tourtelot and Machette, 1979; Asher-Bolinder, 1982). A nearly continuous 100-ft section of the playa facies is exposed in two roadcuts and a clay pit (see fig. 13 on p. 20) sampled along US-60 southwest of Socorro (Fig. 1). The clay pit sediments are the lowest stratigraphically, and the samples from the north side of the highway are the highest stratigraphically in this section. The results of the semi-quantitative XRD analyses of the Popotosa and the other sedimentary units in this study are in Table 3. The variegated green claystones of the pit contain dominantly illite and mixed-layer illite/smectite (I/S). The claystone from the middle of the pit face (sample 27) consists wholly of I/S and illite. The claystone from the top of the face (sample 6) is dominantly illite with minor 1/S and chlorite. Sample 1, a select grab sample of green claystone, contains mostly illite and US with minor chlorite and dioctahedral sodium smectite (montmorillonite). Kaolinite was not found in the pit.

Brown and gray variegated, gypsiferous claystones from the playa facies on the south side of US-60 (Trip 1, mile 11.4 on p. 20) have different clay mineral suites from one another. Both are dominantly illitic, but the brown sample contains more I/S and kaolinite than the gray sample, which contains more dioctahedral sodium smectite (montmorillonite) and chlorite.

Five samples from a 60-ft exposure of the playa facies on the north side of US-60 (Fig. 3; Trip 1, mile 9.8 on p. 20) have a generally uniform clay mineral suite. Except sample 31, the samples are dominantly dioctahedral sodium smectite (montmorillonite) with little or no illite, I/S, chlorite, and kaolinite. Sample 31, a red claystone between gypsiferous siltstone beds, is mostly dioctahedral sodium smec-

TABLE 3—Results of semi-quantitative XRD analyses of the <2 micron-size fraction of sedimentary rocks from Socorro County. Data are in parts in 10 and were calculated using the equations in Table 1. In general, samples are listed, from top to bottom, in descending stratigraphic order at each outcrop. I, illite; NaSm, sodium smectite; I/Sm, mixed-layer illite/smectite; C, chlorite; K, kaolinite; gyp, gypsiferous; sltst, siltstone. Sampling procedure described in text. Sample numbers refer to locations on Fig. 1.

Sample	Formation	Location	Sample description	I	NaSm	I/Sm	C	K
1	Popotosa	36 T3S R2W (clay pit)	green, select	5	1	3	2	0
6	Popotosa	36 T3S R2W (clay pit)	green, select, top	7	0	1	1	0
27	Popotosa	36 T3S R2W (clay pit)	green, select, midwall	4	0	6	0	0
			red, select, lower gyp sltst bed					
2	Popotosa	31 T3S R1W (S side US-60)	brown, select	4	1	3	1	3
			red, channel, between sltst beds					
3	Popotosa	31 T3S R1W (S side US-60)	gray, select	4	3	0	2	1
			red, channel, upper gyp sltst bed					
29	Popotosa	33 T3S R1W 2E (N side US-60)	green, select, between gyp sltst beds	0	10	0	0	0
31	Popotosa	33 T3S R1W 5E (N side US-60)	red, channel, below gyp sltst beds	1	3	3	0	2
28	Popotosa	33 T3S R1W 3E (N side US-60)	brown, select	1	9	0	0	2
23	Popotosa	33 T3S R1W 4E (N side US-60)	white, clayey zone, channel	1	9	0	0	1
30	Popotosa	33 T3S R1W 1W (N side US-60)	white, clayey zone and top of Chinle, channel	1	5	1	1	1
5	Mancos	17 T5S R2E (Fite Ranch)	green, select, **1** ft below white, clayey zone	5	1	2	1	2
24	Dakota	8 T5S R2E (US-380)	purple, channel, 5 ft below white, clayey zone	1	0	1	0	7
21	Dakota/Chinle	8 T5S R2E (US-380)	purple, channel, 30 ft below white, clayey zone	1	2	3	0	3
15	Chinle	8 T5S R2E (US-380)	gray, select, 35 ft below white, clayey zone	1	0	8	0	1
17	Chinle	8 T5S R2E (US-380)	purple, select, 40 ft below white, clayey zone	1	2	1	1	5
18	Chinle	8 T5S R2E (US-380)	green, channel	3	1	6	0	0
14	Chinle	8 T5S R2E (US-380)	red, select	3	1	2	2	1
20	Chinle	8 T5S R2E (US-380)	white, channel	2	0	7	0	0
22	Yeso	19 T3S R2E (Loma de las Carias)	red, select	5	1	1	2	1
12	Yeso	19 T3S R2E (Loma de las Canas)	gray, select	4	0	1	3	2
13	Yeso	19 T3S R2E (Loma de las Canas)	red, channel	4	1	0	3	3
4	Abo	23 T2S R1E (Loma de las Cafias)	gray and minor red, select	3	0	1	3	3
7	Abo	23 T2S R1E (Loma de las Cafias)	red and minor gray, select	3	0	1	3	4
26	Abo	23 T2S R1E (Loma de las Canas)	red, channel	2	0	1	2	6
11	Abo	31 T2S R2E (Loma de las Canas)	green, select	3	1	0	4	2
16	Abo	31 T2S R2E (Loma de las Canas)	red, select	3	0	1	3	2
25	Abo	31 T2S R2E (Loma de las Canas)	brown, channel	3	0	1	3	3
8	Abo	8 T5S R6E (US-380)	red, channel	3	0	2	3	1
9	Abo	8 T5S R6E (US-380)	brown, select	3	0	2	3	2
10	Abo	8 T5S R6E (US-380)	dark gray, select, from mine dump	4	0	2	3	1
19	Abo	8 T5S R6E (US-380)	dark gray, select	4	0	3	2	1
			dark gray, channel					
44	Sandia	2 T3S R1E (Houlett deposit)		1	1	2	0	6
43	Sandia	2 T3S R1E (Houlett deposit)		2	0	3	0	5
42	Sandia	2 T3S R1E (Houlett deposit)		2	0	2	0	6
41	Sandia	2 T3S R1E (Houlett deposit)		2	0	3	0	5

FIGURE 3—Looking northwest from US-60 at exposure of the playa fades of the Popotosa Formation at the base of the Socorro Mountains.

tite, US, and kaolinite with lesser illite. The green claystone (sample 23) has a clay mineral assemblage that is very similar to the red claystones from this outcrop.

Generally, there is little variation vertically in the clay mineralogy within each outcrop, but there is a significant difference between the clay mineralogy of the red claystones and siltstones in the exposure on the north side of US-60 and that of the green, brown, and gray claystones in the exposures on the south side of US-60 and in the clay pit. The samples from the north side of the highway are dominantly smectitic (sodium montmorillonite) and contain little illite, whereas samples from the other two exposures are illitic and 1/S-bearing but generally contain little smectite (Table 3).

The color of the claystones, therefore, seems to be a reflection of the clay mineralogy. But why does the clay mineralogy differ between the three outcrops? Several explanations are possible, based on whether the observed clay mineral assemblages are detrital, authigenic, or both. It is difficult to discern from semi-quantitative analyses whether the clays are detrital or authigenic. A scanning electron microscopy study of the morphological characteristics and spatial and paragenetic relationships of the clays would help resolve this problem.

If the clays are detrital, their varying abundance between the outcrops may be the result of variable detrital input from lithologically different source areas surrounding the playa. Picard and High (1972) examined the clay mineral suite of 40 mostly Recent lakes and found that lacustrinc deposits are characterized by diverse clay mineral assemblages that reflect source materials and climate. These deposits are generally dominated by illite, smectite, and US. Droste (1961a) studied the clay mineralogy of sediments in 45 playas of the Mojave Desert. He found illite and montmorillonite in each playa and determined that they composed at least 70% of the clay minerals present. Chlorite and kaolinite were in the sediments of less than half of the playas and accounted for generally less than 30% of the clay minerals present. The clay mineralogy of desert saline sediments in southern California is controlled almost entirely by the composition of the source rocks surrounding the basins and there is little evidence that any of the clays are unstable in the saline-lake environment (Droste, 1961a, b).

Similarly, the clay mineral assemblage of the Popotosa playa facies may be detrital, unaltered, and a reflection of the composition of the surrounding source rocks. However, these clays may be, in part, authigenic. If they were not altered in the playa proper, they may have been altered after burial by continued exposure to potassium metasomatic alkaline and saline solutions percolating downward into the subsurface from a younger playa.

Domski (unpubl. report 1987) performed semi-quantitative XRD analyses of the <2 micron-size fraction of Popotosa early basin fanglomerate and immediately overlying playa sediments. His playa samples were collected from the same exposures where we collected ours. The two fanglomerate samples both consist wholly of illite (seven parts in 10) and L'S (three parts in 10). The illite content progressively decreases upsection from the fanglomerate samples through the playa samples until dioctahedral sodium smectite (montmorillonite) becomes the dominant species. This trend is also apparent from our analyses (Table 3). The high illite content of the fanglomerate may indicate an initially high detrital illite influx. In contrast, it may be the result of illitization of smectite by potassium metasomatizing fluids. Domski (unpubl. report 1987) found that the amount of US is constant through the sampled vertical interval. He noted that the I/S is randomly interstratified and that the amount of illite in it decreases with depth, from about 20% in the uppermost playa samples, to about 50% in the playa samples nearest the contact with the underlying fanglomcrate, to about 90% in the fanglomerate samples. This trend is, most likely, the result of increasing illitization of smectite with depth by potassium metasomatizing fluids percolating downward through the subsurface, and is probably not a response to varying detrital influx over time.

Mancos Shale

The D-Cross Tongue of the Mancos Shale (Cretaceous) is a transgressive marine shale sequence that is up to 300 ft thick in the Carthage area (Hook, 1983). A brown, silty shale in the D-Cross was sampled in a roadcut on the Fite Ranch (Fig. 1; Trip 2c, between miles 5.45 and 5.55 on p. 36; fig. 1-64.4 of Smith et al., 1983). It consists mostly of illite with lesser, subequal amounts of US, kaolinite, dioctahedral sodiu ▸ smectite (montmorillonite), and chlorite (Table 3).

Chinle Formation

In the Carthage area, the Chinle Formation (Triassic) consists dominantly of nonmarine claystone with thin, discontinuous sandstone, siltstone, and conglomerate interbeds. No single unit is traceable for more than several tens of feet (Smith, 1983). The upper 463 ft is dominated by reddish-brown and gray-red claystones with thin intraformational conglomerates and sandstones (Hunt and Lucas, 1987). A vertical interval from a white, clayey zone at the base of the unconformably overlying Dakota Sandstone (Cretaceous) to about 40 ft below the Chinle-Dakota contact was sampled in a roadcut along US-380 about 2 mi west of Carthage (Fig. 1; Trip 2c, mile 4.1 and fig. 25 on p. 36).

The white, clayey zone was previously assigned to the base of the Dakota but may, alternatively, represent Morrison-like beds (Jurassic) or a weathering zone at the top of the Triassic (Smith, 1983). It consists dominantly of kaolinite with minor illite and US (Table 3). A channel sample of claystone (sample 21) from the base of the white, clayey zone 2 ft into the top of the Chinle is mostly kaolinite and L'S with lesser dioctahedral sodium smectite (montmorillonite) and illite. A select grab sample of green claystone (sample 15) 1 ft below the white, clayey zone is dominantly L'S, similar to the purple claystones (samples 18, 20) downsection. A channel of silty claystone (sample 17) about 5 ft below the white, clayey zone is dominantly kaolinite with minor dioctahedral sodium smectite, illite, US, and chlorite. A channel of purple claystone about 30 ft below the white, clayey zone, and a select grab sample of purple claystone both consist dominantly of liS with minor illite. A select grab sample of gray claystone (sample 14) consists of subequal amounts of illite, US, and chlorite with lesser sodium smectite and kaolinite. The widely variable colors of the claystones may, in part, reflect differences in clay mineralogy. They may also be attributable to oxidation-reduction processes active when meteoric waters, percolating downward along fractures and bedding planes, reacted with pyrite or organic acids.

The high I/5 and illite content of the purple and gray claystones (samples 18, 14, 20) in the Chinle Formation is representative of the terrestrial origin of the unit. The high kaolinite content of the white, clayey zone (samples 24, 21) suggests that it may represent a zone of weathering. Kaolinite formation is favored in non-marine to near-shore, well-leached environments in the presence of fresh to acidic solutions. The uppermost Chinle was deposited in a terrestrial, near-shore environment.

Yeso Formation

The Yeso Formation (Permian) consists of sandstones, shales, limestones, dolomite, and evaporites representing littoral and near-shore deposits between underlying continental deposits of the Abo Formation and overlying marine carbonates of the San Andres Formation. In Socorro County the Torres Limestone Member of the Yeso Formation consists of limestone, sandstone, siltstone, claystone, breech), and gypsum (Smith, 1983). Sandy claystone of the Torres Member was sampled in the Loma de las Carias in a roadcut in sec. 19, T3S, R2E (Fig. 1; Trip 2b, mile 20.15 on p. 30). The three claystone samples are white, red, and green (Table 3). They are all dominantly illite with lesser chlorite and kaolinite and little or no sodium smectite and 1,'S. The uniformity of the clay mineralogy vertically and through the color variations suggests that the clays are detrital and were little affected by the diagenetic processes that induced color changes in the sediments, probably reaction of oxygenated meteoric waters with local pyrite and organic debris.

Abo Formation

In Socorro County the lower Permian Abo Formation is uniformly very dark reddish brown, fine-grained sandstones with interbedded claystones, siltstones, and arkoses, and a few coarser-grained channel sandstones in the lower part of the section (Smith, 1983). They represent continental sediments deposited on a gently, southerly sloping alluvial plain. The Abo conformably overlies the near-shoreishelf sediments of the Bursum Formation and grades upward into the near-shoredittoral Yeso deposits.

Abo claystone and fine-grained sandstone were sampled in two roadcuts in the Loma de las Carias (Trip 2b, miles 7.2 and 10.5 on p. 27) and in a roadcut along US-380 2 mi east of Bingham (Trip 3, mile 37.5 on p. 43; Speer et al., 1983). Gray, green, and brown color hands, which cut across primary sedimentary structures, were selectively sampled (Figs. 1, 4). The Abo rocks consistently contain high, subequal amounts of illite and chlorite with little or no sodium smectite (Table 3). The kaolinite content varies significantly (between one and six parts in 10), and the US content varies slightly between the outcrops. The clay mineralogy generally changes little vertically within each outcrop, regardless of the color of the sediments. This uniformity and the lateral consistency of the clay mineralogy between outcrops suggests a detrital origin for much of the clay minerals. The variable kaolinite contents are ascribed to locally variable detrital influx from the source areas. Like the Chinle and Yeso sediments in Socorro County, the Abo sediments apparently were little affected by diagenetic processes responsible for color changes of the sediments. The gray, green, and brown stringers, transverse to the primary bedding, most likely represent conduits for diagenetic fluids and were variably colored by reduction of pyrite and organic debris.

In studying the clay mineralogy of the Abo in the Sacramento Mountains farther south, Cappa (unpubl. report 1975) noted lateral variations in kaolinite/illite content ratios of the sediments. The kaolinite illite ratios decreased toward the marine basin to the south. Cappa attributes this to kaolinite being less stable in the near-shore environments than in the inland environments and/or "degraded" illite transported from the inland environments being "regraded" by uptake of potassium in the near-shore, more saline environments.

FIGURE 4—Looking north at claystones and sandstones of the Abo Formation along US-380 east of Bingham. Note clay-rich stringers transverse to primary bedding.

Burlbaw and Siemers (unpubl. report 1975) performed semi-quantitative XRD analyses of Pennsylvanian and lower Permian units north of our sample localities, in the Joyita Hills at the southern end of the Los Pinos Mountains, Socorro County. They observed a very uniform clay mineralogy of Abo claystones vertically and laterally. The average of the clay mineral assemblages of the claystones in this area is three parts in 10 illite, two parts in 10 US, four parts in 10 chlorite, and two parts in 10 kaolinite, with no smectite. These values are strikingly similar to our results (Table 3).

Burlbaw and Siemers (unpubl. report 1975) noted that the first appearance of chlorite in the regressive sequence from the marine Pennsylvanian Sandia and Madera Formations to the lower Permian Bursum (transitional) and Abo (continental) Formations is in the Abo, and, consequently, can be a useful stratigraphic indicator. Chlorite formation and preservation is favored by mild leaching conditions and an abundance of magnesium (Grim, 1968; Keller, 1970). The high chlorite content of the Aho here suggests that it was deposited in a semiarid, foreshore environment.

Sandia Formation

In Socorro County, the Sandia Formation (Pennsylvanian) consists of a basal conglomerate with chert boulders in a quartz-arenite matrix overlain by interbedded siltstones, quartz arenites, thin-bedded carbonaceous claystones, and thin limestones (Smith, 1983). These sediments were deposited in marine, near-shore/shelf environments. The limestones contain a diverse fauna of brachiopods, crinoids, corals, and gastropods. Dark-gray and brown carbonaceous claystones were sampled in the Loma de las Carias at the Houlett fireclay deposit (see discussion for Trip 2b, mile 17.5 on p. 29; Van Sandt, 1964), which was exploited in the late 1800's by the Socorro Fire Clay Works for brick making (Figs.. 1, 5). The clay mineralogy is uniformly dominantly kaolinite with lesser IiS and illite, regardless of the color of the sediments (Table 3). Little sodium smectite and no chlorite are present. The consistency of the clay mineralogy vertically and through the color variations suggests that the clays are mostly detrital and were not significantly affected

FIGURE 5—Dark-colored, carbonaceous claystones of the Sandia Formation at the Houlett fireclay deposit in the Loma de las Canas.

by diagenetic solutions responsible for color changes in the sediments.

Burlbaw and Siemers (unpubl. report 1975) analyzed dark-gray to black carbonaceous shales of the Sandia in the Joyita Hills by semi-quantitative XRD and found that they consist evenly of L'S and illite vertically and laterally. No kaolinite, smectite, or chlorite was found. The Sandia sediments in the Joyita Hills were deposited shoreward of those in the Loma de las Callas. Apparently, for reasons not known, the depositional conditions favored the deposition and preservation of illite nearer the shore and kaolinite basinward.

Conclusions

The primary conclusions reached from the semi-quantitative XRD analyses of the <2 micron-size fraction of the selected sedimentary rocks in Socorro County are:

1) Claystones from the playa fades of the Popotosa Formation (Miocene) southwest of Socorro consist dominantly of either illite or dioctahedral sodium smectite (montmorillonite). Variations in the observed clay mineralogy are reflected in color differences of the rock. After burial, the original clay mineral assemblage may have been potassium metasornatized by alkaline solutions descending into the subsurface from a younger playa.

2) The D-Cross Tongue of the Mancos Shale (Cretaceous) near Carthage is dominantly illite, with lesser VS and kaolinite.

3) Near Carthage, white kaolinitic claystones previously assigned to the base of the Dakota Sandstone (Cretaceous) may represent a weathering zone at the top of the Chink Formation (Triassic). Varicolored Chink claystones immediately underlying the Dakota are also kaolinitic, but they grade downsection into dominantly IIS and illite-bearing purple and gray claystones. The variable colors of the claystones may, in part, reflect differences in clay mineralogy, but *were* formed, most likely, by oxidation-reduction processes active when meteoric waters, descending along fractures and bedding planes, reacted with pyrite ancLor organic acids.

4) Sandy claystones in the Torres Limestone Member of the Yeso Formation (Permian) in the Loma de las Canas are illite with lesser, subequal amounts of chlorite and kaolinite. The clay mineralogy is uniform through color variations of green to red to white.

5) Claystones and fine-grained sandstones of the Abo Formation (Permian) in the Loma de las Canas and along US-380 east of Bingham uniformly consist of subequal amounts of illite and chlorite, regardless of the color of the sediments. Gray, green, and brown stringers, which cut across primary sedimentary structures, have clay mineral assemblages similar to the host sediments.

6) Bark-gray and brown carbonaceous claystones of the Sandia Formation (Pennsylvanian) at the Houlett fireclay deposit in the Loma de las Canas are uniformly mostly kaolinite with lesser US and illite.

7) The consistency of the clay mineralogy of the Yeso, Abu, and Sandia sediments vertically and through wide-ranging color variations suggests that most of the clays are detrital and were not significantly affected by diagenetic processes that changed the original color of the sediments.

Acknowledgments

We wish to thank the New Mexico Bureau of Mines and Mineral Resources, in particular, Drs. Frank Kottlowski, Director, and George Austin, Deputy Director, for supporting this work. Kent Cadey prepared oriented slide samples for x-ray analyses. George Austin ran the randomly oriented pressed powder XRD analyses of the tuff from the Luis Lopez Formation. Chris McKee, NMBMMR x-ray laboratory, ran the Socorro Mountain samples on the x-ray fluorescence.

References

Asher-Bolinder, S., 1982, Lithium-rich tuffs in the Popotosa Formation, New Mexico; *in* Austin, G. S., compiler, Industrial rocks and minerals of the Southwest: New Mexico Bureau of Mines and Mineral Resources, Circular 182, pp. 73-76.

Austin, G. S., Glass, H. U., and Hughes, R. E., 1987, Determination of polytype structure *of* some "1Md" illitic clays; in preparation.

Austin, G S., and Leininger, R. K., 1976, Effects of heat-treating mixed-layer illite-smectite as *related* to quantitative clay mineral determinations: Journal of Sedimentary Petrology, v. 46, pp. 206-215.

Brenner-Tourtelot, E. F., and Machette, M. N., 1979, The mineralogy and geochemistry of lithium in the Popotosa Formation. Socorro County, New Mexico: U.S. Geological Survey, Open-file Report 79-839, 23 pp.

Bruning, J. E., 1973, Origin of the Popotosa Formation, north-central Socorro County, New Mexico: Unpublished Ph.D. dissertation, New Mexico Institute of Mining and Technology, Socorro, 132 pp.; New Mexico Bureau of Mines and Mineral Resources, Open-file Report 38, 142 pp.

burlbaw, J., and Siemers, T., 1975, Clay mineralogy of Pennsylvanian and lower Permian beds, Joyita bills, Socorro County, New Mexico, unpublished report.

Cappa, J. A., 1975, Clay mineral assemblage variations in the lower Permian sedimentary rocks of the Sacramento Mountains, New Mexico, unpublished report.

Chamberlin, R. M., 1980, Cenozoic stratigraphy and structure of the Socorro Peak volcanic center, central New Mexico: Unpublished Ph.D. dissertation, Colorado School of Mines, Golden, 495 pp.; New Mexico Bureau of Mines and Mineral Resources, Open-file Report 118, 532 pp.

Chapin, C. F., and Lindley, J. I., 1986, Potassium metasomatism of igneous and sedimentary rocks in detachment terranes and other sedimentary basins—economic implications: Arizona Geological Society Digest, v. 16, pp. 118-126.

Chapin, C. E., and Seager, W. R., 1975, Evolution of the Rio Grande rift in the Socorro and Las Cruces areas: New Mexico Geological Society, Guidebook to 26th Field Conference, pp. 297-321.

Conran, I. P., 198(1. Socorro, a historic survey: University of New Mexico Press, Albuquerque, 124 pp.

D'Andrea-Dinkelman, J. F., Lindley, J. 1., Chapin, C. E., and Osburn, G. R., 1983, 'Me Socorro K0 anomaly—a fossil geothermal system in the Rio Grande rift: New Mexico Geological Society, Guidebook to 34th Field Conference, pp. 76-77.

Denny, C. S., 1940, Tertiary geology of the San Acacia area, New Mexico: Journal of Geology, v. 48, pp. 73-106.

Domski, P., 1987, The clay mineralogy of the Popotosa Formation as a function of the imposed geochemical parameters, unpublished report.

Droste, J. B., 1961a, Clay minerals in the playa sediments of the Mojave Desert, California: California Division of Mines, Special Report 69, 21 pp.

Droste, J. B., 196th, Clay minerals in the sediments of Owens, China, Searles, Panamint, Bristol, Cadiz, and Danby Lake Basins, California: Geological Society of America Bulletin, v. 72, pp. 1713-1721.

Eggleston, T. L., 1982, Geology of the central Cluipadera Mountains, Socorro County, New Mexico: Unpublished M.S. thesis, New Mexico Institute of Mining and Technology, Socorro, 155 pp.; New Mexico Bureau of Mines and Mineral Resources, Open-file Report 141, 162 pp.

Grim, R. E., 1968, Clay mineralogy: McGraw-Hill, Inc., New York, 2nd ed., 596 pp.

Hay, R. L., 1966, Zeolites and zeolitic reactions in sedimentary rocks: Geological Society of America, Special Paper 85, 130 pp.

Hay, R. L., 1978, Geologic occurrence of zeolites; in Sand, L. B., and Mumpton, F. A. (eds.), Natural zeolites-occurrence, properties, use: Pergamon Press, New York, pp. 135-143.

Hook, S. C., 1983, Stratigraphy, paleontology, depositional framework, and nomenclature of marine Upper Cretaceous rocks, Socorro County, New Mexico: New Mexico Geological Society, Guidebook to 34th Field Conference, pp. 165-172.

Hunt, A. P., and Lucas, S. G.. 1987, Triassic stratigraphy, Carthage area, Socorro County, New Mexico and the southeasternmost outcrops of the Moenkopi Formation (abs.): New Mexico Geological Society, Proceedings of 1987 Annual Spring Meeting, p. 47.

Keller, W. D., 1970, Environmental aspects of clay minerals: Journal of Sedimentary Petrology, v. 40, pp. 788-813.

Osborn, G. R., and Chapin, C. E., 1983, Ash-flow tuffs and cauldrons in the northeast Mogollon-Datil volcanic field-a summary New Mexico Geological Society, Guidebook to 34th Field Conference, pp. 197-204.

Osburn. G. K.. Petty, D. M., and Chapin, C. E., 1981, Geology of the Molino Peak quadrangle, Socorro-Magdalena area, Socorro County, New Mexico: New Mexico Bureau of Mines and Mineral Resources, Open-file Report 139a, 24 pp.

Patterson, S. H., and Holmes, R. W., 1965. Clays; in Mineral and water resources of New Mexico: New Mexico Bureau of Mines and Mineral Resources, Bulletin 87, pp. 312-322.

Picard, M. D., and High, L. K., Jr., 1972, Criteria for recognizing lacustrine rocks; *in* Rigby, J. K., and Hamblin, W. K. (eds.), Society of Economic Paleontologists and Mineralogists, Special Publication No. 16, pp. 108-145.

Sheppard, R. A., and Gude, A. J., 111,1968, Distribution and genesis of authigenic silicate minerals in tuffs of Pleistocene I.akeTecopa, Inyo County, California: U.S. Geological Survey, Professional Paper 597, 38 pp.

Smith, C. T., 1983, Structural problems along the east side of the Socorro constriction, Rio Grande rift: New Mexico Geological Society. Guidebook to 34th Field Conference, pp. 103-109.

Smith, C. T., Oshurn, G. R., Chapin, C. E., Hawley, J. W., Osburn, J. C., Anderson, 0. J., Rosen, S. D., Eggleston, T. I.., and Cather, S. M., 1983, First day road log from Socorro to Mesa del Yeso, Joyita Hills, Johnson [till, Cerros de Amado, Lomas *[sic]* de las Jornado *[sic]* del Muerto, Carthage, and return to Socorro: New Mexico Geological Society, Guidebook to 34th Held Conference, pp. 1-28.

Smith, E. W., 1982, Large-scale adobe-brick manufacturing in New Mexico; *in* Austin, G. S. (compiler), Industrial rocks and minerals of the Southwest: New Mexico Bureau of Mines and Mineral Resources, Circular 182, pp. 49-56.

Speer, S. W., Broadhead, R. F., and Kottlowski, F. E., 1983, Road log-second day-Socorro to Bingham, Bent, and to the northern Sacramento Mountains; *in* Guidebook for field trip to the Abu red beds (Permian), central and south-central New Mexico: Roswell Geological Society and New Mexico Bureau of Mines and Mineral Resources, pp. 15-44.

Surdam, R. C., and Sheppard, R. A., 1978, Zeolites in saline, alkaline-lake deposits; *in* Sand, L. B., and Mumpton, F. A. (eds.), Natural zeolites-occurrence, properties, use: Pergamon Press, New York, pp. 145-174.

Talmage, S. B., and Wootton, T. P., 1937, The non-metallic mineral resources of New Mexico and their economic features (exclusive of fuels): New Mexico Bureau of Mines and Mineral Resources, Bulletin 12, 159 pp.

Van Sandt, J., 1964, Refractory clays of Arizona and New Mexico: U.S. Bureau of Mines, unpublished manuscript.

Yoder, H. S., and Eugster, H. P., 1955, Synthetic and natural muscovites: Geochimica et Cosmochimica Ada, v. 8, pp. 225-280.

Geomorphic evolution and soil-geomorphic relationships in the Socorro area, central New Mexico

by Daniel B. McGrath' and John W. Hawley'
'Camp, *Dresser & McKee, Inc., Denver, Colorado 80202 and 'New Mexico Bureau of Mines and Mineral Resources, Socorro, New Mexico 87801*

Introduction

The tour stops on Trips 2a-d of the 1987 Clay Minerals Society annual meeting (this volume) offer excellent vantage points for reviewing the late Cenozoic geomorphic evolution of the Socorro area. This region is the site of pioneering studies on desert-basin geomorphology and hydrogeology by Kirk Bryan (1938) and his students. Much of the early geomorphic research in this area was done by Denny (1940, 1941) and Wright (1946). Recent detailed studies have been made by Machette (1978a, b, c, 1986), and Love and Young (1983). Regional overviews include reports by Hawley et al. (1976), Hawley (1978), and Machette (1985). Machette's work deals not only with geomorphology and late Cenozoic geology, but also with soil-geomorphic relationships and soil stratigraphy. Unpublished work by R. M. Chamberlin on the geology of the Socorro area provided much of the subsurface information and structural interpretations used in preparation of the diagrammatic cross section of the Rio Grande valley (Fig. 1).

Most of the clay mineral analyses and interpretations of soil-clay mineral genesis presented in this paper *were* done by D. B. McGrath as part of a special graduate research project at New Mexico Tech in 1985. Additional information on soil-clay mineral distribution and genesis has been provided by B. G. Jones as part of a clay minerals class project (New Mexico Tech, 1987). The soil survey of Socorro County has been completed recently by the U.S. Soil Conservation Service and cooperators in other federal and state agencies, but it is still unpublished. However, the soil survey manuscript is available for review and was also utilized in the preparation of this paper.

Geomorphic setting

intermontane basin tills and associated geomorphic surfaces of the Socorro area are excellent examples of upper Cenozoic deposits and arid to semiarid landscapes in the Mexican Highland section of the Basin and Range Province (Hawley, 1986a, b). Major mountain and basin landforms are volcano-tectonic features of the Rio Grande rift subprovince (Chamberlin, 1981; Chapin, 1983) that essentially formed by the early Pliocene (4 to 5 m.y. ago). The bulk of the intermontane basin fill (Santa Fe Group) was emplaced by early Pleistocene (>0.75 m.y.), and erosional valleys of the Rio Grande and major arroyo tributaries have only developed in the past half million years. Early rift-basin deposits comprise bolson fill and interbedded volcanics of late Oligocene and Miocene age (lower Santa Fe Group-Popotosa Formation) and are, for the most part, deeply buried by younger basin and valley fills. The older deposits are best exposed in structural uplifts in and adjacent to mountain ranges west of the Rio Grande and are derived from geologic terranes partly obliterated by subsequent tectonism, volcanism, erosion, and burial. Widespread playa-lake deposits in bolson-floor fades assemblages demonstrate that a regional system of through drainage was not present during Miocene and late Oligocene time.

In terms of hydrologic and biologic environments, the physiographic setting during ()Bo-Pleistocene time was probably quite similar to that of the late Quaternary. Paleontological evidence and "caldc" paleosols associated with buried and relict geomorphic surfaces indicate that prevailing climates were semiarid to arid. The stratigraphic record in the form of basin and valley fills clearly shows that ephemeral, high-gradient streams (commonly fan distributaries) dominated piedmont-slope depositional environments, while a perennial, low-gradient fluvial system (the ancestral Rio Grande) and local playa lakes occupied basin floors.

The diagrammatic cross section (Fig. 1) from La Jencia Basin (Trip 2a, Stop 2-1—"Sedillo I sill" surface) across the Rio Grande valley to the Loma de las Canas (Stop 2-2—"Las Callas" surface) illustrates the complex history of basin formation and filling as well as the episodes of middle to late Quaternary valley entrenchment. The earliest ancestral-river deposits (early Pliocene, -.3.5 to 4.5 'my.), which form the lower part of the Sierra Ladrones Formation (upper Santa Fe Group) of Machette (1978b, c), were probably first emplaced along the western margin of the basin (Fig. 1, unit 1). They are now partly incorporated in the uplifted Socorro Mountain block (north of Socorro Canyon; Fig. 1). Sierra Ladrones fluvial sands, exposed along lower Arroyo de la Parida near Pueblito (Trip 2b, mi 2.25, p. 26), contain a Blancan vertebrate fauna of late Pliocene to early Pleistocene age (more than 1.5 m.y.; Tedford, 1981). This unit ((?) on Fig. 1) is extensively preserved in bluffs east of the Rio Grande and intertongues with fan deposits of the eastern piedmont facies of the Sierra Ladrones Formation (seen at Stops 2-2 and 2-3 along Arroyo de las Catlas and Arroyo del Tajo). Between 1.5 and 0.5 m.y. ago the ancestral river continued to deliver sandy sediments to an aggrading central basin floor (Q) on Fig. 1). Volcanic ash and pumice from caldera-forming and intra-caldera eruptions in the Jemez Mountains of northern New Mexico are present in upper Sierra Ladrones fluvial deposits at at least two sites in the Socorro area (Izett et al., 1981). These tephra lenses were deposited by air-fall and debris-flow mechanisms between about 1.5 and 1.1 m.y. ago during the early Pleistocene.

Geologic and soil-geomorphic studies throughout the Albuquerque to El Paso reach of the upper Rio Grande valley indicate that culmination of basin filling and the end of Santa Fe Group deposition occurred about 0.4 to 0.5 m.y. ago (Hawley et al., 1976; Hawley, 1978; Gile et al., 1981; Machette, 1985). The "Sedillo Hill" (Stop 2-1, p. 23) and "Las Cafias" (Stops 2-2 and 2-3, pp. 28, 36) geomorphic surfaces west and east of the river valley, respectively, approximate the ultimate level of piedmont-slope aggradation in the La Jencia, Socorro, and Jornada del Muerto Basins. These surfaces appear to correlate with the Llano de Albuquerque and Jornada I-Lower La Mesa geomorphic surfaces in the Albuquerque and southern Jornada Basins. The history of late stages of basin filling was complicated by recurrent structural deformation (Machette, 1978a, 1986), as well as by shifts in paleohydrologic regimes and effectiveness of vegetation cover.

The present Rio Grande valley (s on Fig. 1), is a narrow erosional feature of a river system that is just beginning to

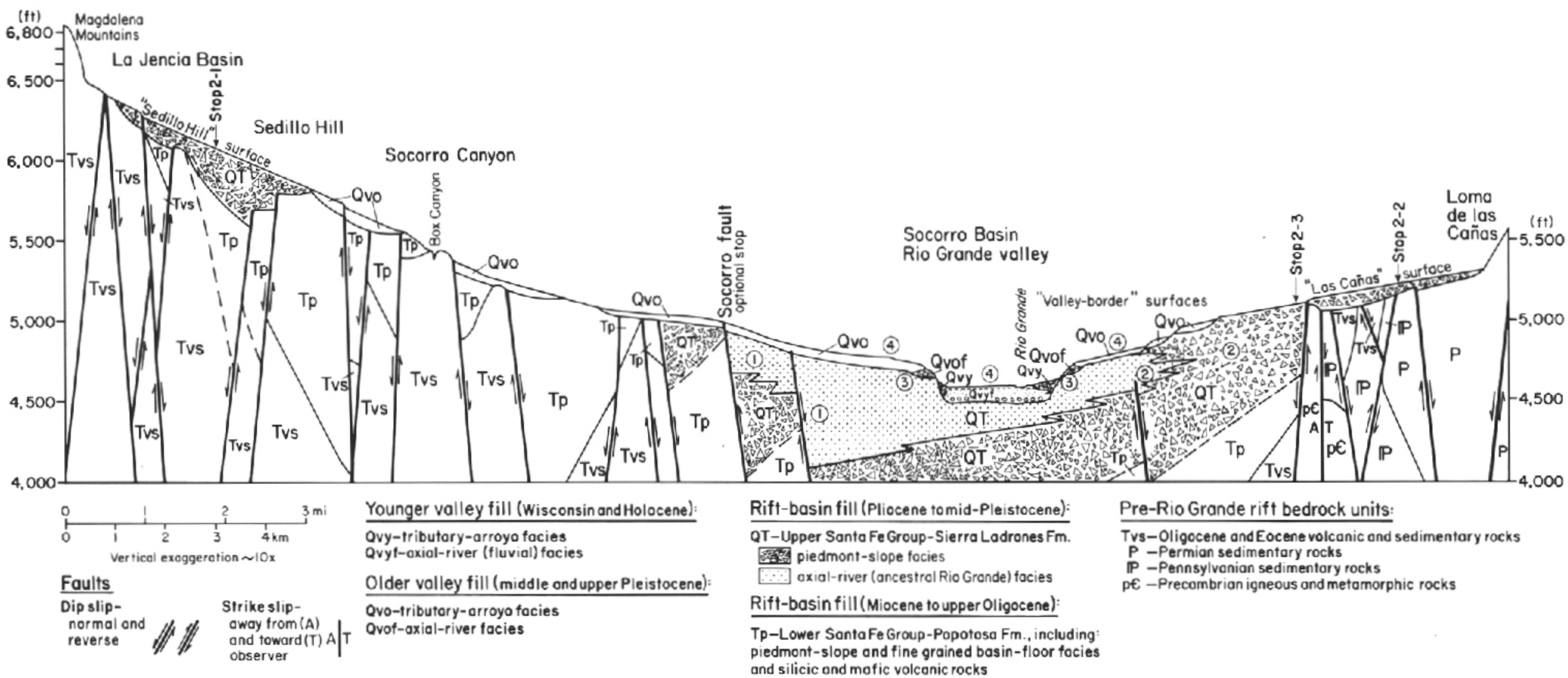

FIGURE 1—Diagrammatic cross section across the Socorro Basin from east-central Magdalena Mountains, west of Sedillo Hill, to western Loma de las Cañas, including the area of Stops 2–1, 2–2, and 2–3 (pp. 23, 28, and 29). The encircled numbers represent units discussed in the text.

entrench itself in an enormous volume of ancient fluvial deposits (upper Santa Fe Group). A stepped sequence of graded ("valley-border") surfaces flanking the modern floodplain, and an erosion surface about 100 ft below the valley floor represent at least four major episodes of river-valley entrenchment. Each of these episodes was followed by long intervals of partial valley backfilling or relatively steady-state conditions with respect to local floodplain base level. Times of widespread valley incision appear to correlate with major expansions of pluvial lakes and alpine glaciers in the eastern Basin and Range and Southern Rocky Mountain provinces (e.g., parts of marine-oxygen-isotope stages 2, 6, 8, 12-14). The extensive remnants of "valley-border" surfaces in this region represent long periods of relative base level stability and surface aggradation subsequent to the major episodes of valley entrenchment (Hawley et al., 1976). These depositional periods probably reflect environments between full-glacial substages when smaller tributary drainage systems delivered more sediment to valley floors and adjacent piedmont slopes than master streams could remove from the upper Rio Grande Basin (parts of 0-isotope stages 1, 3-5, 7, 9-11).

Some principles of soil development in an arid to semiarid area of central New Mexico

The basic principle of soil development in arid and semiarid regions is that precipitation does not remove free cations from the soil during most years. Thus, the soil solution becomes concentrated and alkaline. Weathering proceeds at an extremely slow rate. Gile (1975, 1977), Gile and Grossman (1979), and Gile et al. (1981) provide a large amount of information on soils and soil-geomorphic relations in the arid to semiarid Desert Project region of south-central New Mexico. The following brief overview covers general soil-forming factors and diagnostic-horizon characteristics in the Socorro area. Preliminary data on clay minerals in soils of mid-Pleistocene surfaces (Stops 2--1, 2 2, and 2-5) will also be discussed.

Basin and valley fills of the Socorro area are derived from carbonate rocks (partly dolomitic), sandstone, mudstone, and gypsite of Paleozoic age, Mesozoic sandstone and mudstone, and Cenozoic volcanic and nonmarine sedimentary rocks. The upper Tertiary Quaternary stratigraphic record comprises alluvial, colluvial, lacustrine, and eolian sediments as well as basaltic and silicic volcanics deposited in a tectonically active, intermontane basin and stream-valley setting.

Topographic features range from broad, relatively undissected floors and piedmont slopes, in basins still not integrated with the Rio Grande valley system, to dissected "valley-border" terrains with large local relief and extensive areas of active erosion and sedimentation. Throughout the Holocene the broad Rio Grande valley floor has been the site of active channel and floodplain aggradation, with alluvial fans of tributar v-arrovo systems encroaching on the floodplain margins.

The Rio Grande valley and higher intermontane basin surfaces of the Socorro area have an arid to semiarid climate with mean annual precipitation of about 8-13 inches (20-33 cm) and mean annual temperature of about 50-61 F (10-16'C). Soil and temperature classes include the thermic to mesic transition, and soil-moisture regimes range from aridic (torric) to ustic to possibly xeric. The arid to semiarid. thermic to mesic, and aridic to ustic transitions at this latitude (34' north) occur in the 5,000-6,000 ft (1,524 1,829 m) range. Cooler and moister conditions existed during Wisconsin and earlier Pleistocene glacial-pluvial stages. Xeric moisture regimes may have been prevalent due to shifts from summer-fall-dominant to winter-spring-dominant precipitation. Interglacial temperature and moisture regimes are typified by the warm-dry Holocene and Sangamon intervals (past 10,000 yrs and about 120 to 130 ka, respectively; 0-isotope stages 1 and 5e) are probably not typical of long-term Quaternary environments in this part of the Basin and Range Province (Spaulding, 1984; Van Devender, 1985).

The present vegetative cover is dominated by desert shrubs, grasses, annuals, cacti. and trees of the pifion-juniper zone. During the Pleistocene glacial-pluvial intervals grasslands and mixed forest-grassland were much more extensive at lowland sites. Faunal influence on pedogenesis includes subsurface activity of insects and burrowing vertebrate forms; ubiquitous soil microorganisms also play a major, but often poorly documented, role in desert soil formation.

Tour stops on Trips 2a and 2b emphasize ancient soil landscapes on relict geomorphic surfaces that have been essentially stable for hundreds of thousands of years. Soils examined are associated with piedmont slopes that represent culminating stages of early to middle Pleistocene basin aggradation (upper Santa Fe Group-Sierra Ladrones Formation deposition). These geomorphic surfaces, informally designated "Sedillo Hill" and "Las Cafias" (Fig. 1) include deeply dissected fans and rock pediments that predate mid- to late-Pleistocene entrenchment of the present river-valley system.

Surface soil horizons in arid and semiarid parts of the Socorro area tend to 1) be low in organic matter except on higher undissected basin surfaces, 2) have variable (alkaline to slightly acid) soil solutions, 3) be easily eroded at many sites with sparse vegetative cover, 4) have a thin surface crust at such sites, 5) be exposed to extreme temperature variations, and 6) receive atmospheric fallout (aerosol contributions). Subsurface horizons have fewer oscillations in temperature and soil solution, but are wetted to different depths by each precipitation event. Calcite precipitates in the subsurface of all arid-region soils. Clay translocation occurs, as evidenced by the strong argillic horizon at Stop 2-1, but secondary carbonate commonly disrupts argillans or engulfs argillic horizons. Clay neoformation is possible if soil solution exists for a long enough time at great enough concentrations. Some common horizonation sequences observed are shown in Figure 2. For additional explanation on soil-horizon and fabric nomenclature, see Soil Survey Staff (1975, 1981), Brewer (1976), and Cornell University Agronomy Department (1986).

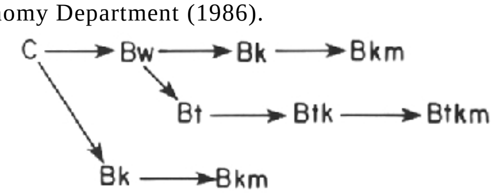

FIGURE 2—Parent material (C), with continued addition of aerosols to a stable geomorphic surface, transforms to cambic (Bw) to calcic (Bk) to petrocalcic (Bkm) horizons, *or* from cambic (Bw) to argillic (Bt) to argillic overprinted with calcic (Btk) to petrocalcic (Btkm) horizons, *or* directly to calcic (Bk) to petrocalcic (Bkm) horizons.

Pedogenic horizons of carbonate accumulation

caliche is the common term used to describe near-surface accumulations of secondary calcium carbonate of both pedogenic and nonpedogenic origin in the American Southwest (Bretz and Horberg, 1949; Aristarain, 1970; Reeves, 1970; Gardner, 1972; Frye et al., 1974). Nonpedogenic varieties formed mainly by precipitation of calcite by deeply percolating subsurface water in both the vadose and underlying saturated (ground-water) zones. Many fanglom erates, conglomerates, and sandstones in the upper Santa Fe Group basin-fill sequence have been cemented by this process, and, where exposed, may be misinterpreted as pedogenic carbonate horizons. These rocks are also transitional to travertine deposits in areas of active or prior spring discharge (Bachman and Machette, 1977; Barker, 1983; Carlisle et al., 1978).

Bates and Jackson (1980) define *calcrete* as a "calcareous duricrust" and a *duricrust* as "a general term for a hard crust . . . or layer in the upper horizons of a soil in a semiarid climate." Calcrete (Lamplugh, 1902; Goudie, 1973) is now commonly used as a synonym for indurated forms of caliche in the southwestern United States (McGrath and Hawley, 1985; Machette, 1985; Sowers, 1985). The general term "calcic soil," introduced by Bachman and Machette (1977), refers to all soils with readily identifiable amounts of illuvial carbonate in the B-horizon position, whether nonindurated or indurated (Bk and Bkm horizons; previously designated Bca, Cca. and Ccam horizons). Soils with calcic and petrocalcic horizons, as well as weaker accumulations of secondary carbonate, are included in the broad "calcic soil" category (Machette, 1983; Gile, 1987).

Gile (1961, 1975, 1977) and Gile et al. (1965, 1966) developed many of the fundamental principles of carbonate horizon genesis and classification in soils of arid and semiarid regions. Their model for soil-carbonate accumulation is described by a bimodal, four-stage (1-IV), morphogenetic sequence for both gravelly and nongravelly parent sediments (Gile et al., 1966). Bachman and Machette (1977), and Machette (1985) expanded this scheme to a six-stage morphogenetic sequence, with stages V and VI used to characterize very strong and morphologically complex pedogenic calcretes (caprock caliches) of the American Southwest. This scheme, as adapted by McGrath and Hawley (1985) is presented in Table 1.

Stages I and II are initial phases of soil-carbonate illuviation and result in the formation of weaker Bk horizons that usually are not diagnostic in soil classification. Nonindurated carbonate accumulations that qualify for calcic horizon designation commonly exhibit stage III morphology. A nearly continuous fabric of carbonate-coated clasts and carbonate-filled voids (K-fabric of Gile et al., 1965) and initial development of irreversible cementation (induration) characterize late stage HI. This incipient phase of petrocalcic horizon and calcrete formation may be followed by stage IV, which is characterized by an indurated layer of dense, multiple-laminar K-fabric that caps the massive to nodular "carbonate-plugged" horizon. Stage IV marks the initial formation of "caliche profile" as defined by Lovelace (1972). Stage V includes development of a thicker "caprock caliche" layer, with several multiple-laminar subhorizons, followed by initial fracturing of this zone and development of coarse-platy structure and zones of brecciation andlor dissolution. Recementation of hrecciated material and solution-rounded fragments to form a pisolitic fabric and additional cycles of brecciation and cementation occur in stage VI. Very long intervals of soil-landscape stability (>10' to 10' yrs) and major changes in paleohydrologic conditions are reflected in the thickness and complexity of the caprock layer in calcretes with stage V and VI morphology.

Soils with petrocalcic horizons, marking the stage III to IV transition, are widely developed on Pleistocene geomorphic surfaces in this region while "calcic soils" with weaker expression of pedogenic carbonate (stages Ito III) are nearly ubiquitous (Machette, 1985). Petrocalcic horizons (pedogenic calcretes) with stage IV to V morphology are locally present ("Las Callas" surface, Stop 2-2), but only on surfaces of mid-Pleistocene or older age (e.g., La Mesa and Jornada 1 surfaces of the Desert Project area; Gile and Grossman, 1979; Gile et al., 1981). Stage VI calcretes are almost everywhere restricted to soils whose formation started in Pliocene to late Miocene time (1.7 to 7 m.y. ago). The only extensive soil landscape (relict and buried) that is preserved in the Southwest is on the Southern High Plains (Llano Estacado) of Texas and New Mexico. However, ancient soils with stages V and VI carbonate morphologies are locally preserved throughout the Basin and Range Province from Trans-Pecos Texas and New Mexico to southern Nevada (Bretz and Horberg, 1949; Gile, 1961; Reeves, 1970; Gardner, 1972; Lattman, 1973; Machette, 1985). In addition to cited publications, recent theses by McGrath (1984), Sowers (1985), and Chitale (1986) give an excellent overview of current research on pedogenic calcretes.

TABLE 1—Stages of carbonate accumulation in gravelly and nongravelly morphogenetic sequences of *calcrete* development.

Stage and general character	Diagnostic carbonate morphology: Gravelly sequence	Diagnostic carbonate morphology: Nongravelly sequence
I Weakest expression of macroscopic carbonate	Thin, discontinuous coatings on gravel clasts	Few filaments or faint coatings on ped surfaces
II Carbonate segregations separated by low-carbonate fabric	Continuous coatings on clasts, some interdast fillings	Few to common nodules
III Carbonate essentially continuous; plugged horizon forms in last part	Many interpebble fillings Upper part of horizon essentially plugged	Many nodules and internodular fillings
IV Laminar horizon develops over plugged horizon; incipient calcrete formation; forms caprock layer up to 0.5 m thick	Indurated laminar horizon over plugged horizon; thin upper zone of platy structure over zone with massive to nodular structure; grades downward into gravelly or nongravelly material with stage III morphology; incipient "caliche profile" of Lovelace (1972) and pedogenic calcrete	
V Multiple laminar horizon develops in upper part of profile; incipient development of degradational features; forms caprock layer up to 2 in thick	Thick, well-indurated upper horizon; platy to tabular structure with multiple laminar internal fabric; zones of dissolution, brecciat ion, and recementation locally present; dry hulk densities up to 2.2 grcm'	
VI Brecciation, dissolution and recementation of upper, multilaminar horizon; multiple generations of calcrete formation and degradation; forms caprock layer up to 4 m thick	Very thick, well-indurated, upper horizon; tabular to platy structure, with pisolitic and multilaminar internal fabric; secondary silica common; dry hulk densities 2.2-2.7 gi cm'	

Clay minerals in mid-Pleistocene soils of the Socorro area

Clay minerals in horizons of carbonate accumulation in soils of the American Southwest have received much attention since early studies of Desert Project calcretes by Vanden Heuval (1966). Of particular interest are authigenic clays of the smectite, illite-smectite (US), and palygorskite-sepiolite (chain-lattice or hormite-clay) groups that commonly occur in both soils and alkaline-lake deposits of the Basin and Range Province, Southern Great Plains l'rovince, and elsewhere in arid and semiarid regions of the world (Parry and Reeves, 1968; Martin-Vivaldi and Robertson, 1971; Gardner, 1972; McLean et al., 1972; Papke, 1972; Frye et al., 1974; Bachman and Machette, 1977; Post, 1978; Bigham et al., 1980; Hay and Wiggins, 1980; Khoury et al., 1982; Jones, 1983; Birkeland, 1984; McGrath, 1984; Sowers, 1985). Models of clay mineral neoformation and transformation in "calcic soils" of arid and semiarid regions are outlined briefly in Table 2.

The relative depletion of sepiolite and palygorskite, particularly sepiolite, with increasing amounts of smectite and associated expansive clays in pedogenic calcretes has been observed by many workers including Frye et al. (1974), Yaalon and Wieder (1976), Bachman and Machette (1977), Bigham et al. (1980), and Jones (1983). Jones (1983) and most other workers (Table 2) consider that neoformation (direct precipitation) of chain-lattice clays can occur in dry-land soils where controlling geochemical parameters (soil-water pH, magnesium, and silica activities, etc.) are at optimum levels. Jones (1983) concluded that the formation of I'S intergrades or interstratifications in pre-existing smectite has competed with neoformation of chain-silicate phases in arid pedogenic environments.

Frye et al. (1974), Bachman and Machette (1977), and

TABLE 2—Models of sepiolite and palygorskite formation in soils of arid and semiarid regions—an overview.

Researcher(s)	Models and regions
Vanden Heuvel (1966)	Formed penecontemporaneously with calcic and petrocalcic horizon development by an unknown mechanism and was later mechanically concentrated within dissolution voids during wetter periods. Desert Project area, southern New Mexico
Gardner	1) detrital component of the parent material, 2) mechanically infiltrated clay derived from colian additions, 3) transformational products from chemical weathering of detrital minerals, 4) "Chemical precipitation of dissolved impurities from evaporating rain water in the soil. Mormon Mesa area, southeastern Nevada
McLean et al.	Transformational product occurring in association with volcanic ash. Texas High Plains
Eswaran and Barzanji (1974) Singer and Norrish	Neoformation (direct precipitation) of palygorskite is possible (if appropriate soil solution exists) in a thin surficial layer characterized by infrequent saturation. Apparent palygorskite-gypsum relationship noted by Eswaran and Barzanji. Middle East, Australia
Frye et al.	Transformation of detrital smectite to palygorskite; in the lower part of caprock caliche profiles in a high magnesium environment; locally associated with formation of opal. Southern Great Plains
Yaalon and Wieder (1976)	Neoformation of palygorskite with Mg supplied by weathering of Mg-carbonates. "The montmorillonite Ito] palygorskite transformation, provided additional Mg is available, seems to be a distinct possibility. . ." Possible relationship between pedogenic gypsum and palygorskite. Israel
Bachman and Machette (1977)	Mineral transformation over hundreds of thousands of years of geologic time and increasing content of calcium carbonate; smectite or mixed-layer clays alter to palygorskite and then to sepiolite. American Southwest

Researcher(s)	Models and regions
Elprince et al. (1979)	Pedogenic palygorskite formed (via the soil solution) at the expense of smectites inherited from the underlying formation. Saudi Arabia
Singer (1979)	Palygorskite precipitates directly from solution in near-surface materials. Overview of arid regions
Bigham et al. (1980)	Neoformation of sepiolite and especially palygorskite can occur; however, these minerals appear to be actively degrading to mixed-layer clays and poorly crystallized material in present-day environments. Semiarid Texas High Plains
I lay and Wiggins (1980)	Sepiolite is the result of precipitation from solution. American Southwest
Khoury et al. (1982)	1) Neoformation by direct precipitation, 2) dissolution of mixed-layer kerolite/stevensite via a dilute ground water. Southwestern Nevada
Viani et al. (1983)	Inherited from colian additions. Saudi Arabia
Jones (1983)	Neoformation of chain-silicate clays in calcic soils by direct precipitation; process enhanced by presence of dolomitic sedimentary and silicic volcanic rocks and calcareous sepiolitic aerosols. Southwestern Nevada
Norrish and Pickering (1983)	Neoformation model supported. Australia; overview of arid-zone soils
Paquet (1983)	Palygorskite formation occurred before or penecontemporaneous with calichification; with increased degree of caliche development, the carbonate replaces the palygorskite. North Africa
McGrath (1984)	"Hormites" form by precipitation (neoformation) in a caliche after an induration threshold is exceeded because moisture is available over a longer time, during which reactions can occur. Southern Great Plains

Bigham et al. (1980) found an increase of palygorskite with depth in well-developed calcic and petrocalcic horizons of the New Mexico-western Texas region; and they also found sepiolite to be most abundant in the middle to lower horizons of the pedons examined. Bachman and Machette (1977) presented a general mineral transformation model in which smectite or US transforms to palygorskite, which in turn is converted to sepiolite. Occurrence of the latter mineral is associated with very ancient soil landscapes and depth zones in petrocalcic horizons where calcium carbonate precipitation and soil-water infiltration are most active. Bigham et al. (1980) point out the sepiolite and palygorskite do not appear to be stable in modern semiarid environments of the Texas High Plains. The geochemical and morphological implications of their work are that these minerals are actively degrading to less well structured IIS and poorly crystallized material. However, they do not argue against neoformation of pedogenic sepiolite and, especially, palygorskite at other places or times.

Profiles of five representative "calcic soils" at or near Stops 2-1, 2-2, and 2-5 are described in Tables 3-7 (pedons la, lb, 2a, 2h, and 3). Figures 3-6 are photographs that illustrate soil-geomorphic and stratigraphic relationships at the field trip stops (pedons la, lb, 2a, and 3). Preliminary interpretations of x-ray diffraction (XRD) analyses of samples from the Paleargids and Paleorthids described at or near Stops 2-1, 2-2, and 2-5 are given in Table 8 (pedons la, 2a, 2h, and 3, respectively). Field and laboratory methodology are discussed below. Inferred distribution of smectite, illite, chlorite, kaolinite, sepiolite, and palygorskite clays, as well as quartz and dolomite, are presented in this table. It must he re-emphasized that these interpretations are very preliminary and may be significantly modified during future, more detailed investigations. However, the chain-silicate (hormite) clays are definitely a substantial component of well-developed soil carbonate horizons that were sampled for this study. The preliminary XRD data on sepiolite occurrence is also supported by use of methyl orange (method described by Hay and Wiggins, 1980; McGrath, 1984; and Sowers, 1985) for rapid field (and laboratory) identification of major zones of sepiolite accumulation in strong soil-carbonate horizons.

The mineralogical contrast between soils of the "Sedillo Hill" (Stop 2-1) and "Las Callas" (Stops 2-2 and 2-5) geomorphic surfaces is striking, particularly when data on smectite and mixed-layer L'S clays are compared with information on sepiolite and palygorskite (Table 8). While both soil landscapes (Figs. 1, 3-6) have been in a relict surface position for about 0.5 m.y., the long-term paleoclimatic setting of the "Sedillo Hill" surface (I.a Jencia Basin, elev. _6,000 ft, 1,829 m) is distinctly less arid and cooler than the "Las Can as" surface (Socorro and Jumada Basins, elev. L5,000 ft, 1,524 m). Furthermore, the "Sedillo Hill" surface at Stop 2-1 is underlain by basin fill derived primarily from silicic volcanic rocks, and dynamic aerosol components of soil parent materials appear to be very low in carbonates relative to nearby valley and basin areas. Major soils in the vicinity of Stop 2-] (Figs. 3 and 4; Tables 4 and 5) have thick, noncalcareous zones in the upper A and (argillic) B position where pH is commonly neutral to slightly acid.

Contrasting soil landscapes of the "Las Callas" surface area, east of the Rio Grande (Figs. 1, 5, and 6) are underlain by basin fill derived from sedimentary and local volcanic terranes that mainly contribute fragments of limestone, dolomite, and calcareous clastic rocks to soil parent materials. Atmospheric additions are also more calcareous in the Socorro Basin area, particularly east (seasonally downwind) of the Rio Grande; and the soil solution is significantly more alkaline than in the southern La Jencia Basin (Fig. 1; Stop 2-1). It has also been noted that beds of volcanic ash and pumice, derived from caldera-forming eruptions in northern New Mexico (Izett et al., 1981), and from elsewhere in the western United States (Hawley et al., 1976; Hawley, 1978; Izett, 1981), are common constituents of axial-river and piedmont facies of the upper Santa Fe Group. These deposits include the upper Sierra I.adrones Formation in the Socorro Basin.

TABLE 3—Field morphological description of Paleargid (pedon la) at Stop 2-1 (p. 23).

Classification:	Ustollic Paleargid; clayey, mixed, mesic
Location:	NW'14, NE' /4, SW' /4, sec. 27, T3S, R2W; in roadcut on west side of US -60 at crest of Sedillo Hill (10 mi west of Socorro)
Geomorphic surface (age):	"Sedillo 11111" (early middle Pleistocene)
Land form:	piedmont slope, medial position; relict alluvial fan
Slope:	4 percent (eastward)
Elevation:	6,095 ft (1,858 in)
Parent material:	Sierra Ladrones Formation, upper piedmont facies; fine loamy to gravelly fan alluvium, primarily derived from silicic volcanic terrane (mid-Tertiary) in east-central Magdalena Mountains; with calcareous aerosol contributions.
Vegetation:	grasses, cacti, annuals
Described by:	D. A. McGrath (7/26/85)
Sampled by:	D. A. McGrath (7i26/85)
Horizon	
A	0-10 cm; dark brown (7.5YR 4i4) silt loam, dark brown (7.5YR 213) moist; weak granular and fine subangular blocky; soft; noncalcareous; few roots to many roots under grass bunches; clear, smooth boundary.
BAt	10-27 cm; reddish brown (5YR 4/4) silty clay, dark reddish brown (5YR 34) moist; weak medium subangular blocky, breaking into moderate very *fine* angular blocky; very hard; noncalcareous; few faint clay films; 10 percent ash-flow-tuff fragments; many tine to medium roots; clear, smooth boundary.
Btkl	27-41 cm, dark red (2.5YR 3/6) clay; weak medium subangular blocky, breaking into moderate very fine angular blocky; very hard; effervesces strongly; distinct clay films on ped faces and rock fragments; carbonate rinds coat clay-film-coated rock fragments; 10 percent ash-flow-tuff fragments; clear, smooth boundary.
Btk2	41-55 cm; red (2.5YR 4/6) gravelly clay, dark red (2.5YR 3/6) moist; moderate medium subangular blocky; very hard; very plastic; effervesces violently; distinct clay films on pod faces and rock fragments; common carbonate nodules; 20 percent ash-flow-tuft fragments, few medium roots; abrupt, wavy boundary.
Btk3 (K)	55-79+ cm; pink (5YR 74) clay yellowish red (5YR 5/6) moist; massive; very hard to indurated (calcrete); plastic; effervesces violently; 60 percent argillic fragments engulfed by carbonate along ped faces; plugged with secondary carbonate; few medium roots.
Remarks:	Calcic horizon, with late stage 111 carbonate morphology (Gile et al., 1966) below 55 cm. Preliminary interpretation of clay mineral distribution by D. A. McGrath and G. S. Austin (Table 8).

The clay mineral assemblages in soils described in this paper are quite similar to occurrences discussed by other workers who have dealt with soil-clay relationships in similar geomorphic and geologic settings (Table 2). The work of Jones (1983) and Bigham et al. (1980) is particularly pertinent to the interpretations of preliminary data on soil-

TABLE 4—Field morphological description of Paleargid (pedon 1b) near Stop 2-1 (p. 23).

Classification:	Ustollic Paleargid; clayey, mixed, mesic
Series:	Magdalena
Location:	SW¼, SE¼, SW¼, sec. 34, T3S, R2W; 1.3 mi south of Sedillo Hill (US-60, 10 mi west of Socorro) and 0.3 mi south of Sixmile Canyon
Geomorphic surface (age):	"Sedillo Hill" (early middle Pleistocene)
Land form:	piedmont slope, medial position; relict alluvial fan
Slope:	6 percent (eastward)
Elevation:	6,120 ft (1,865 m)
Parent material:	fan alluvium primarily derived from silicic volcanic terrane (mid-Tertiary) in east-central Magdalena Mountains; with calcareous aerosol contributions.
Vegetation:	grasses, juniper, cacti, annuals
Described by:	Cooperative Soil Survey Staff (1/13/77)
Sampled by:	Cooperative Soil Survey Staff (1/13/77)
Horizon	
A	0–5 cm; yellowish red (5YR 5/6) gravelly loam, dark reddish brown (5YR 3/4) moist; weak fine platy and weak fine granular structure; loose, very friable, slightly sticky and slightly plastic; many very fine and fine roots; 20 percent pebbles and 5 percent cobbles; neutral; abrupt, smooth boundary.
Bt1	5–18 cm; reddish brown (5YR 4/4) very gravelly sandy clay, dark reddish brown (5YR 4/4) moist; moderate medium subangular blocky structure; slightly hard, friable, sticky, and plastic; many fine and very fine roots; few thin clay films on faces of peds; 35 percent pebbles and 5 percent cobbles; slightly acid; abrupt, wavy boundary.
Bt2	18–36 cm; yellowish red (5YR 4/6) very gravelly clay loam, reddish brown (5YR 4/4) moist; moderate medium subangular blocky structure; hard, friable, sticky, and plastic; common fine and very fine roots; common thin clay films on faces of peds; 40 percent pebbles and 5 percent cobbles; slightly acid; abrupt, wavy boundary.
Bt3	36–58 cm; yellowish red (5YR 4/6) very gravelly clay, moderate fine subangular blocky structure; hard, friable, very sticky, and very plastic; common fine and very fine roots; common moderatelv thick clay films on faces of peds; 45 percent pebbles and 5 percent cobbles; neutral; clear, wavy boundary.
Bt4	58-76 cm; dark red (2.5YR 3/6) very gravelly clay; strong medium angular blocky structure parting to strong fine angular blocky, very hard, firm, very sticky, and very plastic; few fine and very fine roots; continuous, thick clay films on faces of peds; 35 percent pebbles and 5 percent cobbles; neutral; clear, wavy boundary.
Bt5	76-91 cm; red (2.5YR 4/6) gravelly clay; strong, coarse prismatic structure; very hard, firm, very sticky, and very plastic; few fine and very fine routs; continuous thick clay films on faces of peds; 35 percent pebbles; mildly alkaline; abrupt, wavy boundary.
Btk1	91-130 cm; yellowish red (5YR 5/6) very gravelly clay; moderate medium prismatic structure parting to common fine and very fine angular blocky; very hard, firm, very sticky, and very plastic; few very fine and fine roots; continuous thick clay films on faces of peds; effervesces violently, with calcium carbonate occurring as soft masses; 45 percent pebbles and 5 percent cobbles; mildly alkaline; clear, wavy boundary.
Btk2	130-157 cm; yellowish red (5YR 5/6) very gravelly clay; moderate medium prismatic structure parting to moderate fine subangular blocky; very hard, firm, very sticky, and very plastic; few fine and very fine roots; many moderately thick clay films on faces of peds; 50 percent pebbles and 5 percent cobbles; effervesces violently, with calcium carbonate occurring as soft masses; mildly alkaline; clear, wavy boundary.
C	157-188 cm; very gravelly loamy sand.
Remarks:	Contiguous pedons show apparent cyclic alternation (wave length of about 2 in, amplitude less than 1 m) between very gravelly clay and low gravelly to gravelly clay zones. Horizons of soil-carbonate accumulation below 76 cm are much more prominent in the less gravelly clay zones. Interpreted by J. W. Hawley (8/25/77) as a relict patterned-ground feature, possibly related to former gilgai microrelief and action of expansive clays as suggested by Yaalon and Kalmar (1978). The site may also have been affected by freeze-thaw conditions during middle and late Pleistocene glacial stages. Laboratory data available from New Mexico State University Agricultural Experiment Station and U.S. Soil Conservation Service.

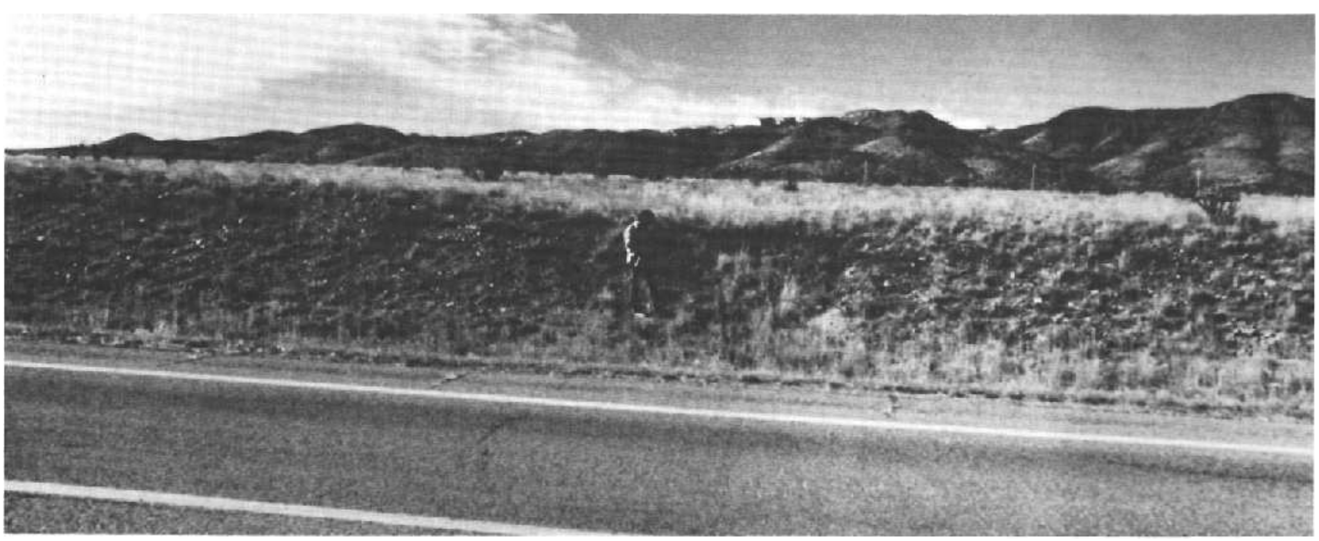

FIGURE 3—"Sedillo Hill" geomorphic surface and Paleargid soil landscape at Stop 2-1 (p. 23). View to west toward Sixmile Canyon area of east-central Magdalena Mountains. Piedmont-slope facies of uppermost Sierra Ladrones Formation and Paleargid pedon la (5' 8" person) exposed in US-60 roadcut.

FIGURE 4—"Sedillo Hill" geomorphic surface and Paleargids exposed in Soil Survey sample pit, 1.3 mi south of Sedillo Hill (Stop 2-1, p. 23). View to west toward Sixmile Canyon area of east-central Magdalena Mountains. Typical pedon of Magdalena soil, at 6-ft tape, is characterized by strong argillic (Bt) horizon developed in piedmont-slope facies of uppermost Sierra Ladrones Formation.

mineralogy obtained in this study. The dominance of VS and illite, and the presence of smectite and kaolinite, in upper soil horizons sampled at Stop 2-1 (Tables 3 and 8, pedon la) agree with observations on clay mineral occurrence in other areas with similar climate and soil-geomorphic settings (Gile and Grossman, 1979; Nettleton and Brasher, 1983). The upper (A, 13t, l3tk) horizons of soils of the "Sedillo Hill" surface do not appear to be sites where "neoformational" or "transformational" processes have led to genesis of chain-lattice clays. However, positive (methyl orange) tests for sepiolite have been obtained from pedogenic calcretes that locally occur in areas of soil-landscape dissection and soil-profile truncation contiguous to the Stop 2 1 study area (Table 3, pedon la). At these places along the rim of the Rio Grande valley, the soil microclimate is distinctly drier than in adjacent undissected areas (well illustrated by pedon lb in Table 7) where an ancient soil landscape is well preserved (also see Gile et al., 1981, pp. 99-102).

The following scenario for genesis of chain-lattice clays in pedogenic calcretes of the "Las Car'las" geomorphic surface (Tables 5-7, pedons 2a, 2h, and 3) is in essential agreement with models described by Jones (1983) in southern Nevada and McGrath (1984) in the Southern High Plains. Calcic-petrocalcic horizon sequences (late stage III and stronger carbonate morphologies) serve as holding tanks for a concentrated soil solution. It is inferred that the chain-lattice clays form after the carbonate cementation (incipient induration) threshold has been crossed. When the solution

TABLE 5—Field morphological description of Paleorthid (pedon 2a) at Stop 2-2 (p. 28).

Classification:	Typic Paleorthid; loamy-skeletal, carbonatic, thermic, shallow
Location:	NW¼, SE¼, SE¼, SE¼, sec. 24, T3S, R1E; in west face of roadcut on ranch road 0.05 mi south of BLM road to Arroyo del Tajo interpretive site.
Geomorphic surface (age):	"Las Cañas" (early middle Pleistocene)
Land form:	piedmont slope, proximal position; relict constructional surface
Slope:	2–3 percent (westward)
Elevation:	5,225 ft (1,593 m)
Parent material:	Sierra Ladrones Formation, upper piedmont facies; loamy to gravelly alluvium (valley fill) derived from sedimentary terrane (Permian) in Loma de las Cañas highlands. Limestone, dolomite, sandstone, and mudstone, with calcareous aerosol contributions.
Vegetation:	surface locally disturbed, creosotebush, annuals
Described by:	J. W. Hawley (2/24/87)
Sampled by:	J. W. Hawley, B. G. Jones, V. T. McLemore (2/24/87)
Horizon	
ABk (AK1)	0–30 cm; surface disturbed; light brown (7.5YR 6/4) very gravelly loam; common platy, gravel- to cobble-size fragments of laminar to massive calcrete (pinkish white, 7.5YR 8/2); weak subangular blocky; soft; effervesces violently; sepiolitic; common roots; clear to abrupt, smooth to wavy boundary.
Bkm (K21m)	30–91 cm; pinkish white (5 to 7.5YR 8/2) calcrete (loamy sediment plugged with secondary carbonate); massive to nodular, with platy zones; well indurated; effervesces violently; sepiolitic, gradual boundary.
Bk1 (K22)	91–122 cm; pinkish white (5 to 7.5YR 8/2) carbonate-plugged loamy sediment, with common, well-indurated nodules in carbonate-cemented, but non-indurated matrix, pink (5–7.5YR 7/4) moist; massive; very hard; effervesces violently; gradual boundary.
Bk2 (K23)	122–183 cm; pink (5 to 7.5YR 8/4), carbonate-plugged material,with some nodules as above (91–122 cm), light reddish brown to light brown (5–7.5 YR 6/4) moist; clear irregular boundary.
2Bk3 (2K3)	183–229 cm; pink (7.5YR 7/4) very gravelly loamy sand, light brown (7.5YR 6/4) moist; massive; very hard; effervesces violently; clear irregular boundary.
2C	229+ cm; pebble and cobble gravel to very gravelly loamy sand, with few small boulders. Upper gravelly unit, including 2Bk3 horizon, rises abruptly to the south and occupies most of roadcut below thin surficial calcrete horizon (general lateral equivalent of Bkm).
Remarks:	Petrocalcic horizon with well-developed stage IV to incipient stage V carbonate morphology (Gile et al., 1966; Machette, 1985) 30 to 91 cm. Preliminary interpretation of clay mineral distribution by B. G. Jones and G. S. Austin (Table 8). Geoffrey Jones (May 1987) noted that with increasing depth sepiolite content generally decreases, with possibly a sepiolite low between 61 and 91 cm, and palygorskite content increases. Active carbonate precipitation in the upper 61 cm is indicated by greater abundance of clay-size carbonate in that zone.

is rich in Mg, neoformation of palygorskite and/or sepiolite would occur. Palygorskite could form as long as quantities of collodial or solute Al were available (Jones, 1983). When free Al has been consumed, or if it was never present,

Continued on page 65

TABLE 6—Field morphological description of Paleorthid (pedon 2b) near Stop 2–2 (p. 28).

Classification:	Typic Paleorthid, fine-loamy, mixed (carbonatic?), thermic
Location:	SW¼, SE¼, NW¼, sec. 5, T4S, R2E; 3 mi south southeast of Stop 2–2 (mi 24.35, p. 31); in caliche pit on east side of Socorro County road A129, 11.3 mi north of US–380
Geomorphic surface (age):	"Las Cañas" (early middle Pleistocene)
Land form:	piedmont slope, proximal position; relict pediment (thin gravelly veneer)
Slope:	5 percent (westward)
Elevation:	5,300 ft (1,615 m)
Parent material:	Sierra Ladrones Formation, upper piedmont facies; gravelly to loamy alluvium, derived from sedimentary terrane (Permian) in Loma de las Cañas highlands; dolomite, limestone, sandstone, and mudstone; with minor eolian sand and calcareous aerosol contributions.
Vegetation:	creosotebush, lechuguilla, juniper, snakeweed, grasses, annuals
Described by:	D. A. McGrath (8/13/85)
Sampled by:	D. A. McGrath (8/13/85)
Horizon	
A	0–13 cm; light brown (7.5YR 6/4) sandy clay loam, dark brown (7.5YR 4/4) moist; weak subangular blocky; soft; effervesces violently; common fine and few medium roots; clear, smooth boundary. Soil surface has sparse vegetation and about 25 percent rock-fragment cover (including calcrete clasts).
Bw	13–30 cm; light brown (7.5YR 6/4) sandy clay loam; brown (7.5YR 5/4) moist; weak subangular blocky; soft; effervesces violently; non-sepiolitic; common fine and few medium roots; clear, smooth boundary.
Bk1	30-50 cm; pale brown (10YR 6i3) gravelly clay loam; yellowish brown (10YR 5/4) moist; weak subangular blocky; soft; effervesces violently; 3-mm carbonate rinds on gravel clasts, which include calcrete fragments; few fine and medium roots; clear, smooth boundary.
Bk2 (K1)	50-60 cm; light gray (10YR 7/2) gravelly clay loam, yellowish brown (10YR 514) moist; weak subangular blocky; hard; effervesces violently; 3-mm carbonate rinds on gravel clasts, which include calcrete fragments; few fine and medium roots; abrupt, smooth boundary.
Bkm1 (K21m)	60-61 cm; white (10YR 9.:1) laminar calcrete crust; pale brown (10YR 6/3) moist; very well indurated; effervesces violently; solution-cupped limestone fragments; some 2-mm brown siliceous bands; sepiolitic; abrupt, smooth boundary.
Bkm2 (K22m)	61-86 cm; white (10YR 8/1) very gravelly calcrete, pale brown (10YR 6/3) moist; well indurated; effervesces violently; plugged and cemented with secondary carbonate; sepiolitic; common fragments of dolomite and mudstone; some dolomite fragments fractured and recemented by pedogenic calcite; clear, smooth boundary.
Bk (K3)	86-180 cm; pinkish white (7.5YR 8/2) very gravelly loam with indurated nodular *calcrete* zones, light brown (7.5YR 6/4) moist; massive; partly indurated; effervesces violently; plugged with secondary carbonate; sepiolitic in upper part; common fragments of mudstone and dolomite.
Bk&C	180-245 cm; pink (7.5YR 714) gravelly sandy clay loam; brown (7.4YR 514) moist; massive; soft; effervesces strongly; non-sepiolitic. Upper part of veneer of gravelly alluvium (upper Sierra Ladrones Formation-piedmont facies) that caps Las Camas geomorphic surface (pediment phase).
Remarks:	I'etrocalcic horizon with stage IV carbonate morphology (tile et al., 1966) 60-86 cm. l'reliminary interpretation of clay mineral distribution by ID. A. McGrath and G. S. Austin (Table 8).

FIGURE 5—Remnants of "Las Cañas" geomorphic surface and Paleorthid soil landscape at Stop 2–2 (p. 28). View to south across valley of Arroyo de las Cañas toward Las Cañas pediment cut on west-dipping beds of the Yeso Formation. Roadcut in foreground is gravelly to loamy valley fill of the uppermost Sierra Ladrones Formation–piedmont facies. Described pedon (2a) with low, gravelly pedogenic calcrete located in right center of photo (5′ 8″ to 6′ people).

TABLE 7—Field morphological description of Paleargid (pedon 3) near Stop 2–5 (p. 36).

Classification:	Petrocalcic Paleargid, fine-loamy, mixed, thermic
Location:	NW1/4, SW1/4, NE1/4, sec. 17, T5S, R2E; in roadcut on east side of Socorro County road A153, 1.2 mi south of US–380; 0.5 mi northwest of Fite Ranch Headquarters
Geomorphic surface (age):	"Las Cañas" (early middle Pleistocene)
Land form:	piedmont slope, distal position; relict constructional surface
Slope:	2 percent (westward)
Elevation:	4,990 ft (1,521 m)
Parent material:	Sierra Ladrones Formation, upper piedmont facies, loamy low gravelly alluvium, primarily derived from mixed sedimentary (Cretaceous–early Tertiary) and volcanic (mid-Tertiary) rocks; with major eolian sand and calcareous aerosol contributions.
Vegetation:	creosotebush, grasses, annuals
Described by:	D. A. McGrath (8/15/85)
Sampled by:	D. A. McGrath (8/15/85)
Horizon	
A	0–9 cm; brown (7.5YR 5/4) fine sandy loam, dark brown (7.5YR 4/4) moist; weak subangular blocky; upper 1 cm is platy; soft; effervesces strongly; common medium roots; clear smooth boundary. Soil surface has sparse vegetation and 10 percent rock fragment cover.
BAt	9–22 cm; brown (7.5YR 5/4) sandy clay loam, dark brown (7.5YR 4/4) moist; weak subangular blocky; soft; effervesces strongly; faint thin clay films; common medium roots; clear smooth boundary.
Btk1	22–42 cm; light brown (7.5YR 6/4) sand clay loam, dark brown (7.5YR 4/4) moist; medium subangular blocky; hard; effervesces strongly; faint thin clay films; common carbonate threads and filaments of carbonate; few medium roots; wavy boundary.
Btk2 (K1)	42–51 cm; light brown (7.4YR 6/4) sandy clay loam; dark brown (7.5YR 4/4) moist; weak subangular blocky; hard; effervesces violently; faint thin clay films; many carbonate modules; non-sepiolotic; few medium roots; abrupt, wavy boundary. Horizon is discontinuous through the outcrop area.
Btkm (K2m)	51–136 cm; white (10YR 9/2) calcrete (incipient), very pale brown (10YR 7/4) moist; massive; indurated; effervesces violently; 10 percent argillic material; plugged non-sepiolitic; clear, smooth boundary. Common pipes and vertical joints with hard, laminar carbonate coatings (one pipe is a krotovina, which widens with depth; one joint has clay films (t) to 1 m below top of calcrete, with common fine roots). Faint laminar structure or bedding. Small krotovinas filled with argillic material (engulfed argillic horizon) out of termite chambers. Top of calcrete has many platy nodules.
Btkb?1 (K3)	136–157 cm; pinkish white to pink (7.5YR 8/2 to 7/4) clay loam, very pale brown (7.5YR 7/4 to 6/4) moist; massive; indurated; effervesces violently; 5 percent argillic material; non-sepiolitic; clear, smooth boundary.
Btkb?2	157+ cm; very pale brown to light brown (7.5YR 7/4 to 6/4) sandy clay loam, brown (7.5YR 5/4) moist; weak subangular blocky; hard; effervesces violently; few faint thin clay films; carbonate nodules and filaments along structural planes; non-sepiolitic.
Remarks:	Incipient petrocalcic horizon, stage III–IV carbonate morphology (Gile et al., 1966) 51–157 cm. Preliminary interpretation of clay mineral distribution by D. A. McGrath and G. S. Austin (Table 8).

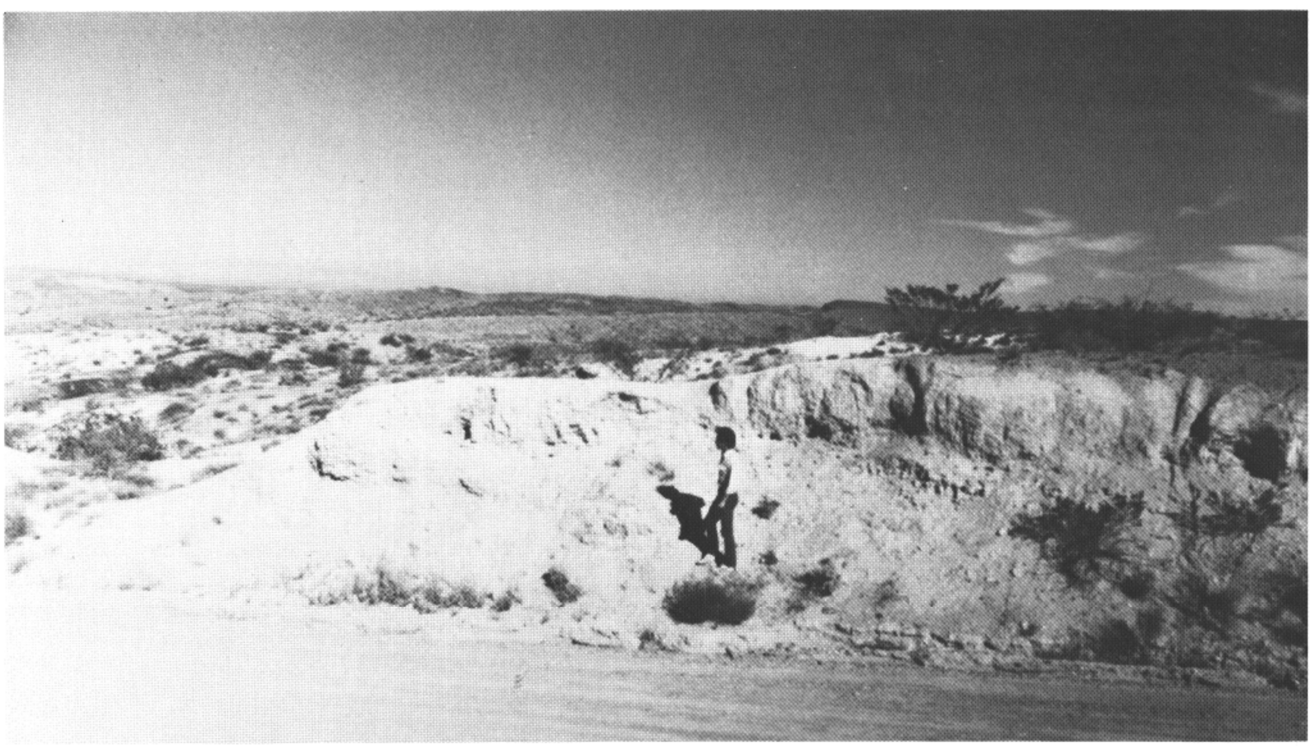

FIGURE 6—Las Cañas geomorphic surface and Paleorthid–Calciorthid soil landscape at Stop 2–5 (p. 36). View is to northeast from Las Cañas surface at west edge of Carthage coal field across valley of San Pedro Arroyo. Roadcut (county road A–153) in loamy to sandy piedmont-slope facies of uppermost Sierra Ladrones Formation. Described pedon (3) with low, gravelly pedogenic calcrete located at right edge of photo (5′ 8″ person).

TABLE 8—Clay mineral distribution in Paleargids and Paleorthids at or near Stops 2–1, 2–2, and 2–5 (pedons 1a, 2a, 2b, 3). Remarks: based on preliminary XRD analyses by D. A. McGrath (1a, 2b, 3) and B. G. Jones (2a), and interpretations by G. S. Austin, McGrath, and Jones. **VA,** very abundant; **A,** abundant; **P,** present; **tr,** trace; **N,** not present; **Q,** quartz; **D,** dolomite; **calc,** calcite in original sample was not completely destroyed during treatment before XRD analysis.

Stop (pedon)	Horizon	Depth (cm)	Smectite	Illite	Illite/ smectite	Chlorite	Kaolinite	Sepiolite	Palygorskite	Non-clay minerals in <2 μm fraction
2–1 (1a)	A	0–10	N	A	P	N	A	N	N	Q, poor record
	BAt	10–27	N	P	A	N	P	N	N	
	Btk1	27–41	N	P	A	N	P	N	?	calc
	Btk2	41–55	P	P	P	N	P	N	N	calc
	Btk3	55–79	P	P	P	N	P	N	tr	calc?
2–2 (2a)	ABk	0–30	N	P	tr	N	P	VA	tr	
	Bkm	30–61	N	P	tr	N	P	A	N	
	Bkm	61–91	N	N	N	N	P	P	?	
	Bk1	91–122	N	P	P	N	tr	P	P	
	Bk2	122–152	N	P	N	N	tr	P	P	
	Bk2	152–183	N	P	tr	N	P	tr	N	
2–2 (2b)	A	0–13	P	P	P	P	P	P	N	Q
	Bw	13–30	P	A	A	tr	tr	N	N	Q
	Bk1	30–50	P	P	P	P	P	P	N	Q
	Bk2	50–60	tr	A	P	P	P	P	N	Q, D
	Bkm1	60–61	N	P	P	tr	tr	VA	N	Q, D, calc
	Bkm2	61–86	P	P	P	P	N	A	N	D, calc
	Bk upper	86–180	P	P	P	P	P	A	N	Q, D
	Bk lower		A	A	N	N	P	N	N	D?
	Bk&C	180–245	tr	P	P	P	A	N	N	Q
2–5 (3)	A	0–9	P	P	P	P	P	N	N	Q
	BAt	9–22	P	P	P	tr	A	N	N	Q
	Btk1	22–42	P	P	P	P	P	N	N	Q
	Btk2	42–51	P	P	P	P	P	N	tr	Q
	Btkm	51–136	P	P	P	P	P	N	P	Q
	Btkb?1	136–157	P	P	P	P	P	N	P	Q
	Btkb?2	157+	P	P	P	tr	P	N	P	Q

sepiolite neoformation would occur. Chain-lattice clays, rather than the ubiquitous smectites, form because of the low pMg. The necessary Mg could be supplied by degradation of phyllosilicates, volcanic ash, and/or other detrital minerals. However, if the parent sediment (including aerosol contributions) contained a significant dolomite component, then the Mg supply problem would be greatly simplified. Free Ca in solution would precipitate on the existing calcite resulting in a still greater degree of induration and calcrete development. Free Ca" would be obtained from dissolution of detrital carbonates and the weathering of other Ca-bearing materials.

Free Si in the system not used in clay neoformation would precipitate as an independent opal phase (opal—CT). However, this phase has not been observed in "Las Calias" pedons. If volcanic ash, even in relatively small increments, were to be deposited on the surface, or if a grassland soil was buried or climatically altered, with resulting dissolution of opal phytoliths, then silica cementation of the subsoil might also be expected. The necessary Si could also be obtained from the degradation of clay phyllosilicates or detrital primary silicates. If a trend of decreasing feldspar/quartz ratio with increasing degree of calcrete development is observed in future studies, an inference could be made that Al" would also be available for clay neoformation. Another possible Al" source would be from degradation of phyllosilicates. Thus, Al' liberated in the system would be readily available for clay neoformation when a flux of the other necessary cations existed. With increasing age of the deposit and advancing stages of diagenesis and pedogenesis, the probability of more than one of the above events occurring would be increased greatly.

Methodology

Samples were collected from hand-dug excavations in roadcut and natural exposures, and pedons were described using standard U.S. Cooperative Soil Survey nomenclature (Soil Survey Staff, 1981). Samples were air-dried and indurated samples were ground to pass a 60-mesh sieve. Carbonates were destroyed by placing approximately 20 g of sample in 150 ml of 10 percent acetic acid (HOAc; McLean et al., 1972). Samples were washed (by decantation) until dispersion occurred. Dispersion was aided by adding 5 ml of 5 percent sodium hexametaphosphate. Clay was extracted based on a settling time of 45 minutes per cm for <2μm-sized particles. Clay extract volume was controlled by using 10 percent CaC1 to induce flocculation. Samples were oriented using the filter membrane peel technique of Dreyer (1973).

X-ray diffraction (XRD) was conducted on the Rigaku diffractometer at the New Mexico Bureau of Mines and Mineral Resources. The machine was operated at a speed of 4°/minute with a time constant of 0.2. Occasional powder samples were examined from 2-50° 2θ. Oriented clay slides were examined from 2-32° 2θ. Ethylene glycol solvated slides were examined from 2-15° 2θ, with the glycolation obtained by allowing the samples to remain in a room-temperature desiccator containing ethylene glycol. Glycolated slides were exposed to 350°C temperatures for one hour then examined from 8-10° 2θ immediately upon removal from the oven and then examined from 2-15° 2θ (Austin and Leininger, 1976). Clay minerals were identified with the aid of procedures described by Brindley (1980), Brown (1980), and Brown and Brindley (1980).

Acknowledgments

Assistance by George Austin, Richard Chamberlin, Geoffrey Jones, David Love, Virginia McLemore, and Deborah Shaw in preparation of this paper is gratefully acknowledged.

References

Aristarain, L. P., 1970, Chemical analyses of caliche profiles from the High Plains, New Mexico: Journal of Geology, v. 78, pp. 201-212.

Austin, G. S., and Leininger, R. K., 1976, The effect of heat-treating sedimented mixed-layer illite-smectite as related to qualitative clay mineral determinations: Journal of Sedimentary Petrology, v. 46, pp. 206-215.

Bachman, G. O., and Machette, M. N., 1977, Calcic soils and calcretes in the southwestern United States: U.S. Geological Survey, Open-file Report 77-794, 163 pp.

Barker, J. M., 1983, Preliminary investigation of the origin of the Riley travertine, Socorro County, New Mexico: New Mexico Geological Society, Guidebook to 34th Field Conference, pp. 269-276.

Bates, R. L., and Jackson, J. A., 1980, Glossary of geology, second edition: American Geological Institute, pp. 89, 191.

Bigham, J. M., Jaynes, W. F., and Allen, B. L., 1980, Pedogenic degradation of sepiolite and palygorskite on the Texas High Plains: Soil Science Society of America Journal, v. 44, pp. 159-167.

Birkeland, P. W., 1984, Soils and geomorphology.: Oxford University Press, New York, NY, 372 pp.

Bretz, J. H., and Horberg, L. H., 1949, Caliche of southeastern New Mexico: Journal of Geology, v. 57, pp. 492-511.

Brewer, R., 1976, Fabric and mineral analysis of soils: R. E. Krieger Publishing Co., Huntington, NY, 482 pp.

Brindley, G. W., 1980, Qualitative x-ray mineral analysis of clays; *in* Brindley, G. W., and Brown, G. (eds.), Crystal structures of clay minerals and their x-ray identification: Mineralogical Society, London, pp. 411-438.

Brown, G., 1980, Associated minerals; in Brindley, G. W., and Brown, G. (eds.), Crystal structures of clay minerals and their x-ray identification: Mineralogical Society. London, pp. 361-410.

Brown, G., and Brindley, G. W., 1980, X-ray diffraction procedures for clay mineral identification; *in* Brindley, G. W., and Brown, G. (eds.), Crystal structures of clay minerals and their x-ray identification: Mineralogical Society, London, pp. 305-359.

Bryan. Kirk, 1938, Geology and ground-water conditions of the Rio Grande depression in Colorado and New Mexico; *in* [U.S.] Natural Resources Planning Board, the Rio Grande joint investigations in the upper Rio Grande Basin: U.S. Government Printing Office, v. 1, pt. 2, pp. 196-225.

Carlisle, D., Merifield, P. M., Orme, A. K., Kohl, M. S., and Kolker, O., 1978, The distribution of calcretes and gyperetes in southwestern United States and their uranium favorability based on deposits in western Australia and southwest Africa (Namibia): U.S. Department of Energy, Open-file Report GJBX-29(78), 274 pp.

Chamberlin, R. M., 1981, Cenozoic stratigraphy and structure of the Socorro Peak volcanic center, central New Mexico--a summary: New Mexico Geology, v. 3, no 2, pp. 22-24.

Chapin, C. E. (ed.), 1983, Socorro region II: New Mexico Geological Society, Guidebook to 34th Field Conference, 344 pp.

Chitale, J. D., 1986, A study of petrography and internal structures in calcretes of west Texas and New Mexico: Unpublished Ph.D. dissertation, Texas Tech University, Lubbock, 107 pp.

Cornell University Department of Agronomy, 1986, Designations of master horizons and layers in soils: Soil Management Support Service, Soil Conservation Service, Washington, DC 20013, 16 pp.

Denny, C. 5., 1940, Tertiary geology of the San Acacia area, New Mexico: Journal of Geology, v. 48, pp. 73-106.

Denny, C. S., 1941. Quaternary geology of the San Acacia area, New Mexico: Journal of Geology, v. 49, pp. 225-260.

Dreyer, J. 1., 1973, The preparation of oriented clay mineral specimens for XRD analysis by a filter-membrane peel technique: American Mineralogist, v. 58, pp. 553-554.

Elprince, A. M., Mashady, A. S., Aba-Husayn, M. M., 1979, The occurrence of pedogenic palygorskite (attapulgite) in Saudi Arabia: Soil Science, v. 128, pp. 214-218.

Eswaran, H., and Barzanji, A. F., 1974, Evidence of neoformation of attapulgite in some soils of Iraq: Transactions of the 10th International Congress of Soil Sciences, Moscow, v. 7, pp. 154-161.

Frye, J. C., Glass, H. D., Leonard, A. B., and Coleman, D. U., 1974, Caliche and clay mineral zonation of Ogallala Formation, central-eastern New Mexico: New Mexico Bureau of Mines and Mineral Resources, Circular 144, 16 pp.

Gardner, L. R., 1972, Origin of the Mormon Mesa caliche, Clark County, Nevada: Geological Society of America, Bulletin 83, pp. 143-156.

Gile, L. H., 1961, A classification of ca horizons in soils of a desert region, Dona Ana County, New Mexico: Soil Science Society of America Proceedings, v. 25, pp. 52-61.

Gile, I.. II., 1975, Holocene soils and soil-geomorphic relations in an arid region of southern New Mexico: Quaternary Research, v. 5, pp. 321-360.

Gile, L. H., 1977, Holocene soils and soil-geomorphic relations in a semi-arid region of southern New Mexico: Quaternary Research, v. 7, pp. 112-132.

Gile, L. H., 1987, Book review of Weide, D. L. (ed.), Soils and Quaternary geology of the southwestern United States: Quaternary Research, v. 27, pp. 335-336.

Gile, L. H., and Grossman, R. B., 1979, The Desert Project soil monograph: National Technical Information Service, Document no. PB80-13534, Springfield, VA 22161, 984 pp.

Gile, L. H., Hawley, J. W., and Grossman, R. B., 1981, Soils and geomorphology in the Basin Range area of southern New Mexico-guidebook to the Desert Project: New Mexico Bureau of Mines and Mineral Resources, Memoir 39, 222 pp.

Cite. L. H., Peterson, F. F., and Grossman, R. B., 1965, The K horizon-master soil horizon of carbonate accumulation: Soil Science, v. 99, pp. 74-82.

Gile, L. H., Peterson, F. F., and Grossman, R. B., 1966, Morphological and genetic sequences of carbonate accumulation in desert soils: Soil Science, v. 101, pp. 347-360.

Goudie, A., 1973, Duricrusts in tropical and subtropical landscapes: Clarendon Press, Oxford, England, 174 pp.

Hawley, J. W. (compiler), 1978, Guidebook to Rio Grande rift in New Mexico and Colorado: New Mexico Bureau of Mines and Mineral Resources, Circular 163, 241 pp.

Hawley, J. W., 1986a, Physiographic provinces of New Mexico; *in* Williams, J. L. (ed.), New Mexico in maps: University of New Mexico Press, Albuquerque, pp. 28-31.

I lawley, J. W., 1986b, Landforms of New Mexico; *in* Williams, J. L. (ed.), New Mexico in maps: University of New Mexico Press, Albuquerque, pp. 32-35.

Hawley, J. W., Bachman, G. O., Manley, K., 1976, Quaternary stratigraphy in the Basin and Range and Great Plains provinces, New Mexico and western Texas; *in* Mahaney, W. C. (ed.), Quaternary stratigraphy of North America: Dowden, Hutchinson, and Ross, Inc., Stroudsburg, PA, pp. 235-274.

Hay, R. L., and Wiggins, B., 1980, Pellets, ooids, sepiolite, and silica in three calcretes in the southwestern United States: Sedimentology, v. 27, pp. 559-576.

Izett. G. A., 1981, Volcanic ash beds-Recorders of upper Cenozoic silicic pyroclastic volcanism in the western United States: Journal of Geophysical Research, v. 86, no. B11, pp. 10,200-10,222.

Izett, G. A., Obradovich, J. D., Naeser, C. W., and Cebula, G. T., 1981, Potassium-argon and fission-track ages of Cerro Toledo Rhyolite tephra in the Jemez Mountains, New Mexico: U.S. Geological Survey, Professional Paper 1199-D, pp. 37-43.

Jones, B. F., 1983, Occurrence of clay minerals in surficial deposits of southwestern Nevada; in Nahon. D., and Noak, Y. (eds.), Petrologie des alterations des sols: Universite Louis Pasteur de Strasbourg, Institut de Geologie, Sciences Geologiques, Memoir 73, v. II, pp. 81-92.

Khoury, H. N., Eberl, D. D., and Jones, B. F., 1982, Origin of magnesium clays from the Armagosa Desert, Nevada: Clays and Clay Minerals, v. 5, pp. 327 336.

Lamplugh, G. W., 1902, Calcrete: Geological Magazine, v. 9, p. 75.

Lattman, L. H., 1973, Calcium carbonate cementation of alluvial fans in southern Nevada: Geological Society of America Bulletin, v. 84, pp. 3013-3028.

Love, D. W., and Young, J. D., 1983, Progress report on the late Cenozoic geologic evolution of *the* lower Rio Puerco: New Mexico Geological Society; Guidebook to 34th Field Conference, pp. 277-284.

Lovelace, A. D., 1972, Aggregate resources in central eastern New Mexico: New Mexico Geological Society, Guidebook to 23rd Field Conference, pp. 187-191.
Machette, M. N., 1978a, Dating Quaternary faults in southwestern United States by using buried calcic paleosols: U.S. Geological Survey, Journal of Research, v. 6, no. 3, pp. 369-381.
Machette, M. N., 1978b, Geologic map of the San Acacia quadrangle, Socorro County, New Mexico: U.S. Geological Survey, Geologic Quadrangle Map GQ-1415, scale 1:24,000.
Machette, M. N., 1978c, Late Cenozoic geology of the San Acacia-Bernardo area; *in* Hawley, J. W. (compiler), Guidebook to Rio Grande rift in New Mexico and Colorado: New Mexico Bureau of Mines and Mineral Resources, Circular 163, pp. 135-137.
Machette, M. N., 1985, Calcic soils of the southwestern United States; *in* Weide, D. L. (ed.), Quaternary soils and geomorphology of the American Southwest: Geological Society of America, Special Paper 203, pp. 1-21.
Machette, M. N., 1986, History of Quaternary offset and paleoseismicity along the La Jencia fault, central Rio Grande rift, New Mexico: Bulletin of the Seismological Society of America, v. 76, pp. 259-272.
Martin-Vivaldi, J. L., and Robertson, R. H. S., 1971, Palygorskite and sepiolite (the hormites); in Gard, J. A. (ed.), The electron optical investigation of clays: Mineralogical Society, London, pp. 255-275.
McGrath, D. B., 1984, Morphological and mineralogical characteristics of indurated caliches of the Llano Estacado: Unpublished M.S. thesis, Texas Tech University, Lubbock, 206 pp.
McGrath, D. B., and Hawley, J. W., 1985, Calcretes of the Santa Rosa area: New Mexico Geological Society, Guidebook to 36th Field Conference, pp. 4-6.
McLean, S. A., Allen, B. L., and Craig, J. R., 1972, The occurrence of sepiolite and attapulgite on the southern High Plains: Clays and Clay Minerals, v. 20, pp. 143-149.
Nettleton, W. D., and Brasher, B. R., 1983, Correlation of clay minerals and properties of soils of the western United States: Soil Science Society of America Journal, v. 47, pp. 1032-1036.
Norrish, K., and Pickering, J. G., 1983, Clay minerals; in Soils, an Australian viewpoint: Division of Soils, Commonwealth Scientific and Industrial Research Organization, Melbourne, Australia, Academic Press, London, pp. 281-308.
Papke, K., 1972, A sepiolite-rich playa deposit in southern Nevada: Clays and Clay Minerals, v. 20, pp. 211-215.
Paquet, H., 1983, Stability, instability, and significance of attapulgite in calcretes of Mediterranean and tropical areas with marked dry seasons; *in* Nahon, *D.*, and Noak, Y. (eds.), Petrologie des alterations et des sols: Universite Louis Pasteur de Strasbourg, Institut de Geologic, Sciences Geologiques, Memoir 73, v. II, pp. 131-140.
Parry, W. T., and Reeves, C. C., Jr., 1968, Sepiolite from pluvial Mound Lake, Lynn and Terry Counties, Texas: American Mineralogist, v. 53, pp. 984-993.
Post, J. L., 1978, Sepiolite deposits of the Las Vegas, Nevada area: Clays and Clay Minerals, v. 26, pp. 58-64.
Reeves, C. C., Jr., 1970, Origin, classification, and geologic history of caliche on the southern High Plains, Texas and eastern New Mexico: Journal of Geology, v. 78, pp. 352-362.
Singer, A., 1979, Palygorskite in sediments: Detrital. diagenetic or neoformed—a critical review: Geologisch Rundschau, v. 68, pp. 996-1008.
Singer, A., and Norrish, K., 1974, Pedogenic palygorskite occurrences in Australia: American Mineralogist, v. 59, pp. 508-517.
Soil Survey Staff, 1975, Soil taxonomy—a basic system of soil classification for making and interpreting soil surveys: U.S. Department of Agriculture, Soil Conservation Service, Handbook 436, 753 pp.
Soil Survey Staff, 1981, Examination and description of soils in the field; *in* Soil survey manual: U.S. Department of Agriculture, Soil Conservation Service, Handbook 430, chapter 4, pp. 4-14-107.
Sowers, J. M., 1985, Pedogenic calcretes of the Kyle Canyon alluvial fan, Nevada—morphology and development: Unpublished Ph.D. dissertation, University of California, Berkeley, 159 pp.
Spaulding, W. C., 1984, The last glacial interglacial climatic cycle—its effects on woodlands and forests in the American West; *in* Proceedings, North American Biology Workshop: Utah Department of Forest Research, Logan, pp. 42-69.
Tedford, R. H., 1981, Mammalian biochronology of the late Cenozoic basins of New Mexico: Geological Society of America Bulletin, v. 92, part I, pp. 1008-1022.
Vanden Heuvel, R. C., 1966, The occurrence of sepiolite and attapulgite in the calcareous zone of a soil near Las Cruces, New Mexico; *in* Clays and clay minerals: Proceedings of the 13th National Clay Conference on Clay Minerals, Pergamon Press, New York, NY, pp. 193-207.
Van Devender, T. R., 1985, Climatic cadences and the composition of Chihuahuan desert communities—the late Pleistocene packrat midden record; *in* Diamond, J., and Case, T. J. (eds.), Community ecology: Harper and Row, New York, NY, pp. 285-299.
Viani, B. E., Al-Mashhady, A. S., and Dixon, J. B., 1983, Mineralogy of Saudi Arabian soils—central alluvial basins: Soil Science Society of America Journal, v. 47, pp. 149-157.
Wright, 1-1. E., 1946, Tertiary and Quaternary geology of the lower Puerco area, New Mexico: Geological Society of America Bulletin, v. 57, pp. 383-456.
Yaalon, D. H., and Kalmar, D., 1978, Dynamics of cracking and swelling clay soils—displacement of skeletal grains, optimum depth of slickensides, and rate of intra-pedonic turbation: Earth Surface Processes, v. 3, pp. 31-42.
Yaalon, D. H., and Wieder, M., 1976, Pedogenic palygorskite in some arid brown (Caldorthid) soils of Israel: Clay Minerals, v. 1, pp. 73-80.

Mineralization in the Luis Lopez mining district Socorro County, New Mexico—a summary

by Robert M. North and Virginia T. McLemore

New Mexico Bureau of Mines and Mineral Resources Socorro, New Mexico 87801

Introduction

The Luis Lopez mining district,. located southwest of Socorro, was one of the largest manganese producers in New Mexico. Manganese oxides occur along fractures and breccia zones in Tertiary volcanic rocks. By 1957, total production from this district amounted to about 97,000 short tons of concentrate that averaged 41% Mn and 18,000 short tons of crude ore that averaged 28% Mn (Farnham, 1961; Willard, 1973; Eggleston et al., 1983a). Production continued into the 1970's; however, figures are not available. Production was by both underground and open pit methods.

This report is a summary of published accounts describing the geology and mineralization in the district as well as observations by the authors. For more detailed information, the reader is referred to the references cited.

Geology

The Luis Lopez mining district is located near the northeast edge of the mid-Tertiary Datil-Mogollon volcanic field. The geology of the area is dominated by silicic ash-flow tuffs erupted from a number of mid-Tertiary cauldrons (Fig. 1). The district is located within the eastern portion of the Socorro cauldron, a mid-Tertiary volcanic feature subsequently modified by late Tertiary extension. The Socorro cauldron was formed approximately 32.04 m.y. B.P. (McIntosh et al., 1986; 'Art'Ar on sanidine) by the explosive evacuation of a high-level silicic magma chamber; the pyroclastic debris became the hells Mesa Tuff. The roof of the magma chamber subsided as material was erupted, resulting in a volcanic collapse basin (Fig. 2). The gradual subsidence allowed the accumulation of a thick sequence of Hells Mesa Tuff within the cauldron (cauldron facies) as compared to the outflow sheet (outflow facies), which spread for several tens of kilometers around the cauldron (Osburn, 1983). Continued subsidence caused oversteepened cliffs to form, which periodically spilled into the cauldron and became interbedded with the tuff. At some point, the central portion of the fractured, subsiding block was forced upward. This is known as a resurgent dome, resulting in a topographically high central section surrounded by a moat, which in this case, was subsequently filled by about 1,000 m of volcaniclastic sediments, rhyolite domes and flows, and local ash flows known as the Luis Lopez Formation (Chamberlin, 1980; Eggleston, 1982).

The eastern margin of the Sawmill Canyon cauldron is near the western edge of the mining district. The Sawmill Canyon cauldron is a small cauldron nested within the much larger Socorro cauldron (Fig. 3). La Jencia Tuff was formed by the contemporaneous eruption of the Sawmill Canyon-Magdalena cauldrons about 28.78 m.y. B.P. (Osburn and Chapin, 1983a; McIntosh et al., 1986). The outflow facies of La Jencia Tuff is preserved within the margins of the Socorro cauldron south of the Luis Lopez district. Later, the I .emitar Tuff probably erupted from a cauldron in the northern San Mateo Mountains about 27.97 m.y. B.P. (Osburn and Chapin, 1983a; McIntosh et al., 1986), and partially filled the moat of the Sawmill Canyon and Socorro cauldrons (Eggles ton, 1982; Eggleston et al.. 1983b). The South Canyon Tuff, also probably erupted from the northern San Mateo Mountains, overlies the Lemitar Tuff and hosts some mineralization in the northern part of the district. McIntosh et al. (1986) reported an age of 27.36 m.y. B.P. for the South Canyon Tuff. Mid- to late-Tertiary extension of up to, perhaps, 100% has modified the cauldron, burying its eastern rim in the Rio Grande rift and exaggerating the east-west dimension (Fig. 3). The approximate present outline of the cauldron is 16 mi from north to south and 22 mi from east to west (Osburn and Chapin, 1983b).

Structure

The structure of the Luis Lopez district is dominated by cauldron structures and faulting and tilting related to regional extension. Pre-volcanic structure is dominated by a transverse shear zone (Precambrian wrench fault?) of the Morenci lineament north of the district (Chapin et al., 1978). This zone of crustal weakness, locally referred to as the Socorro transverse shear zone, is the focus for the repeated volcanism and high heat flow in the area. The zone is expressed at the surface by a change in the regional dip of the volcanic rocks from west- north of the zone to east-south of the zone (Chapin et al., 1978).

Regional extension related to the Rio Grande rift began about 31 m.y. B.P. (Aldrich et al., 1986), shortly after the eruption of the Socorro cauldron, contemporaneous with the eruption of the Sawmill Canyon-Magdalena cauldrons. High-angle, normal faults were formed, resulting in east-dipping fault blocks in the Luis Lopez mining district. The dip of the fault blocks increases from about 20 to 70° from south to north in the district, probably indicating a greater degree of extension in the northern part of the area (Eggleston, 1982). In some cases, the original high-angle faults might he rotated to lower angles as extension continues and subsequently cut by high-angle faults. Structure of this type is referred to as domino-style crustal extension because in cross section it resembles toppled dominoes (Chamberlin, 1983).

Mineralization

Mineralization in the district occurs along joints, minor faults, and in breccia zones related to faulting and perhaps in breccias formed by hydrothermal explosive events (T. L. Eggleston, pers. comm. 1987). At the MCA (Red Hill) mine, mineralization occurs along steeply dipping parallel structures in the Hells Mesa Tuff, which strike north to N20°W and have small displacements. At the Nancy and Tower mines, the major mineralization is along parallel structures in the Lemitar Tuff, South Canyon Tuff, and basaltic andesite striking N15'W to N30°W (Eggleston et al., 1983a, b).

The mineralization has not been dated, but structural evidence cited by Chamberlin (1980) suggests an age of 3 to 7 m.y. B.P., possibly associated with rhyolitic volcanism and high heat flow on Socorro Peak, north of the district. Individual veins of manganese oxides vary from less than 1 cm to

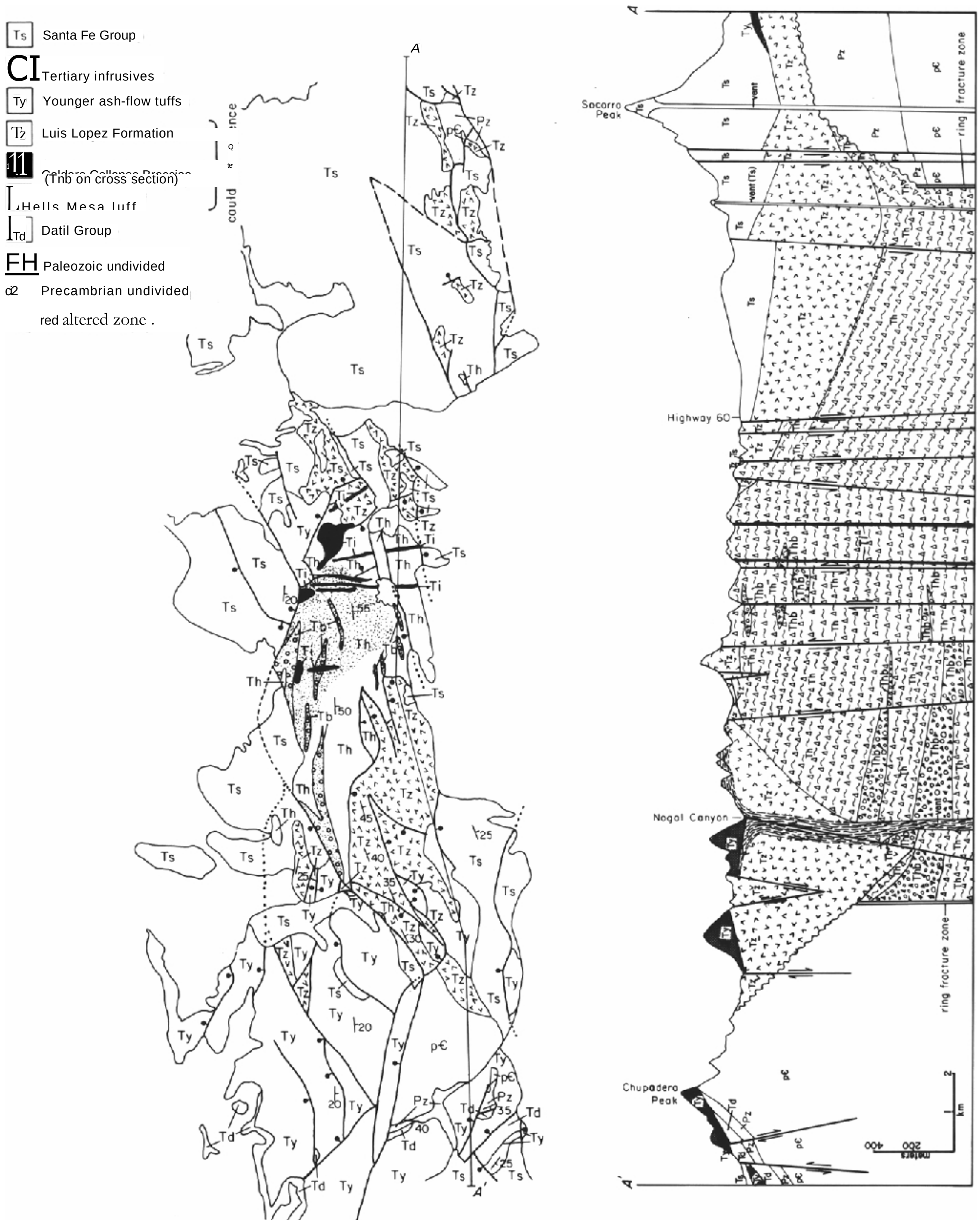

FIGURE 1—Generalized geologic map and cross section of the Luis Lopez mining district and vicinity. *(From Eggleston, et al .,19831;: used with permission.)*

nearly 1 m. The breccia zones consist of tuff fragments coated by manganese oxides and cemented by manganese oxides and/or calcite.

Mineralogy

The mineralogy of the veins has been the subject of considerable discussion and debate. The hard manganese oxides have been commonly referred to as psilomelane. This material is a mixture of acicular manganese oxides, most commonly hollandite ($Ba(Mn^{4+},Mn^{2+})_8O_{16}$), a monoclinic (pseudotetragonal) mineral with a structure related to the ruffle group. Commonly, the last stage of manganese mineralization is a fine-grained aggregate of intertwining crystals resembling black velvet (Fig. 4). Among mineral collectors this material is referred to as "rat's hair" psilomelane. Other end-members with a structure related to the ruffle group include cryptomelane ($K(Mn^{4+},Mn^{2+})_8O_{16}$; monoclinic, pseudotetragonal) and coronadite ($Pb(Mn^{4+},Mn^{2+})_8O_{16}$; tetragonal?). Pyrolusite (MnO_2) is also probably present. Using high-resolution transmitted electron microscopy, Turner and Buseck (1979) showed that individual crystal fibers from the district are composed of single unit-cell layers of romanechite ($BaMn^{2+}Mn_8^{4+}O_{16}(OH)_4$; monoclinic) randomly distributed within a dominant hollandite crystal lattice. Using electron microprobe analysis, Modreski (1983) showed the material to be chemically zoned from nearly pure barium-manganese oxide, with some potassium (5-15 mole percent cryptomelane with no lead), to coronadite (20 weight percent PbO). Willard (1973) reported microprobe

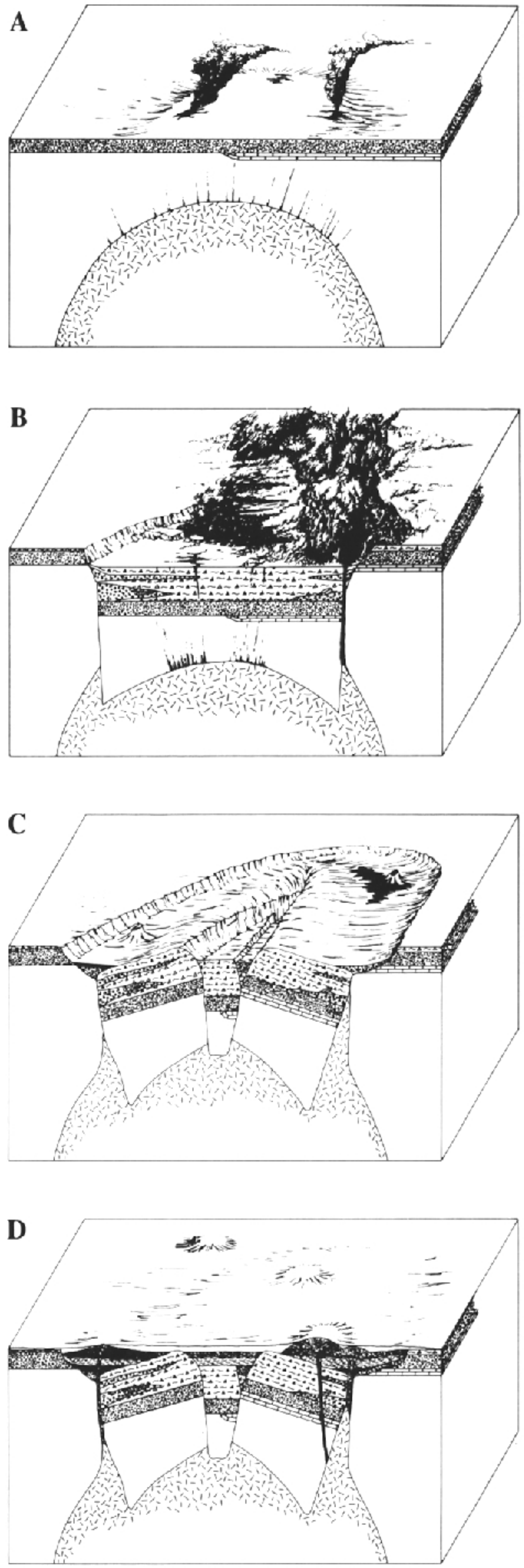

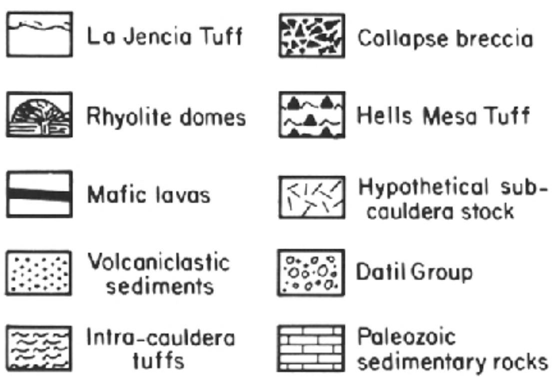

FIGURE 2—Diagrams depicting development of Socorro cauldron (12x vertical exaggeration). Diagram **A** shows a differentiating silicic pluton at a few kilometers depth. Surface deposits at that time were lavas and volcaniclastic rocks of the Datil Group, slightly upwarped by the pluton. Some hot spring and fumarolic activity and minor eruptions are also shown.

Diagram **B** simplistically depicts part of the major Hells Mesa eruption with large volumes of magma ascending to the surface via ring fractures and being projected high into an eruptive column that is periodically collapsing to generate ash flows. The ash flows are distributing erupted material in a wide apron around the cauldron. The Hells Mesa Tuff within the cauldron is much thicker and interbedded with breccias generated by collapse of cauldron walls.

Diagram **C** shows the cauldron after eruptions ceased and the intracauldron block had been resurgently uplifted and fractured. A symmetrical resurgent dome is shown although structural complexities prevent observation of this shape within Socorro cauldron. Erosion of the cauldron walls is continuing with concurrent deposition of conglomeratic sediments and mafic lavas (black).

Diagram **D** shows the completely filled cauldron and next overlying regional ash-flow tuff, La Jencia Tuff (thin white layer). The moat was nearly filled by this time with various materials including rhyolite domes and flows, local ash-flow tuffs, volcaniclastic sediments, and mafic lavas. *(From Osburn, 1983; used with permission. Legend by R. M. North)*

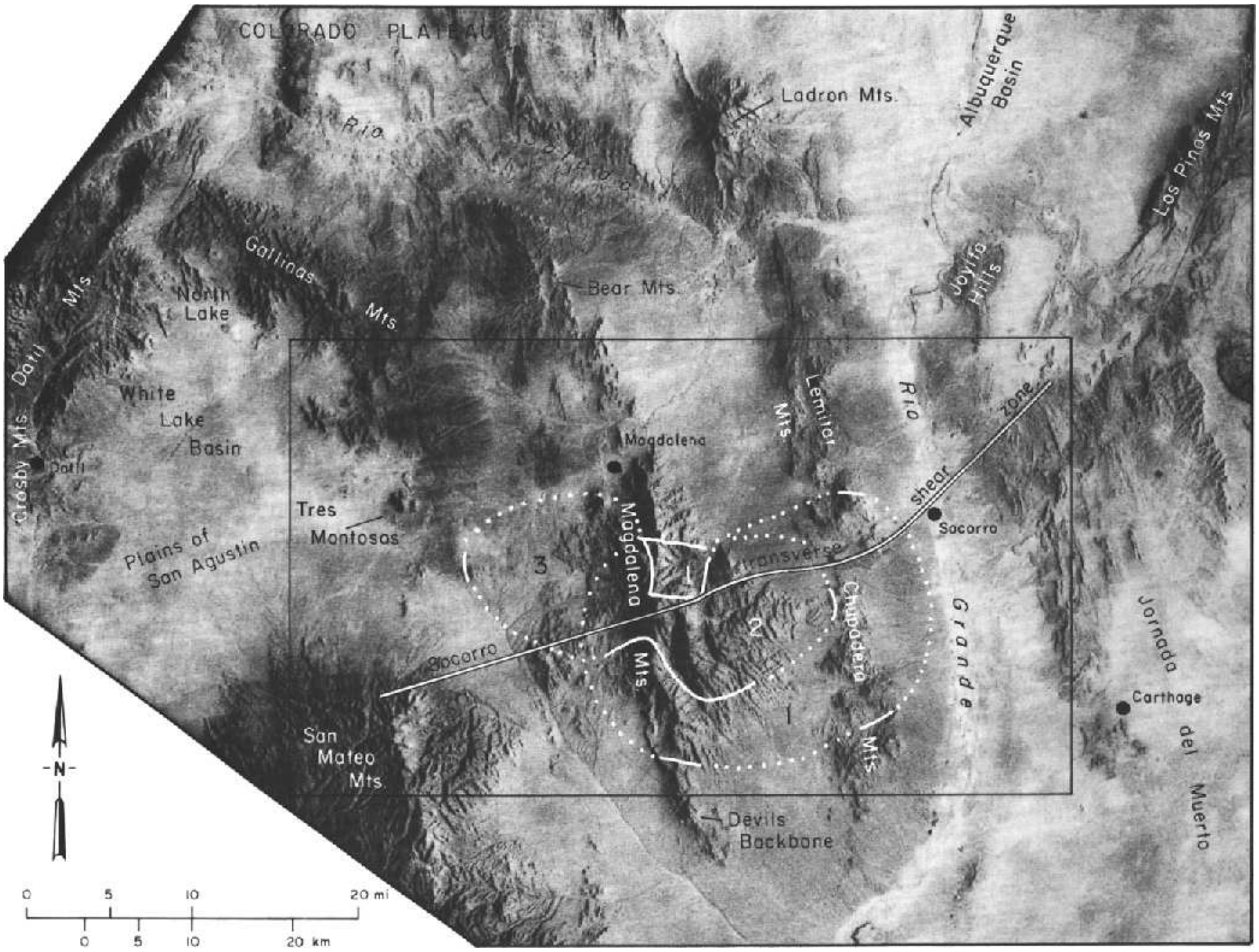

FIGURE 3—Approximate location of mid-Tertiary cauldrons in the Socorro area. 1, Socorro cauldron; 2, Sawmill Canyon cauldron; 3, Magdalena cauldron. The Socorro transverse shear zone separates two structural domains with rocks north of the zone dipping west and south of the zone dipping east. *(From °shun' and Chapin, 1983a).*

analyses, which indicated the banded material (Fig. 5) showed as much chemical variation along the bands as across them. lie concluded that the banding is due to physical, not chemical, changes during deposition. Because of this uncertainty, psilomelane is probably the best name for the material, keeping in mind that it is most often hollandite with a unit-cell of crvptomelane, coronadite, and!or romanechite thrown in here and there, perhaps admixed with pyrolusite. The common gangue minerals include calcite, quartz, hematite, and barite.

Trace-element chemistry

Trace-element studies of the Luis Lopez manganese deposits have shown that the manganese veins contain considerable amounts of some interesting trace elements. The most detailed geochemical study of the ore is the unpublished report of Willard (1973; Table 1), who reported a variety of minor and trace elements from the district. Lead, due to the presence of coronadite, is widespread in the district. Tungsten, in concentrations between 0.1 and 0.3 percent, is common in the district (Willard, 1973; Norman et al., 1983). Silver and gold have been detected in several samples (Table 1). Other elements generally present include

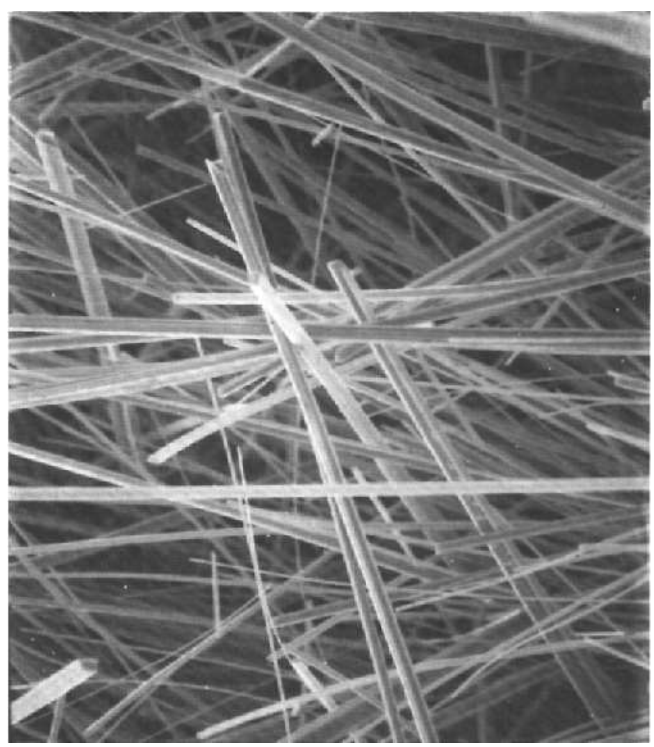

FIGURE 4—Scanning Electron Microscope photo of "rat's hair" psilomelane from the Nancy mine. Field of view is approximately 0.18 mm by 0.23 mm. *(Photo try Martha Cather.)*

FIGURE 5—Banded, hard manganese oxides (psilomelane). Material of this type has been found to he dominately hollandite with intergrown cryptomelane and coronadite. Sample is 6 cm wide.

arsenic, antimony, beryllium, nickel, cobalt, strontium, and thallium (Willard, 1973). Molybdenum is erratic in the district. ranging from undetectable to nearly 0.2%.

Genesis of the deposits

The Luis I.opez deposits have been described as an oxidized epithermal system (Norman et al., 1983). The main manganese deposits in the district are adjacent to a large area of red alteration (oxidized iron) superimposed on a large area of potassium metasomatism. The potassium metasomatism has resulted in replacement of plagioclase by K-feldspar (adularia?) and is thought to represent a widespread fossil hydrothermal system associated with rifting (D'Andrea-Dinkelman et al., 1983). The K_20 anomaly is Miocene or younger, and the mineralization at Luis Lopez and the silver-lead epithermal mineralization in the Socorro Peak district may be parts of this fossil geothermal system. The red, altered rock is depleted in manganese and is thought to he the source of the element in the adjacent Luis Lopez deposits. Manganese (1.2) was leached and oxidized from the altered rocks by hydrothermal solutions and deposited in open fractures and breccias adjacent to the altered area (Eggleston et al., 1983a; Fig. 6). Fluid inclusion and stable isotope analyses of the manganese ores indicate that the main mineralization in the district was formed from boiling; low-salinity solutions between 175 and 375°C formed approximately 500 in beneath the surface (Norman et al., 1983).

Future potential

As long as imports are stable, it is doubtful that the Luis Lopez ores will be mined again for manganese. Currently, the United States imports 100% of its manganese needs, 73% coming from Gabon, Brazil, and South Africa (Jones, 1987). In the event that the import sources were cut off, mining of sea-floor nodules would probably be as attractive as reopening the mines of the Luis Lopez district exclusively for manganese. However, some of the trace elements in the ore are interesting. Metallurgical studies on the ore may discover ways to recover some of the more abundant or valuable trace elements such as tungsten, silver, and perhaps even gold (Ahmad, 1972).

TABLE 1—Trace elements in the Luis Lopez mining district (from Willard, 1973).

Element	Range	Analytical method
P		
b	0.001-20%	atomic absorption
B	5.0-19%	atomic absorption
a	1.0-10%	atomic absorption
F	0.8-0.58% 0-0.13%	atomic absorption
e		atomic absorption
C	0-0.014%	atomic absorption
u	0-0.070%	atomic absorption
Z	0-1.7%	atomic absorption
n	0-0.181%	atomic absorption
Ni	0-2.0%	atomic absorption
C	0 0.1%	atomic absorption
o	0.7-1.5%	spectrographic
	0-0.7%	spectrographic
Mo	0-0.7%	spectrographic
K	0.003-0.007%	spectrographic
Sr	0.03-0.15%	spectrographic
A	0.03-1.5%	spectrographic
	0.00-0.02 oziton	fire assay
s	(0.68 ppm)	
S		*fire* assay
b	0.00-3.30 oz/ton	
TT	(113 ppm)	

Norman et al. (1983) stated that it is unlikely to find precious- or base-metal sulfide mineralization below the manganese oxide veins. They cited the lack of organic compounds and H2S in the fluid inclusions, and they also noted that the manganese mineralization is at the boiling level in the system, a level at which precious metals are found in many epithermal systems (Buchanan, 1981). However, they do suggest that *a* silver base-metal deposit similar to the Hardshell deposit in the Patagonia Mountains of Arizona could underlie the manganese oxide veins of the Luis Lopez district. This is a rather unlikely possibility. The 1 lardshell deposit is thought to have formed from the in-situ oxidation of a manganese sulfide (albandite)-base-metal sulfide deposit (Koutz, 1984). No evidence of any sulfide mineralization has been found at Luis Lopez. Also, the Hardshell mineralization is probably part of a Laramide porphyry-copper system (Keith et al., 1983), a much different geologic setting than the mid-Tertiary Luis Lopez district. This does not preclude some type of base- or precious-metal mineralization at depth, but it is unlikely that anything similar to Hardshell will be found.

Acknowledgments

The manuscript was reviewed by Dr. Ted L. Eggleston, and discussions with him aided the authors in understanding the geology of the district. The New Mexico Geological Society kindly allowed the reproduction of several figures front their Guidebook to the 34th Field Conference, Socorro Region II.

References

Ahmad, U. M. U., 1972, Recovery of manganese and by-products from manganese ores in Socorro County, New Mexico: Unpublished M.S. thesis, New Mexico Institute of Mining and Technology' 91 PP.

Aldrich, M. J., Jr., Chapin, C. E., and Laughlin, A. W., 1986, Stress history and tectonic development of the Rio Grande rift, New Mexico: Journal of Geophysical Research, v. 91, no. 86, pp. 6199-6211.

Buchanan, L. J., 1981, Precious metal deposits associated with volcanic environments in the Southwest; *in* Dickinson, W. R., and Payne, W. D. (eds.), Relations of tectonics to ore deposits in the southern Cordillera: Arizona Geological Society Digest, v. 14, pp. 237-262.

Chamberlin, R. M., 1980, Cenozoic stratigraphy and structure of the Socorro Peak volcanic center, central New Mexico: Unpublished Ph.D. thesis, Colorado School of Mines, 495 pp.; New Mexico Bureau of Mines and Mineral Resources, Open-file Report 118, 532 pp.

Chamberlin, R. M., 1983, Cenozoic domino-style crustal extension in the Lemitar Mountains, New Mexico—a summary: New Mexico Geological Society, Guidebook to 34th Field Conference, pp. 111-118.

Chapin, C. E., Chamberlin, R. M., Osburn, G. R., White, D. W., and Sanford, A. R., 1978, Exploration framework of the Socorro geothermal area, New Mexico; *in* Chapin, C. E., and Elston, W. E. (eds.), Field guide to selected cauldrons and mining districts of the Datil-Mogollon volcanic field New Mexico: New Mexico Geological Society, Special Publication 7, pp. 115-129.

D'Andrea-Dinkleman, J. F., Lindley, J. 1., Chapin, C. E., and Osburn, G. R., 1983, The Socorro K_2O anomaly—a fossil geothermal system in the Rio Grande rift: New Mexico Geological Society, Guidebook to 34th Field Conference, pp. 76-77.

Eggleston, T. L., 1982, Geology of the central Chupadera Mountains, Socorro County, New Mexico: Unpublished M.S. thesis, New Mexico institute of Mining and Technology, 164 pp; New Mexico Bureau of Mines and Mineral Resources, Open-file Report 141, 162 pp.

Eggleston, T. I., Norman, D. 1., Chapin, C. E., and Savin, S., 1983a, Geology, alteration, and genesis of the Luis Lopez manganese district, New Mexico: New Mexico Geological Society, Guidebook to 34th Field Conference, pp. 241-246.

Eggleston, T. I., Osburn, G. R. „ind Chapin, C. E., 1983b, Third day road log from Socorro to San Antonio, Nogal Canyon, Chupadera Mountains, Luis Lopez manganese district, and the MCA mine: New Mexico Geological Society, Guidebook to 34th Field Conference, pp. 61-81.

Farnham, L. L., 1961, Manganese deposits of New Mexico: U.S. Bureau of Mines, Information Circular 8030, 176 pp.

Jones, T. S., 1987, Manganese; in Mineral commodity summaries, 1987: U.S. Bureau of Mines, Government Printing Office, Washington, D.C., pp. 98-99.

Keith, S. B., Gest, D. E., DeWitt, E., Toll, N. W., and Everson, B. A., 1983, Metallic mineral districts and production in Arizona: Arizona Bureau of Geology and Mineral Technology, Bulletin 194, 58 pp., scale 1:1,000,000.

Koutz, F. R., 1984, The Hardshell silver, base-metal, manganese oxide deposit, Patagonia Mountains, Santa Cruz County, Arizona—a held trip guide; *in* Wilkins, J., Jr. (ed.), Gold and silver deposits of the Basin and Range Province, western U.S.A.: Arizona Geological Society Digest, v. 15, pp. 199-217.

McIntosh, W. C., Sutter, J. F., Chapin, C. E., Osburn, C. R., and Ratte, J. C., 1986. A stratigraphic framework for the eastern Mogollon-Datil volcanic field based on paleomagnetism and high-precision ^{41}Art^{39}Ar dating of ignimbrites—a progress report: New Mexico Geological Society, Guidebook to 37th Field Conference, pp. 183-195.

Modreski, P. J., 1983, Manganese oxides (psilomelane) from Socorro County, New Mexico (abs): New Mexico Geology, v. 5, no. 4, p. 84.

Norman, D. 1., I3azrafshan, K., and Eggleston, T. L., 1983, Mineralization of the Luis Lopez epithermal manganese deposits in light of fluid inclusion and geologic studies: New Mexico Geological Society, Guidebook to 34th Field Conference, pp. 247-251.

Osburn, G. R., 1983, Ash-flow tuffs, ignimbrites, cauldrons, and calderas: New Mexico Geological Society, Guidebook to 34th Field Conference, pp. 66-67.

Osburn, G. R., and Chapin, C. E., 1983a, Nomenclature for Cenozoic rocks of northeast Mogollon-Datil volcanic field, New Mexico: New Mexico Bureau of Mines and Mineral Resources, Stratigraphic Chart 1.

Osburn, G. R., and Chapin, C. E., 1983b, Ash-flow tuffs and cauldrons in the northeast Mogollon-Datil volcanic field—a summary: New Mexico Geological Society, Guidebook to 34th Field Conference, pp. 197-204.

Turner, S., and Buseck, P. R., 1979, Manganese oxide tunnel structures and their intergrowths: Science, v. 203, pp. 456-158.

Willard, M. E., 1973, Geology of Luis Lopez manganese district, New Mexico: New Mexico Bureau of Mines and Mineral Resources, Open-file Report 186, 81 pp.

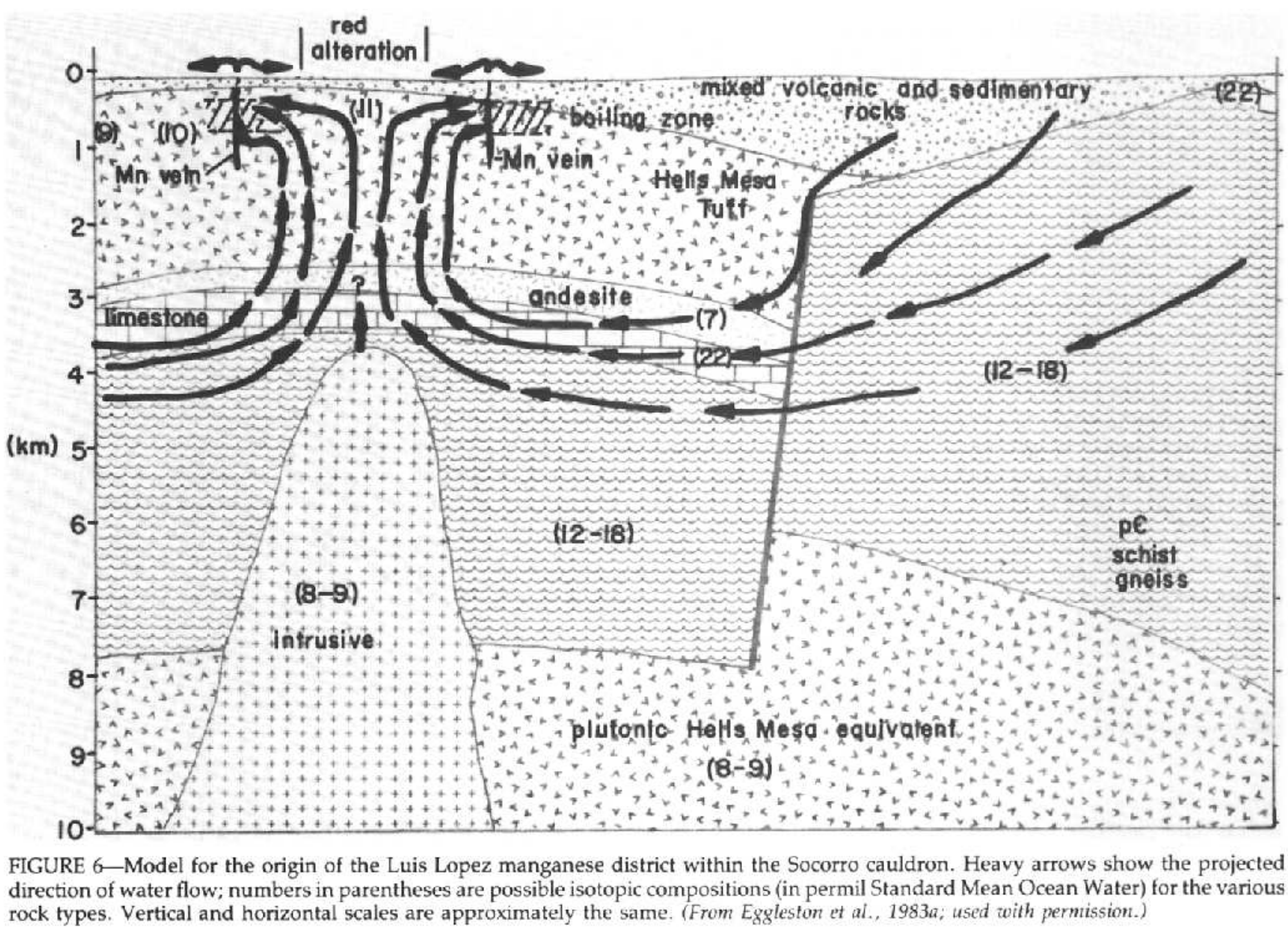

FIGURE 6—Model for the origin of the Luis Lopez manganese district within the Socorro cauldron. Heavy arrows show the projected direction of water flow; numbers in parentheses are possible isotopic compositions (in permil Standard Mean Ocean Water) for the various rock types. Vertical and horizontal scales are approximately the same. *(From Eggleston et al., 1983a; used with permission.)*

Glossary

alluvial fan—body of stream, sheetwash, and debris-flow deposits whose surface forms the segment of a cone that radiates downslope from the point where a stream emerges from a narrow valley or canyon onto a plain.
alluvium—unconsolidated elastic material deposited by running water, including various mixtures of gravel, sand, silt, and clay.
ammonite—extinct marine invertebrate related to the present-day chambered nautilus.
andesite—volcanic rock intermediate in composition between rhyolite and basalt.
anticline—archlike fold in which strata dip in opposite directions from a common ridge or axis.
arroyo—flat-floored and steep-walled channel or gully of an ephemeral stream, usually dry but can be transformed into a temporary watercourse or short-lived torrent after heavy rainfall.
ash—fine pyroclastic material that is less than 4.0 mm in diameter.

basalt—fine-grained, dark-colored volcanic rock composed chiefly of calcium-rich plagioclase, pyroxene, and olivine.
basement—the oldest rocks recognized in a given area; usually a complex of Precambrian igneous and metamorphic rocks underlying l'aleozoic and younger sedimentary formations.
bed—thin layer of rock, usually sedimentary or pyroclastic.
breccia—coarse-grained, elastic rock composed of very angular fragments; may be sedimentary, volcanic, or tectonic in origin.

calcrete—see caliche.
caliche--a common term, used in Hispanic North America, for a prominent zone of secondary carbonate accumulation in surficial materials of semiarid to arid areas formed by both geologic and pedogenic processes; finely crystalline calcium carbonate forms a nearly continuous surface-coating and void-filling medium in parent sediments and rocks; cementation ranges from weak and discontinuous to well-indurated (calcrete) forms; and accessory cements may include other carbonate, silicate, and sulphate minerals.
clastic—rock and mineral fragments (clasts) derived from pm-existing rocks and transported from their place of origin by water, wind, ice, volcanic, or mass-wasting processes.
colluvium—unconsolidated elastic material deposited on and at the base of steep hillslopes and mountain fronts by mass wasting and unconcentrated runoff.
conglomerate—clastic sedimentary rock composed predominantly of rounded to subangular gravel, cementing minerals, and lesser amounts of sand, silt, and clay.
contact—the place or surface where two different kinds of rocks meet.

dike—tabular igneous intrusion that cuts across the planar structures of surrounding rocks.
dip—the angle that a bed or fault plane makes with an imaginary horizontal plane.
dome—round or elliptical upwarp of strata.

extrusive rock—volcanic rock emplaced on the surface of the earth.

fault—fracture in rocks along which the two sides have moved relative to each other.
flow unit—group of sheets or beds of lava that were formed by a single eruption.
fold—archlike or troughlike undulations of rocks best seen in layered rocks; usually caused by compressional forces in the earth's crust.
formation—the fundamental unit in rock stratigraphic classification; a mappable body of rock characterized by lithologic homogeneity or distinctive lithologic features that is prevailingly, but not necessarily, tabular.
fossil—identifiable remains or traces of an ancient animal or plant preserved in rock.

gabbro—dark-colored, medium- to coarse-grained igneous rock consisting mainly of pyroxene and calcium plagioclase.
granite—light-colored, medium- to coarse-grained intrusive igneous rock consisting chiefly of orthoclase, sodium-plagioclase, and quartz with minor mica.
gypsum—common evaporite mineral used in making plaster of Paris ($Ca50_4 \cdot 2H_20$).

igneous rock—rock formed by solidifying and crystallizing from magma within the earth's crust (plutonic) or from lava and pyroclastic material on the earth's surface (volcanic).
intrusive rock—body of igneous rock that penetrated preexisting rocks as magma and cooled within the earth's crust.

laccolith —concordant, usually lenticular, igneous instrusion with known or assumed flat floor and a postulated dike-like feeder somewhere beneath its thickest point.
Laramide—of or relating to mountain-making (orogenic) movements in late Mesozoic and early Cenozoic time, approximately 75-40 m.y. ago in New Mexico.
lava—magma or molten rock that has reached the surface.
limestone—sedimentary rock composed of calcium carbonate; the consolidated equivalent of calcite mud, calcareous sand, or shell fragments.

magma—the molten rock material that forms igneous rocks when it cools.
mesa—isolated, nearly flat-topped, upland mass standing distinctly above the surrounding country and hounded by steeply sloping scarps; in Hispanic North America the term is also used for broad alluvial terraces and erosional benches that occur as intermediate platforms bordering stream valleys and canyons; Spanish for table.
metamorphic rock—sedimentary or igneous rock that has been altered chemically and structurally by extreme heat and pressure, causing new structures and minerals to form.
monzonite—grayish, medium- to coarse-grained intrusive rock consisting of approximately equal amounts of orthoclase and plagioclase with minor biotite and hornblende.

paleontology—the study of fossils, their environment, and the record of evolutionary development.
pediment—broad, gently sloping erosion surface developed at the foot of a receding hillslope or mountain front; the surface may be essentially hare, exposing rocks that extend beneath adjacent uplands, or it may be thinly mantled with alluvium and colluvium.
petroglyphs—figures and inscriptions pecked, carved, or hammered into rock surfaces.
phenocryst—conspicuous, relatively large crystal, inset in a more finely crystalline groundmass of an igneous rock.
pictograph—picture painted on a rock and used as a sign.
piedmont slope—the dominant gentle slope at the foot of a mountain, including footslope erosion surfaces (pedi-

ments) and constructional surfaces (fans, coalescent fans, and alluvial plains).

pluton—large igneous intrusion formed at depth in the crust.

porphyry—igneous rock consisting of distinct crystals (phenocrvsts) set in a very fine crystalline base or groundmass.

pyroclastic—pertaining to clastic materials produced by explosive aerial ejection of rock and mineral particles from a volcanic vent.

rhyolite—light-colored, silicic, very fine grained volcanic rock; extrusive equivalent of granite.

sandstone—clastic sedimentary rock composed predominantly of sand grains, cementing minerals, and lesser amounts of silt, clay, and gravel.

sedimentary rock—indurated deposit of clastic particles, chemical precipitates, and organic remains; primarily material transported by water, wind, or ice, or mass-wasting processes.

semiarid—type of climate characterized by 10-20 inches of annual rainfall and high evapotranspiration.

shale—clastic sedimentary rock, composed of indurated clay-silt mixtures, that tends to split apart easily into very thin layers.

sill—tabular igneous intrusion that parallels the planar structure of surrounding rocks.

siltstone--clastic sedimentary rock composed predominantly of particles between 0.062 and 0.004 mm in diameter.

stock—large, irregular igneous intrusion that cuts through surrounding rocks.

stratification—recognizable parallel beds of considerable lateral extent in sedimentary formations.

stratigraphic column—list of formations, by age, that compose the geologic history of an area. syncline—trough-like fold in layered rocks.

talus—sloping heap of coarse rock fragments at the foot of a cliff or steep slope.

tectonic—pertaining to the forces involved in, or the resulting structure of, the broader deformational features of the upper part of the earth's crust.

terrace—one of a series of level surfaces in a stream valley, elongated more or less parallel to the stream channel, representing the dissected remnant of an abandoned floodplain or valley floor produced during a former state of erosion or deposition.

tipple—apparatus by which loaded cars (as with coal or mineral ore) are emptied by tipping, sometimes including an elevated trackway upon which the cars are run for tipping.

unconformity—surface of erosion or nondeposition representing an undocumented period of geologic time and hence a gap in the stratigraphic record.

volcano—localized vent in the earth's crust from which molten or hot rock and gases issue; a hill or mountain composed wholly or in part of the material ejected from such a vent and often having a crater at its top.

Selected conversion factors*

TO CONVERT	MULTIPLY BY	TO OBTAIN
Length		
inches, in	2.540	centimeters, cm
feet, ft	3.048×10^{-1}	meters, m
yards, yds	9.144×10^{-1}	m
statute miles, mi	1.609	kilometers, km
fathoms	1.829	m
angstroms, Å	1.0×10^{-8}	cm
Å	1.0×10^{-4}	micrometers, μm
Area		
in^2	6.452	cm^2
ft^2	9.29×10^{-2}	m^2
yds^2	8.361×10^{-1}	m^2
mi^2	2.590	km^2
acres	4.047×10^{3}	m^2
acres	4.047×10^{-1}	hectares, ha
Volume (wet and dry)		
in^3	1.639×10^{1}	cm^3
ft^3	2.832×10^{-2}	m^3
yds^3	7.646×10^{-1}	m^3
fluid ounces	2.957×10^{-2}	liters, l *or* L
quarts	9.463×10^{-1}	l
U.S. gallons, gal	3.785	l
U.S. gal	3.785×10^{-3}	m^3
acre-ft	1.234×10^{3}	m^3
barrels (oil), bbl	1.589×10^{-1}	m^3
Weight, mass		
ounces avoirdupois, avdp	2.8349×10^{1}	grams, gr
troy ounces, oz	3.1103×10^{1}	gr
pounds, lb	4.536×10^{-1}	kilograms, kg
long tons	1.016	metric tons, mt
short tons	9.078×10^{-1}	mt
oz mt^{-1}	3.43×10^{1}	parts per million, ppm
Velocity		
ft sec^{-1} (= ft/sec)	3.048×10^{-1}	m sec^{-1} (= m/sec)
mi hr^{-1}	1.6093	km hr^{-1}
mi hr^{-1}	4.470×10^{-1}	m sec^{-1}
Pressure, stress		
lb in^{-2} (= lb/in^2), psi	7.03×10^{-2}	kg cm^{-2} (= kg/cm^2)
lb in^{-2}	6.804×10^{-2}	atmospheres, atm
lb in^{-2}	6.895×10^{3}	newtons (N)/m^2, N m^{-2}
atm	1.0333	kg cm^{-2}
atm	7.6×10^{2}	mm of Hg (at 0° C)
inches of Hg (at 0° C)	3.453×10^{-2}	kg cm^{-2}
bars, b	1.020	kg cm^{-2}
b	1.0×10^{6}	dynes cm^{-2}
b	9.869×10^{-1}	atm
b	1.0×10^{-1}	megapascals, MPa
Density		
lb in^{-3} (= lb/in^3)	2.768×10^{1}	gr cm^{-3} (= gr/cm^3)
Viscosity		
poises	1.0	gr cm^{-1} sec^{-1} *or* dynes cm^{-2}
Discharge		
U.S. gal min^{-1}, gpm	6.308×10^{-2}	l sec^{-1}
gpm	6.308×10^{-5}	m^3 sec^{-1}
ft^3 sec^{-1}	2.832×10^{-2}	m^3 sec^{-1}
Hydraulic conductivity		
U.S. gal day^{-1} ft^{-2}	4.720×10^{-7}	m sec^{-1}
Permeability		
darcies	9.870×10^{-13}	m^2
Transmissivity		
U.S. gal day^{-1} ft^{-1}	1.438×10^{-7}	m^2 sec^{-1}
U.S. gal min^{-1} ft^{-1}	2.072×10^{-1}	l sec^{-1} m^{-1}
Magnetic field intensity		
gausses	1.0×10^{5}	gammas
Energy, heat		
British thermal units, BTU	2.52×10^{-1}	calories, cal
BTU	1.0758×10^{2}	kilogram-meters, kgm
BTU lb^{-1}	5.56×10^{-1}	cal kg^{-1}
Temperature		
°C + 273	1.0	°K (Kelvin)
°C + 17.78	1.8	°F (Fahrenheit)
°F − 32	5/9	°C (Celsius)

**Divide by* the factor number to reverse conversions.
Exponents: for example 4.047×10^{3} (see acres) = 4,047; 9.29×10^{-2} (see ft^2) = 0.0929.

Editor: Deborah A. Shaw
Drafters: Monte M. Brown

Type face: Palatino

Presswork: Miehle Single Color Offset
Harris Single Color Offset

Binding: Smyth sewn with softbound cover

Paper: Cover on 17-pt. Kivar
Text on 70-lb White Matte

Ink: Cover—PMS 320
Text—Black

Quantity: 900

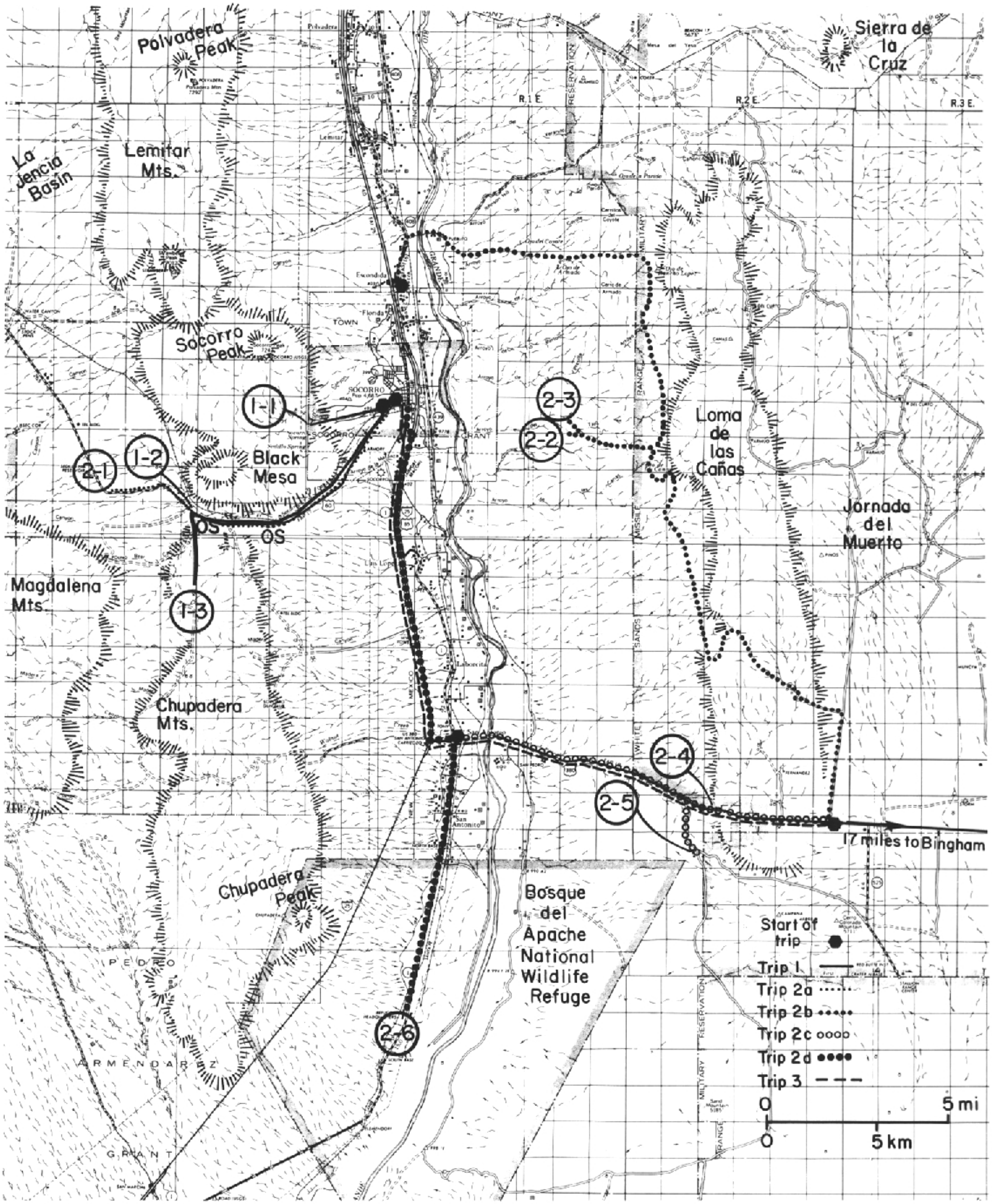

Polvadera Peak
Sierra de la Cruz
La Jencia Basin
Lemitar Mts.
Socorro Peak
1-1
2-3
2-2
Loma de las Cañas
2-1
1-2
Black Mesa
OS
OS
Jornada del Muerto
Magdalena Mts.
1-3
Chupadera Mts.
2-4
2-5
17 miles to Bingham
Chupadera Peak
Bosque del Apache National Wildlife Refuge
Start of trip
Trip 1
Trip 2a
Trip 2b
Trip 2c
Trip 2d
Trip 3
2-6
0
5 mi
0
5 km